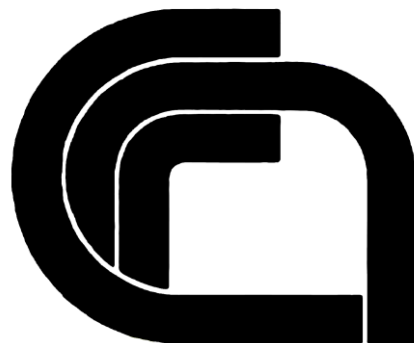


NATIONAL RESEARCH COUNCIL

ADVISORY COMMITTEE
ON TECHNICAL RECOMMENDATIONS FOR CONSTRUCTION

**Guide for the Design and Construction
of Externally Bonded FRP Systems
for Strengthening Existing Structures**

Materials, RC and PC structures, masonry structures



CNR-DT 200 R1/2013

This document is subject to copyright.

**No part of this publication may be stored in a retrieval system, or
transmitted in any form or by any means
– electronic, mechanical, recording, or otherwise –
without the prior written permission
of the Italian National Research Council.**

**The reproduction of this document is permitted
for personal, noncommercial use.**

CONTENTS

1 FOREWORD	1
1.1 SCOPE	1
1.2 SYMBOLS	2
2 Materials	6
2.1 INTRODUCTION.....	6
2.2 CLASSIFICATION OF FRP STRENGTHENING SYSTEMS.....	6
2.2.1 Mechanical properties of FRP strengthening systems	7
2.2.2 Pre-cured systems.....	9
2.2.3 Wet lay-up systems	9
2.2.4 Pre-impregnated systems	12
2.3 QUALITY CONTROL	12
2.3.1 Tasks and responsibilities of professionals	12
2.4 TRANSPORTATION, STORAGE, PRESERVATION, HANDLING AND USE	13
3 BASIS OF DESIGN FOR FRP STRENGTHENING	15
3.1 BASIC REQUIREMENTS	15
3.2 DURABILITY REQUIREMENTS.....	16
3.3 GENERAL PRINCIPLES OF THE STRENGTHENING DESIGN	16
3.3.1 Introduction	16
3.3.2 Service life and design load	16
3.3.3 Properties of FRP materials and related design load	17
3.3.4 Design capacity	17
3.4 PARTIAL FACTORS	18
3.4.1 Partial factor γ_m for FRP	18
3.4.2 Partial factors γ_{Rd} for resistance models.....	18
3.5 SPECIAL DESIGN PROBLEMS AND RELEVANT CONVERSION FACTORS	18
3.5.1 Environmental factors	18
3.5.2 Load condition and conversion factors for long-term effects	20
3.5.3 Impact and explosive loading.....	20
3.5.4 Vandalism	20
3.6 STRENGTHENING LIMITATIONS IN CASE OF FIRE.....	20
4 STRENGTHENING OF REINFORCED AND PRESTRESSED CONCRETE STRUCTURE	22
4.1 DEBONDING MECHANISMS	22
4.1.1 Failure mechanisms due to debonding.....	22
4.1.2 Fracture energy.....	23
4.1.3 Ultimate design strength for laminate/sheet end debonding (mode 1)	24
4.1.4 Ultimate design strength for intermediate debonding (mode 2)	25
4.1.5 Interfacial stress for serviceability limit state	25
4.2 FLEXURAL STRENGTHENING.....	27
4.2.1 Introduction	27
4.2.2 Analysis at ultimate limit state.....	27
4.2.3 Analysis at serviceability limit state	31
4.2.4 Ductility.....	33
4.3 SHEAR STRENGTHENING	34
4.3.1 Introduction	34
4.3.2 Strengthening configurations	34

4.3.3	Shear capacity of FRP strengthened members.....	35
4.4	TORSIONAL STRENGTHENING	38
4.4.1	Introduction	38
4.4.2	Strengthening configurations	38
4.4.3	Torsional capacity of FRP strengthened members.....	38
4.5	CONFINEMENT	39
4.5.1	Introduction	39
4.5.2	Axial capacity of FRP-confined members	40
4.5.3	Ductility of FRP-confined members under combined bending and axial load.....	44
4.6	FLEXURAL STRENGTHENING OF PRESTRESSED CONCRETE MEMBERS	45
4.6.1	Use of FRP for prestressed concrete members	45
4.7	DESIGN FOR SEISMIC APPLICATIONS	46
4.7.1	Introduction	46
4.7.2	Selection criteria for FRP strengthening	46
4.8	INSTALLATION, MONITORING, AND QUALITY CONTROL.....	49
4.8.1	Quality control and substrate preparation	49
4.8.2	Recommendations for the installation.....	50
4.9	NUMERICAL EXAMPLES	51
5	STRENGTHENING OF MASONRY STRUCTURES	52
5.1	INTRODUCTION.....	52
5.1.1	Scope	52
5.1.2	Strengthening of historical and monumental buildings	52
5.1.3	FRP strengthening design criteria	52
5.2	DESIGN ASSUMPTIONS	53
5.2.1	Structural modeling	53
5.2.2	Failure modes	53
5.2.3	Design requirements.....	53
5.3	EVALUATION OF DEBONDING STRENGTH	55
5.3.1	General considerations and failure modes	55
5.3.2	Design strength for laminate/sheet end debonding	56
5.3.3	Design strength for intermediate debonding	59
5.3.4	Bond strength with stresses perpendicular to the bond surface	59
5.3.5	Mechanical anchorage devices.....	59
5.4	SAFETY REQUIREMENTS	60
5.4.1	Strengthening of masonry panels	60
5.4.2	Lintel and tie areas	68
5.5	STRENGTHENING OF STRUCTURAL MEMBERS WITH SINGLE OR DOUBLE CURVATURE.....	69
5.5.1	Arches	70
5.5.2	Single curvature vaults: barrel vaults	71
5.5.3	Double curvature vaults: domes.....	71
5.5.4	Double curvature vaults on a square plane	72
5.6	CONFINEMENT OF MASONRY COLUMNS.....	73
5.6.1	Design of axially loaded confined members.....	73
5.6.2	Confinement of circular columns.....	75
5.6.3	Confinement of prismatic columns	76
5.7	DESIGN FOR SEISMIC APPLICATIONS	79
5.7.1	Design objectives	79
5.7.2	Selection criteria for FRP strengthening	80
5.8	INSTALLATION AND CONSTRUCTION DETAILS.....	80

5.8.1	Quality control and substrate preparation	81
5.8.2	Recommendations for the installation.....	82
5.9	NUMERICAL EXAMPLES	83
6	CONTROL AND MONITORING	84
6.1	QUALITY CONTROL ON THE CONSTRUCTION SITE	84
6.2	QUALITY CONTROL DURING INSTALLATION.....	84
6.2.1	Semi-destructive tests.....	84
6.2.2	Non destructive tests	85
6.3	PERSONNEL QUALIFICATION.....	86
6.4	MONITORING OF THE STRENGTHENING SYSTEM	87
7	APPENDIx A (CHARACTERISTICS OF COMPOSITES AND THEIR CONSTITUENTS).....	88
7.1	INTRODUCTION.....	88
7.2	FIBERS USED IN COMPOSITES	90
7.2.1	Types of fibers available in the market and their classification.....	91
7.2.2	Non-impregnated fabrics.....	96
7.3	MATRICES.....	97
7.3.1	Epoxy resins	98
7.3.2	Polyester resins.....	98
7.3.3	Other types of resins.....	99
7.4	ADHESIVES.....	99
8	APPENDIx b (MANUFACTURING TECHNIQUES).....	100
8.1	INTRODUCTION.....	100
8.1.1	Pultrusion	100
8.1.2	Lamination	101
8.1.3	Wet lay-up.....	102
9	APPENDIX C (STRESS-STRAIN RELATIONSHIP OF FRP)	103
9.1	MECHANICAL BEHAVIOR OF COMPOSITES.....	103
9.2	PLANE STRESSES	105
9.2.1	Effect of loading acting on directions other than that of material symmetry.....	106
9.3	FAILURE CRITERIA.....	108
10	APPENDIx D (DEBONDING)	111
10.1	FAILURE DUE TO DEBONDING	111
10.2	BOND BETWEEN FRP AND CONCRETE	112
10.2.1	Specific fracture energy	113
10.2.2	Bond-slip law	114
10.2.3	Optimal bond length.....	115
10.2.4	Debonding due to flexural cracks	116
10.3	BOND BETWEEN FRP AND MASONRY	116
10.3.1	Specific fracture energy	116
10.3.2	Bond-slip law	118
10.3.3	Optimal bond length.....	119
10.3.4	Debonding due to flexural cracking	120
11	APPENDIX C (STRENGTHENING FOR COMBINED BENDING AND AXIAL load OF REINFORCED CONCRETE MEMBERS)	121

11.1 FLEXURAL CAPACITY OF FRP STRENGTHENED MEMBERS SUBJECTED TO COMBINED BENDING AND AXIAL LOAD.....	121
12 APPENDIX D (CONFINED CONCRETE).....	123
12.1 CONSTITUTIVE LAW OF CONFINED CONCRETE	123
13 APPENDIX E (EXAMPLES OF FRP STRENGTHENING DESIGN on RC structures)	125
13.1 GEOMETRICAL, MECHANICAL AND LOADING DATA	125
13.2 INCREASE OF APPLIED LOADS	127
13.3 DESIGN OF FLEXURAL REINFORCEMENT	127
13.4 DESIGN OF SHEAR REINFORCEMENT	131
13.5 DESIGN OF COLUMNS REINFORCEMENT.....	133
13.5.1 Confinement of columns subjected to slightly eccentric axial force	134
13.5.2 Confinement and flexural strengthening of columns subjected to combined bending and axial force	136
14 APPENDIX H (EXAMPLES OF FRP STRENGTHENING DESIGN on masonry structures)	138
14.1 GEOMETRICAL, MECHANICAL AND LOADING DATA	138
14.2 COMBINED AXIAL AND BENDING MOMENT CAPACITY	141
14.3 DESIGN OF FRP FOR COMBINED AXIAL AND BENDING MOMENT.....	144
14.4 SHEAR CAPACITY	144
14.5 DESIGN OF FRP FOR SHEAR.....	147
14.6 DESIGN FOR SIMPLE OVERTURNING	148

1 FOREWORD

More than five years after the approval notice of CNR-DT 200/2004, the CNR *Committee for the preparation and analysis of technical recommendations for construction* has promoted a revision of the document. The original study group was entrusted with the task of updating the document based on the results of the latest researches, both theoretical and experimental, undertaken at an international level during the last five years. This was achieved using research performed in Italy under the project Reluis (2005-2008), founded by the Department of Civil Protection, in which a specific chapter was dedicated to the “Innovative Materials for Risk Mitigation of Existing Structures.”

During the revision process, the Committee also took into consideration of the latest version of the following international guidelines:

- 440.2R-08: “Guide for the Design and Construction of Externally Bonded FRP Systems for Strengthening Concrete Structures”, American Concrete Institute (ACI), committee 440, 2008;
- ISIS Design Manual No. 4: “FRP Rehabilitation of Reinforced Concrete Structures”. ISIS Canada Corporation, 2008.

The document has been subjected to public hearing from April to June of 2013. Modifications and/or integrations were then implemented.

On October 10, 2013 at the CNR headquarters in Rome (Italy) the updated document was discussed and approved by the “Advisory committee on technical recommendations for construction.”

We would like to thank those Professional, Institutional, Industrial and Academic individuals who have actively participated in the process.

1.1 SCOPE

The purpose of this guide is to provide, within the framework of the Italian regulations, a document for the design and construction of externally bonded FRP systems for strengthening existing structures. A guide, by definition is not a binding regulation, but merely represents an aid for practitioners interested in the field of composites. Nevertheless, the responsibility remains with the user of this guide.

The following topics will be addressed:

- Materials
- Basic concepts on FRP strengthening
- Strengthening of reinforced and prestressed concrete structures
- Strengthening of masonry structures

Specific guidelines for the strengthening and construction of reinforced concrete, prestressed concrete and masonry structures subjected to earthquakes according to the most recent national and international design codes are provided.

The first topic includes a summary of several advantages and some disadvantages of FRP materials. Also included are Appendices A, B and C that present notions on the mechanical characterization of composite materials. The peculiar differences between FRP compared to traditional materials, such as their anisotropic behavior and emphasis to their constitutive laws, are highlighted.

The remaining topics are addressed using the approach of the Eurocodes and typical style of technical documents published by CNR. Sections are divided into *Principles* and *Application Rules*. Each section is numbered progressively, and the principles are marked with the label P. *Principle* statements include the following:

- *General statements and definitions of mechanical-structural nature.*

- *Recognized needs and/or analytical models accepted by the scientific community, whose value is universally deemed to be pre-eminent with respect to possible alternatives, unless otherwise explicitly stated.*

Application Rules are procedures of widely recognized value, following the Principles and meeting their requirements.

The document contains following Appendices:

- Appendix A, Mechanical Characterization of FRP;
- Appendix B, Production Techniques;
- Appendix C, Constitutive Law and Failure Modes;
- Appendix D, Debonding;
- Appendix E, Strengthening of Prestressed Concrete;
- Appendix F, Constitutive Law for Confined Concrete;
- Appendix G, Design Examples for FRP Strengthening of Reinforced Concrete Members
- Appendix H, Design Examples for FRP Strengthening of Masonry.

1.2 SYMBOLS

General notations

- (.)_c value of quantity (.) for concrete
- (.)_{cc} value of quantity (.) for confined concrete
- (.)_d design value of quantity (.)
- (.)_f value of quantity (.) for fiber-reinforced composite
- (.)_{fib} value of quantity (.) referred to the fiber itself
- (.)_k characteristic value of quantity (.)
- (.)_m value of quantity (.) for masonry
- (.)_{mat} value of quantity (.) referred to the matrix
- (.)_{mc} value of quantity (.) for confined masonry itself
- (.)_R value of quantity (.) as resistance
- (.)_s value of quantity (.) for steel
- (.)_S value of quantity (.) as demand

Uppercase Roman letters

- A_c cross-sectional area of concrete
- A_f area of FRP reinforcement
- A_{fib} area of fiber
- A_{s1} area of steel reinforcement subjected to tension
- A_{s2} area of steel reinforcement subjected to compression
- E_c Young's modulus of elasticity of concrete
- E_f Young's modulus of elasticity of FRP reinforcement
- E_{fib} Young's modulus of elasticity of fiber itself
- E_{mat} Young's modulus of elasticity of matrix
- E_s Young's modulus of elasticity of steel reinforcement
- FC confidence factor
- $F_{max,d}$ design value of the maximum tensile force transferred by FRP reinforcement to the concrete support
- F_{pd} design value of the maximum anchorage force transferred by FRP reinforcement bonded on a masonry structure in the presence of a force perpendicular to the bonded surface area
- G_a shear modulus of adhesive
- G_c shear modulus of concrete

I_o	moment of inertia of cracked and un-strengthened reinforced concrete section
I_1	moment of inertia of cracked and FRP-strengthened reinforced concrete section
I_c	moment of inertia of transformed section
I_f	moment of inertia of FRP reinforcement about its centroidal axis, parallel to the beam neutral axis
M_{Rd}	flexural capacity of FRP-strengthened member
M_{Sd}	factored moment
M_o	bending moment acting before FRP strengthening
M_1	bending moment applied to the RC section due to loads applied after FRP strengthening
$N_{Rcc,d}$	axial capacity of FRP-confined concrete member
$N_{Rmc,d}$	axial capacity of FRP-confined masonry
N_{Sd}	factored axial force
P_{fib}	weight percentage of fibers
P_{mat}	weight percentage of matrix
T_g	glass transition temperature of the resin
T_{mat}	melting temperature of the resin
T_{Rd}	torsional capacity of FRP-confined concrete member
$T_{Rd,f}$	FRP contribution to the torsional capacity
$T_{Rd,c}$	concrete contribution to the torsional capacity
$T_{Rd,l}$	longitudinal steel contribution to the torsional capacity
$T_{Rd,s}$	vertical steel contribution to the torsional capacity
T_{Sd}	factored torsion
T_x	Yarn count in x direction
V_{fib}	volume percentage of fibers
V_{Rd}	shear capacity of FRP-strengthened member
$V_{Rd,c}$	concrete contribution to the shear capacity
$V_{Rd,s}$	steel contribution to the shear capacity
$V_{Rd,f}$	FRP contribution to the shear capacity
V_{Sd}	factored shear force
$V_{Rd,m}$	masonry contribution to the shear capacity

Lowercase Roman letters

b	width of the section
b_f	width of FRP reinforcement
d	distance from extreme compression fiber to centroid of tension reinforcement
f_{bm}	mean value of compressive strength of masonry blocks
f_{btm}	mean value of tensile strength of masonry blocks
f_{bd}	design bond strength between FRP reinforcement and concrete (or masonry)
f_c	concrete compressive strength (cylindrical)
f_{ccd}	design strength of confined concrete
f_{cd}	design concrete compressive strength
f_{cm}	mean value of concrete compressive strength
f_{ctm}	mean value of concrete tensile strength
f_{fd}	design strength of FRP reinforcement
f_{idd}	design debonding strength of FRP reinforcement (mode 1)
$f_{idd,2}$	design debonding strength of FRP reinforcement (mode 2)
f_{fed}	effective design strength of FRP shear reinforcement
f_{fib}	characteristic strength of the fiber itself
f_{fk}	characteristic strength of FRP reinforcement
f_{fpd}	design debonding strength of FRP reinforcement
f_l	confining lateral pressure

$f_{l,eff}$	effective confining pressure
f_{mat}	characteristic strength of the matrix
f_{mm}	characteristic compressive strength of masonry
f_{mm}^h	characteristic compressive strength of masonry in the horizontal direction
f_{mcd}	characteristic compressive strength of FRP-confined masonry
f_{md}	design compressive strength of masonry
f_{md}^h	design compressive strength of masonry in the horizontal direction
f_{mtm}	mean value of characteristic tensile strength of masonry
f_{vd}	design shear strength of masonry
f_{vm}	mean value of masonry shear strength
f_y	yield strength of longitudinal steel reinforcement
f_{yd}	design yield strength of longitudinal steel reinforcement
h	height of the section
k_{eff}	coefficient of efficiency for confinement
k_H	coefficient of efficiency in the horizontal direction
k_V	coefficient of efficiency in the vertical direction
k_α	coefficient of efficiency related to the angle α of fibers respect to the longitudinal axis of confined member
l_b	bond length
l_{ed}	optimal bond length
p_b	distance between layers of bars in the confinement of masonry columns
p_f	spacing of FRP strips or discontinuous FRP U-wraps
s	interface slip
s_u	interface slip at full debonding
t_f	thickness of FRP laminate
x	distance from extreme compression fiber to neutral axis

Lower case Greek letters

Γ_{Fk}	characteristic value of specific fracture energy
Γ_{Fd}	design value of specific fracture energy

Lowercase Greek letters

γ_m	partial factor for materials
γ_{Rd}	partial factor for resistance models
ϵ_o	concrete strain on the tension fiber prior to FRP strengthening
ϵ_c	concrete strain on the compression fiber
ϵ_{ccu}	design ultimate strain of confined concrete
ϵ_{co}	concrete strain on the tension fiber prior to FRP strengthening
ϵ_f	strain of FRP reinforcement
ϵ_{fd}	design strain of FRP reinforcement
$\epsilon_{fd,rid}$	reduced design strain of FRP reinforcement for confined members
ϵ_{fk}	characteristic rupture strain of FRP reinforcement
ϵ_{fdd}	maximum strain of FRP reinforcement before debonding
ϵ_{mcu}	ultimate compressive strain of confined masonry
ϵ_{mu}	ultimate compressive strain of masonry
ϵ_{s1}	strain of tension steel reinforcement
ϵ_{s2}	strain of compression steel reinforcement
ϵ_{yd}	design yield strain of steel reinforcement
η	conversion factor
ν_{fib}	Poisson's ratio of fibers
ν_{mat}	Poisson's ratio of matrix

ρ_{fib}	fiber density
ρ_{mat}	matrix density
σ_c	stress in the concrete
σ_f	stress in FRP reinforcement
σ_s	stress in tensile steel reinforcement
σ_{Sd}	stress normal to masonry face acting on the bonded surface area between FRP reinforcement and masonry
$\tau_{\text{b,e}}$	equivalent shear stress at the adhesive-concrete interface

2 MATERIALS

2.1 INTRODUCTION

This guide addresses specific structural applications of composite materials comprised of continuous long carbon, glass or aramid fibers immersed in polymeric matrices and commonly referred to as *Fiber Reinforced Polymer* (FRP). More properly FRP can be identified using the acronyms CFRP, GFRP and AFRP when comprised of carbon, glass or aramid fiber, respectively. Continuous fiber-reinforced materials with polymeric matrix can be considered as composite, heterogeneous, and anisotropic materials with a prevalent linear elastic behavior up to failure. They are widely used for the strengthening of civil structures. There are many advantages of using FRP: it is lightweight, possesses good mechanical properties, and is corrosion-resistant.

Composites are available in several geometries types ranging from laminates with regular surfaces to bi-directional fabrics that are easily adaptable to the shape of the member being strengthened. Composites are also suitable for applications where the aesthetic preservation of the original structures is required (buildings of historic or artistic interest) or where traditional strengthening techniques cannot be effectively employed.

There are also other types of commercial composite materials characterized by the nature of the matrix (inorganic matrix) or the fibers (discontinuous or continuous fibers, made of steel, basalt, or PBO).

Chapter 2 the classification, the qualifications certification and the acceptance criteria of systems made of FRP as well as duties and responsibilities of the users.

The reader who wishes to acquire further knowledge on the production technologies of FRP, the mechanical properties and design criteria shall use Appendices A, B and C of these Instructions, in addition to the many books available in the literature.

2.2 CLASSIFICATION OF FRP STRENGTHENING SYSTEMS

(1) From a morphological point of view, FRP strengthening systems are divided into:

- Pre-cured systems (Section 2.2.2), Manufactured in various shapes by pultrusion or lamination, pre-cured systems are directly bonded to the structural member to be strengthened;
- Wet lay-up systems (Section 2.2.3), Manufactured with fibers lying in one or more directions as FRP sheets or fabrics and impregnated with resin at the job site to the support;
- Prepreg systems (Section 2.2.4), Manufactured with unidirectional or multidirectional fiber sheets or fabrics pre-impregnated at the manufacturing plant with partially polymerized resin. They may be bonded to the member to be strengthened with (or without) the use of additional resins.

(2) From a mechanical point of view, the FRP strengthening systems are classified based on their values of modulus of elasticity and ultimate capacity. These values are measured under uniaxial tension in the direction of the fibers. Pre-cured systems shall be referred to by unit area of the FRP (fiber and matrix) and Wet lay-up system to the area of dry fibers only. Values of modulus of elasticity and tensile strength must be durable with respect to the environmental degradation induced on the FRP composite.

This classification is consistent with the *Guideline for qualification and acceptance criteria of fiber reinforced composites for strengthening applications of existing structures*, currently under approval from the Italian Ministry of Infrastructures and Transportation.

2.2.1 Mechanical properties of FRP strengthening systems

(1)P In FRP materials, fibers provide both loading carrying capacity and stiffness to the composite while the matrix ensures sharing of the load among fibers and protects the fibers from the environment. Most FRP materials are comprised of fibers with both high strength and stiffness, while their strain at failure is lower than that of the matrix.

Figure 2-1 shows the stress-strain relationship for the fiber, matrix, and resulting FRP material. The FRP material has a lower stiffness than the fibers and fails at the same strain, $\epsilon_{fib,max}$, of the fibers alone. In fact, beyond such ultimate strain, load sharing from the matrix to fibers is not recommended.

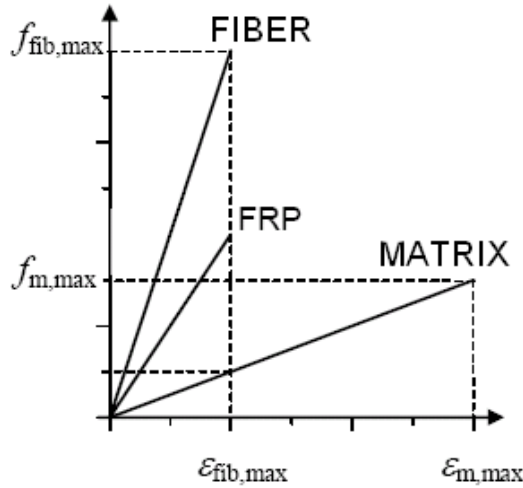


Figure 2-1 – Stress-strain relationship of fibers, matrix and FRP.

Table 2-1 summarizes the mechanical properties of a pre-cured laminate compared to the average values of the corresponding fibers. The values of Young modulus of elasticity, E_f , and ultimate strength at failure, f_f , of the laminate are lower than those of the fiber itself, while the ultimate tensile strain is of the same order of magnitude for both materials.

Table 2-1 – Comparison between mechanical properties of a pre-cured laminate and fibers.

Pre-cured systems	Modulus of elasticity [GPa]		Ultimate strength [MPa]		Ultimate strain [%]	
	FRP E_f	Fiber E_{fib}	FRP f_f	Fiber f_{fib}	FRP ϵ_{fu}	Fiber $\epsilon_{fib,u}$
CFRP (low modulus)	160	210-230	2800	3500-4800	1.6	1.4-2.0
CFRP (high modulus)	300	350-500	1500	2500-3100	0.5	0.4-0.9

(2) For FRP material made of unidirectional fibers, the mechanical behavior of the composite can be estimated using micro-mechanical models. For example, using the rule of mixtures (eq. (9.5) in Appendix C):

$$E_f = V_{fib} \cdot E_{fib} + (1 - V_{fib}) \cdot E_{mat}, \tag{2.1}$$

$$f_f \cong V_{fib} \cdot f_{fib} + (1 - V_{fib}) \cdot f_{mat}, \tag{2.2}$$

In addition to the quantities already introduced in Table 2-1, V_{fib} is the volumetric fraction of fibers (ratio between the volume of fibers and the overall volume of the composite), and E_{mat} and f_{mat} Young’s Modulus of elasticity and the tensile strength of the matrix, respectively.

The rule of mixtures is based on the hypothesis of a perfect bond between the fibers and matrix. For unidirectional composites, it provides an accurate assessment of the modulus of elasticity. The same accuracy cannot be obtained for ultimate strength.

(3) For proper definition of the modulus of elasticity and strength properties in a specific direction of FRP composites impregnated *in-situ*, the area of the dry fiber disposed perpendicular to that direction shall be used for computation. This is justified by the difficulty in calculating the volume percentage of the amount of resin installed.

For example, a unidirectional 100 mm wide fabric (fibers area: $A_{\text{fib}} = 70 \text{ mm}^2$) impregnated with variable quantities of resin is considered. The properties of each component are reported in Table 2-2. The importance of resin content on the mechanical properties in the direction of the fibers, calculated using Equations (2.1) and (2.2), is summarized in Table 2-3 and Figure 2-2.

Table 2-2 – Properties of components.

Fiber	Matrix
$E_{\text{fib}} = 220 \text{ GPa}$	$E_{\text{mat}} = 3 \text{ GPa}$
$f_{\text{fib}} = 4000 \text{ MPa}$	$f_{\text{mat}} = 80 \text{ MPa}$

Table 2-3 – Importance of fiber volumetric fraction, V_{fib} , on the FRP mechanical properties.

A_{fib} [mm ²]	A_{mat} [mm ²]	A_f [mm ²]	V_{fib} [%]	E_f [GPa]	f_f [MPa]	ϵ_{fu} [%]	F_{fu} [kN]	$E_f \cdot A_f$ [kN]
70	0	70	100	220.0	4000	1.81	280.0	15400
70	30	100	70	154.9	2824	1.82	282.4	15490
70	70	140	50	111.5	2040	1.83	285.6	15610

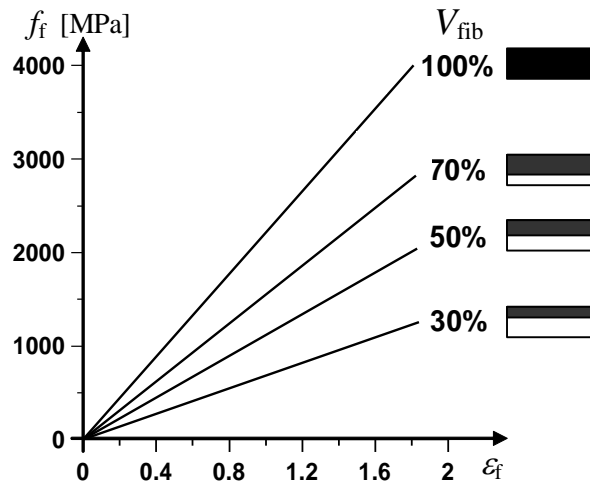


Figure 2-2 – Stress-strain relationship as a function of the volumetric fraction.

Table 2-3 and Figure 2-2 refer to values of V_{fib} between 30 % and 70 %. As a limit case, the volumetric fraction of fibers equal to 100% is also taken into consideration.

Table 2-3 shows how the mechanical properties of the composite (E_f and f_f) are dependent on the volumetric fraction, V_{fib} . Adversely, the ultimate tensile load, $F_{\text{fu}} = f_f \cdot A_f$, and axial stiffness, $E_f \cdot A_f$, present less variability (3-4%), and preferred due to the decreasing in values of E_f and f_f which are compensated by increasing the total cross sectional area of the impregnated fiber, A_f .

2.2.2 Pre-cured systems

(1) The mechanical properties of pre-cured systems, f_f and E_f , are computed using the following equations:

$$f_f = F_{fu} / A_f, \quad (2.3)$$

$$E_f = F_{fu} / (A_f \cdot \varepsilon_{fu}), \quad (2.4)$$

where F_{fu} and ε_{fu} are the experimentally determined ultimate load and deformation, respectively, and A_f , the cross sectional area of the pre-cured system.

(2) Pre-cured composites are characterized by a unidirectional fiber orientation that allows for the use of the rule of mixtures to determine the strength and stiffness of the composite. However, such values only represent an estimate (typically an overestimation) because other relevant parameters, such as adhesion properties between fibers and matrix, presence of manufacturing defects, voids, or fibers misalignment, are not considered. Reliable values of FRP mechanical properties shall be obtained with experimental testing to ensure determination of appropriate statistical parameters accounting for the adopted manufacturing process.

(3) Volumetric fractions usually vary between 50 and 70 %.

2.2.3 Wet lay-up systems

(1) In the case of wet lay-up systems, final thickness of the FRP laminate cannot be estimated in a deterministic fashion. Therefore, it is recommended to refer to both mechanical and geometrical properties of dry fabric according to the technical data sheets provided by the FRP manufacturer.

In the case of manual impregnation, it is recommended to limit the mass of texture present in a single layer of reinforcement to guarantee the grammage, or area density, will not overcome the value of 600 g/m² (Section 7.2.2.1). For higher levels of grammage it is recommended to verify that the impregnation is complete. In these cases it is also suggested to use mechanical systems of installation.

(2) It is not advised to use more than five layers.

2.2.3.1 Determination of A_{fib}

(1) For the laminate cross sectional area, A_{fib} , reference shall be made to the technical data sheet provided by the FRP manufacturer.

Laminate cross sectional area per unit width can be expressed as follows (Section 7.2.2.1)

$$A_{fib} = \frac{T_x \cdot N_f}{10^4 \cdot \rho_{fib}} \cdot b_f, \quad (2.5)$$

where T_x is the yarn count in the principal direction expressed in TEX [g/km], N_f is the number of yarns per unit width in the principal direction expressed in [n^o/cm], ρ_{fib} is the fiber density [g/cm³], and b_f is the width of the fiber [mm].

In case of fabrics with equal number of fibers in two orthogonal directions (balanced fabrics), the area of fabric in both directions can be computed by using the following equation:

$$A_{\text{fib}} = \frac{p_t}{2 \cdot \rho_{\text{fib}}} \cdot \frac{b_f}{10^3} \quad (2.6)$$

Where p_t is defined as the fabric mass per unit area, expressed in g/m^2 . For unidirectional fabric (2.6) the area may be evaluated as follows:

$$A_{\text{fib}} = \frac{p_t}{\rho_{\text{fib}}} \cdot \frac{b_f}{10^3} \quad (2.7)$$

However, for practical purposes limited to unidirectional or balanced fabrics, it is common to refer the area of fabric to the thickness of an equivalent plate made of only fiber, which can be obtained as follows:

$$t_f = \frac{A_{\text{fib}}}{b_f} \quad (2.8)$$

Table 2-4 summarizes the parameters deemed necessary for the determination of the laminate cross sectional area for three different fabrics: 1) unbalanced plain weave fabric (fabric A), 2) balanced plain weave fabric (fabric B), and 3) unidirectional fabric (fabric C).

Table 2-4

Property		Measurement unit	Fabric A	Fabric B	Fabric C
Fabric mass		g/m^2	187	286	304
Fiber density		g/cm^3	1.76	1.76	1.8
No. of yarns/cm	weft	no/cm	4	6	-
	warp	no/cm	8	6	3.8
Count	weft	Tex	67	200	-
	warp	Tex	200	200	800

In case of an unbalanced fabric (fabric A), Equation (2.5) yields:

$$A_{\text{fib}}^{\text{trama}} = \frac{67 [\text{Tex}] \cdot 4 [\text{fili/cm}]}{10^4 \cdot 1.76 [\text{g/cm}^3]} \cdot 100 [\text{mm}] = 1.52 \text{ mm}^2 \quad (\text{area resistente nella direzione della trama}),$$

$$A_{\text{fib}}^{\text{ordito}} = \frac{200 [\text{Tex}] \cdot 8 [\text{fili/cm}]}{10^4 \cdot 1.76 [\text{g/cm}^3]} \cdot 100 [\text{mm}] = 9.09 \text{ mm}^2 \quad (\text{area resistente nella direzione dell'ordito}).$$

For fabric B, the cross sectional area can be written as follows (both directions):

$$A_{\text{fib}} = \frac{200 [\text{Tex}] \cdot 6 [\text{fili/cm}]}{10^4 \cdot 1.76 [\text{g/cm}^3]} \cdot 100 [\text{mm}] = 6.82 \text{ mm}^2 ,$$

$$t_f = \frac{6.82 [\text{mm}^2]}{100 [\text{mm}]} = 0.068 \text{ mm} .$$

Alternatively, the same result can be obtained from Equation (2.6), as follows:

$$A_{\text{fib}} = \frac{240[\text{g/m}^2]}{2 \cdot 10^3 \cdot 1.76 [\text{g/cm}^3]} \cdot 100 [\text{mm}] = 6.82 \text{ mm}^2.$$

Finally, for fabric C, Equations (2.7) e (2.8), provide:

$$A_{\text{fib}} = \frac{304[\text{g/m}^2]}{10^3 \cdot 1.80[\text{g/cm}^3]} \cdot 100 [\text{mm}] = 16.89 \text{ mm}^2,$$

$$t_f = \frac{16.89[\text{mm}^2]}{100[\text{mm}]} = 0.17 \text{ mm}.$$

2.2.3.2 Mechanical characteristics of wet lay-up systems

(1) In this document, the wet lay-up systems are considered similar to an equivalent system of only dry fabric ($A_f = A_{\text{fib}}$). The mechanical proprieties of the impregnated composite, f_f and E_f , shall be evaluated by using the following equations:

$$f_f = F_{\text{fu}} / A_{\text{fib}}, \tag{2.9}$$

$$E_f = F_{\text{fu}} / (A_{\text{fib}} \cdot \varepsilon_{\text{fu}}). \tag{2.10}$$

For practical purposes, the thickness of wet lay-up systems, t_f , shall be computed in accordance with equation (2.8).

2.2.3.3 Comparison between characteristics of pre-cured and wet lay-up systems

Table 2-5 shows the mechanical proprieties of two systems: a wet lay-up with a unidirectional carbon fabric and a pre-cured carbon fiber laminate. The mechanical proprieties of these systems are evaluated by using the technical data sheet of each material. For design purpose some simplifications can be made (Table 2-6).

Table 2-5

System 1	System 2
Type: Unidirectional fabric CFRP and epoxy <i>Wet lay-up</i>	Type: Pre-cured laminate CFRP and epoxy resin <i>Pre-cured</i>
Mechanical properties*	Mechanical properties **
$t_f = 0.45 \text{ mm}$	$t_f = 1.2 \text{ mm}$
$f_f = 4200 \text{ N/mm}^2$	$f_f = 2800 \text{ N/mm}^2$
$\varepsilon_f = 1.8\%$	$\varepsilon_f = 1.7\%$
$E_f = 235000 \text{ N/mm}^2$	$E_f = 165000 \text{ N/mm}^2$

* Properties referred to the fiber itself (equations (2.9)(2.10))

** Properties referred to the total area of the system (equations (2.3)(2.4)).

Table 2-6

System 1	System 2
Type: Unidirectional fabric CFRP and epoxy <i>Wet lay-up</i>	Type: Pre-cured laminate CFRP and epoxy resin <i>Pre-cured</i>
1) Ultimate tensile load by unit width	1) Ultimate tensile load by unit width
$f_f \cdot t_f = 1890 \text{ N/mm}$	$f_f \cdot t_f = 3360 \text{ N/mm}$

2) Modulus of elasticity by unit width

$$E_f \cdot t_f = 105750 \text{ N/mm}$$

2) Modulus of elasticity by unit width

$$E_f \cdot t_f = 198000 \text{ N/mm}$$

3a) Comparison of ultimate tensile loads

$$\frac{f_f^{(2)} \cdot t_f^{(2)}}{f_f^{(1)} \cdot t_f^{(1)}} = 1.77$$

3b) Comparison of moduli of elasticity

$$\frac{E_f^{(2)} \cdot t_f^{(2)}}{E_f^{(1)} \cdot t_f^{(1)}} = 1.87$$

Two layers of the unidirectional fabric (System 1) are necessary to generate an equivalent stress and stiffness of the pre-cured laminate (System 2).

2.2.4 Pre-impregnated systems

(1) Pre-impregnated (*prepreg*) systems are impregnated directly at the manufacturer plant and delivered in rolls. Resin may receive pre-polymerization treatments. A pre-impregnated system is a thin sheet (0.15 mm typical thickness), flexible and moderately sticky, with a detaching film (silicon paper or similar) applied on the surface to preserve the system from external contamination. Proper storing shall be performed under controlled moisture and temperature conditions and system cross-linking shall occur at the time of application by means of thermal treatments.

2.3 QUALITY CONTROL

As of today, FRP classification and acceptance criteria for strengthening applications are not covered by the European codes.

Information can be found in the Italian document “*Guide for the qualification and acceptance criteria of fiber-reinforced composites for strengthening of existing structures*”, currently under review.

2.3.1 Tasks and responsibilities of professionals

(1) This section addresses the responsibility of manufacturers, designers, contractors, etc. As stated in the Guideline of “Consiglio Superiore dei Lavori Pubblici” (Supreme Council responsible for overseeing public works), the term *Supplier* is attributed to different qualified individuals. In the case of pre-cured reinforcement systems, the term supplier refers to persons who, having purchased pre-cured systems by qualified manufactures, are eligible to re-introduce them into the market with their own brand or logo without any further processing. The supplier also refers to individuals who have been authorized to sell complete systems made of specific resins and fibers.

Designer:

- Shall clearly state the quality and characteristics of the strengthening system.
- Depending on the importance and extent of the applications, designers shall inform the construction manager on the need for quality control tests for debonding, as reported in Chapter 6.

Contractor/subcontractors:

- Shall be qualified for the application of composite materials to concrete and masonry structures. Qualifications shall be demonstrated through documentation of previous experiences. In particular, the personnel responsible for the installation shall have a specific and qualified ability in the application of FRP strengthening systems for structural purposes.
- Shall make sure that the products comply with the provisions indicated by the designer. If the material and corresponding indicated requirements is not available, then agreement upon

viable alternatives shall be made with the designer or the construction manager.

Construction manager:

- Shall make decisions regarding the acceptance of products.
- Shall check the compliance of the material with the designer's provisions.
- Shall check the origin of the supplied material.
- Shall check the mechanical and physical characteristics of products using the test certificates provided by the manufacturer.
- Based on the importance of the application, the construction manager may request experimental tests to evaluate both the quality of materials and compliance with the values provided by the manufacturer or supplier. Such tests shall be carried out in laboratories of proven experience and appropriately equipped to characterize FRP materials.
- Based on the importance of the application, the construction manager may request the performance of specific test to characterize the debonding with regard to the design requirements.

Inspector:

If the FRP strengthened structure has to be tested, the inspector shall:

- check the quality of the materials is in compliance with the manufacturer specifications.
- verify that all materials used have been accepted by the construction manager.
- check the results of experimental tests required by the construction manager and determine if further are required.

2.4 TRANSPORTATION, STORAGE, PRESERVATION, HANDLING AND USE

(1) Proper transportation, storage, preservation, handling and use of FRP material to ensure that properties of each components are not altered and are compliance with safety laws and meet regulations.

- Transportation: Each component of the selected FRP system shall be suitably packaged and transported according to safety laws and regulations.
- Storage: To preserve the properties of FRP material and ensure compliance with safety laws and regulations, FRP material shall be stored according to the recommendations provided by the supplier/manufacturer.

To preserve the properties of fibers and resins, storage shall be performed under suitable temperature conditions (suggested range is 10-24 °C), in a dry environment (moisture less than 20%), unless otherwise suggested by the manufacturer/supplier.

Laminate and other preformed material may be damaged due to bending or improper stacking.

Due to safety reasons, some constituents such as reactive reticulating agents, initiators, catalysts, solvents for surface cleaning, etc., shall be stored according to manufacturer/supplier requirements or official standards. Catalysts and initiators (typically peroxides) shall be stored separately from other reagents to avoid any accidental contact leading to premature polymerization.

- Preservation: The properties of non-polymerized resins can change over time and are affected by moisture and temperature conditions. The latter can also affect the mixture reactivity and properties of the polymerized resin. Manufacturers shall indicate the storage time (shelf life) that ensures the properties of thermo-setting resins are adequately maintained. Constituents exceeding their shelf time, or suffering degradation or contamination, shall not be used. All constituents deemed unusable shall be disposed of according to the manufacturer specifications as well as the provisions of safety laws and regulations.

- Handling: The manufacturer shall provide a technical data sheet reporting all information relevant to safety (MSDS – *Materials Safety Data Sheet*) for all the constituents of FRP material).
- Use: Substances used in combination with thermoset resins are typically hardeners, cross-linkers, initiators (peroxides), and fillers. Some potential dangers using thermoset resins include:
 - Skin irritation and sensitization.
 - Inhalation of vapors of solvents, diluents, and monomers.
 - Fire or blast risk due to large concentrations of flammable substances in the air or contact with flames or sparks (including cigarettes).
 - Exothermic reactions between reagents that may cause fire or harm to the personnel involved.
 - Presence of dust from working or handling FRP material.

Therefore, it is necessary to adopt precautions when working with such products or with their constituents.

Potential risks associated with their use requires that all operators read the labels and MSDS carefully in order to mitigate possible hazards.

For handling of fibers or resins, the use of disposable gloves, work-suits, and protection glasses is recommended. Rubber or plastic gloves shall be solvent-resistant. In the presence of fiber fragments, dusts or solvent vapors, or when mixing and applying resins, respiratory protection devices are required, as specified by FRP manufacturers/suppliers. The working site shall always be properly ventilated.

3 BASIS OF DESIGN FOR FRP STRENGTHENING

(1) This chapter discusses the FRP strengthening of existing reinforced and prestressed structures as well as masonry structures for which building code requirements are not met.

The same principles also apply to existing structures comprised of steel and timber, not included in this document.

(2)P The following assumption are made:

- The choice and the design of the strengthening system are made by a qualified and experienced engineer.
- The installation phase is carried out by personnel having the appropriate skills and experience.
- Proper supervision and quality control is provided during installation.
- Construction materials are identifiable, qualified, traceable and accepted on the work site.

(3) The FRP strengthening system shall be designed to have appropriate strength, and meet serviceability, durability and strength requirements. In case of fire, the strength of the selected FRP system shall be adequate for the required period of time.

(4) The FRP strengthening system shall be located in areas where tensile stresses are to be occur. The FRP strengthening system shall not carry compression stresses, unless well confined (within the strengthened members) or pre-cured systems adequately provide axial and flexional stiffness.

3.1 BASIC REQUIREMENTS

(1)P Design of FRP strengthening system shall be performed in compliance with the following principles:

- The risks to which the structure can be subjected shall be accurately identified, removed or mitigated;
- The strengthening configuration shall not be very sensitive to the above risks and capable of withstanding to acceptable localized damages;
- Strengthening systems shall eliminate or postpone brittle failures proceeding to the installation of the strengthening system itself.

(2)P The above-defined basic requirements can be considered met if the following are satisfied:

- materials are chosen based on the indication of Chapter 2;
- design, installation and inspection of the strengthening material are in compliance to the requirements of this and the following Chapters.

(3)P If FRP strengthening concerns structures of historical and monumental interest, a critical evaluation of the strengthening technique is required with respect to the standards for preservation and restoration, according to the Guide of the President of the Italian Cabinet “Presidente del Consiglio dei Ministri” released on 12/10/2007 (GU n. 24 del 29/01/2008).

The actual effectiveness of the strengthening technique shall be objectively proven, and the adopted solution shall guarantee compatibility (physical-chemical and mechanical), durability, and reversibility.

3.2 DURABILITY REQUIREMENTS

(1)P Design of the strengthening system shall ensure the durability of the system, and effectiveness for the entire service life of the strengthened structure also in relationship to the expected degradation.

(2) To ensure durability of the FRP strengthened members the following shall be taken into account:

- Intended use of the strengthened structure.
- Expected environmental conditions and load application process.
- Composition, properties, and performance of the existing structure and FRP materials along with the products used for their installation.
- Choice of the strengthening system, its configuration, and construction details.
- Quality of workmanship and the level of control.
- Particular protective measures (*e.g.*, fire, humidity or impact).
- Intended maintenance program during the service life of the strengthened structure.

(3) Special design problems (regarding environmental issues, loading, etc.) shall be identified at the design stage to evaluate their relevance from a durability point of view, assign proper values of the conversion factors (§ 3.5), and take the necessary provisions for protection of the adopted FRP system.

(4) When conversion factors for a particular FRP system are not available, any possible reason of degradation of the adopted strengthening configuration shall be accurately estimated. Such estimation can be accomplished through theoretical models, experimental investigations, experience in previous applications, or any combination of the above.

3.3 GENERAL PRINCIPLES OF THE STRENGTHENING DESIGN

3.3.1 Introduction

(1)P Design with FRP composites shall be carried out both in terms of serviceability limit state (SLS) and ultimate limit state (ULS), as defined by the current building code.

(2)P Structures and structural members strengthened with FRP shall be designed for a design strength, R_d , at all sections at least equal to the required strength, E_d , calculated for the factored load and forces in such combinations as stipulated in the current building code. The following equation shall be met:

$$E_d \leq R_d, \quad (3.1)$$

(3) The design values are obtained from the characteristic values through different appropriate partial factors for each limit state as indicated in the current building code. Specific partial factors for FRP materials are indicated in this document.

3.3.2 Service life and design load

(1)P When designing FRP strengthened members, the service life of the structure shall be in compliance with the requirements of the current building code. Therefore, the same partial factors for existing materials and the same design loads prescribed by the current building code for new constructions shall be adopted.

3.3.3 Properties of FRP materials and related design load

- (1)P The properties of FRP materials to be used for strengthening existing structures shall be determined in accordance with the indications of Chapter 2.
- (2)P Properties of the existing materials in the structure to be strengthened shall be obtained from on-site or laboratory tests and, when available, from any additional source of information (original documents of the project, further documentation obtained subsequently, etc.).
- (3) Characteristic (5%) values shall be used to compute the ultimate strength and ultimate deformation of the FRP materials. The average values shall be used to compute the mechanical properties of existing materials.
- (4) The average value shall be used to compute the modulus of elasticity of FRP and preexistent materials.
- (5) For the generic property of a FRP material, the design value, X_d , can be expressed as follows:

$$X_d = \eta \cdot \frac{X_k}{\gamma_m} \quad (3.2)$$

where η , is a conversion factor accounting for special design problems (Section 3.5), X_k is the characteristic value of the property being considered, and γ_m is the partial factor of the material that takes into account the type of application (Section 3.4).

If both the environmental and serviceability limit state factors are used, the conversion factor η is obtained as product of the environmental factor (Section 3.5.1), η_a , and the serviceability limit state factor (Section 3.5.2), η_l . In case of ultimate limit state, the conversion factor η is equal to η_a (Section 3.5.1).

- (6) The value of the generic property of a preexisting material, X_d , is obtained by the ratio between the average value of the property, X_m , and a calibrated factor of confidence, FC, related to the level of knowledge. If required by the applicable code, this ratio is divided by the material safety factor.

3.3.4 Design capacity

- (1) The design strength, R_d , can be expressed as follows:

$$R_d = \frac{1}{\gamma_{Rd}} \cdot R\{X_{d,i}; a_{d,i}\} \quad (3.3)$$

In Equation (3.3), $R\{\}$ is a suitable function for the specific type of force effect being considered (e.g., flexure, shear, etc.), and γ_{Rd} is a partial factor accounting for uncertainties in the assumed model. The variables in the function $R\{\}$ are typically the design values of the materials, $X_{d,i}$, used for strengthening or the existing materials. The nominal values of the geometrical parameters, $a_{d,i}$, involved in the model are also considered.

(2) As a rule, the FRP contribution to the strengthened member can not increase the structural capacity more than 50% of that of the unstrengthen member. Such limitation does not apply to exceptional or seismic loads.

3.4 PARTIAL FACTORS

3.4.1 Partial factor γ_m for FRP

(1) For the ultimate limit state, the value assigned to the partial factor of FRP materials $\gamma_m = \gamma_f$ is equal to 1.10. Only when debonding occurs in the case of limit state, the values of $\gamma_m = \gamma_{f,d}$ can be chosen by the designer in a range between 1.20 to 1.50, depending on the higher or lower probability of failure due to debonding. In this case, tests performed on the specific application by the manufacturer/supplier can help optimize the design process.

(2) For the serviceability limit state, values of $\gamma_m = \gamma_f$ can be equal to 1.

3.4.2 Partial factors γ_{Rd} for resistance models

(1) For ULS, values to be assigned to the partial factors γ_{Rd} are reported in Table 3-1.

Table 3-1 – Partial factors γ_{Rd} .

Resistance model	γ_{Rd}
Bending/Combined Bending and Axial Load	1.00
Shear/Torsion	1.20
Confinement	1.10

3.5 SPECIAL DESIGN PROBLEMS AND RELEVANT CONVERSION FACTORS

(1) Hereafter, some reference values to be assigned to the conversion factor, η , (Section 3.3.3(5)) that affects both durability and behavior of FRP materials are reported.

3.5.1 Environmental factors

(1)P Mechanical properties of FRP systems (*e.g.*, tensile strength, ultimate strain, and Young’s modulus of elasticity) degrade under specific ageing conditions such as alkaline environment, moisture (water and chloride solutions), extreme temperatures, thermal cycles, freeze and thaw cycles, and ultraviolet radiations (UV).

(2) Effects of alkaline environment: In some circumstances the alkaline solution present in porous concrete may cause degradation of the resin and/or the interface between FRP and the substrate. Epoxy resins are generally characterized by excellent durability against alkaline environment, separate from the polyurethane resins normally used for internal reinforcement bars. Therefore, vinylester based resins preferred. If glass fibers with high content of zirconia are used, the FRP system might result in a lower strength compared to the GFRP traditionally used for structural application. Damage of the resin due to alkaline environment is typically more dangerous than that due to moisture. The resin shall complete its curing process before being exposed to alkaline environment.

(3) Effects of moisture (water and chloride solutions). The main effects of moisture absorption

concern the resin; and can be summarized as follows: plasticization, reduction of glass transition temperature, and strength and stiffness (the latter less significant). Moisture absorption depends on the type of resin, thickness, curing conditions, resin-fiber interface, working conditions, composition and quality of the laminate.

(4) Effects of extreme temperatures and thermal cycles. The primary effects of temperature concern the viscous response of both the resin and the composite. As the temperature rises, Young modulus of elasticity of the resin decreases. If the temperature exceeds the glass transition temperature, the performance of FRP materials significantly decreases. In general, thermal cycles do not have harmful effects on FRP, however they may cause micro-fractures in systems with high modulus resins. For standard temperatures in civil infrastructures, undesired performance can be avoided by choosing a system where the glass transition temperature is always higher than the maximum service temperature of the structure or component being strengthened. The use of FRP in the presence of service temperatures higher than the glass transition temperature minus 15° C is not recommended. As a precaution, special protection systems shall be designed in order to provide thermal isolation to the FRP system.

(5) Effects of freeze and thaw cycles. In general, exposure to freeze and thaw cycles does not have an impact on FRP performance, but decreases the performance of the resin as well as the fiber-resin interface. For temperatures below 0 °C, performance of polymeric-based resin systems may improve by developing higher strength and stiffness. The effects of the degradation induced by freeze and thaw cycles may be magnified by the presence of moisture.

(6) Effects of ultraviolet radiations (UV). Ultraviolet radiations rarely degrade the mechanical performance of FRP-based systems, but may cause some resins to have a certain degree of brittleness and surface erosion. In general, the most harmful effect linked to UV exposure is the penetration of moisture and other aggressive agents through the damaged surface. FRP-based systems may be protected from such damages by adding fillers to the resin or by providing appropriate coatings.

(7) Table 3-2 summarizes the values to assign to the environmental conversion factor η_a depending upon fiber/resin type and exposure conditions. The reported values are precautionary estimations. Designer shall use these values when more information on test evidence for the material in use and expected environmental condition are missing.

Values as reported in the table may be increased by 10 % (however, $\eta_a \leq 1$ shall always be satisfied) whenever protective coatings are used. Such coatings need to be maintained on the strengthened structure for its entire life and be experimentally tested and proven effective in protecting the FRP system from environmental exposure.

Table 3-2– Environmental conversion factor η_a for different exposure conditions or FRP systems.

Exposure conditions	Type of fiber/resin	η_a
Internal	Glass/Epoxy	0.75
	Aramid/Epoxy	0.85
	Carbon/Epoxy	0.95
External	Glass/Epoxy	0.65
	Aramid/Epoxy	0.75
	Carbon/Epoxy	0.85
Aggressive environment	Glass/Epoxy	0.50
	Aramid/Epoxy	0.70
	Carbon/Epoxy	0.85

3.5.2 Load condition and conversion factors for long-term effects

- (1)P Mechanical properties (*e.g.*, tensile strength, ultimate strain, and Young modulus of elasticity) of FRP-based systems experience degradation as a result of creep, relaxation, and fatigue.
- (2) Effects of creep and relaxation. For FRP-based systems, creep and relaxation depend on the properties of both the resins and fibers. Typically, thermosetting resins (unsaturated polyesters, vinyl esters, epoxy, and phenolic resins) are less viscous than thermo-plastic resins (polypropylenes, nylon, polycarbonates, etc.). Since the presence of fibers reduces the resin creep, such phenomena are more distinct when the load is applied transversely to the fibers or when the composite has a low volume ratio of fibers. Creep may be reduced by ensuring low serviceability stresses. CFRP, AFRP, and GFRP systems are respectively the least, moderately, and most prone to creep rupture.
- (3) Fatigue effects. The performance of FRP systems under fatigue conditions needs to be considered as well. Such performance depends on the matrix composition and, moderately, on the type of fiber. In particular, the type of fiber can oppose to the formation and propagation of cracks.
- (4) To avoid failure of FRP strengthened members under continuous stress or cyclic loading, the stress level in service can be limited by reducing the design values and using a conversion factor, η_1 , whose values are reported in Table 3-3.

Table 3-3 – Conversion factor for long-term effects η_1 for several FRP systems at SLS.

Loading mode	Type of fiber/resin	η_1
Continuous (creep and relaxation)	Glass/Epoxy	0.30
	Aramid/Epoxy	0.50
	Carbon/Epoxy	0.80
Cyclic (fatigue)	All	0.50

3.5.3 Impact and explosive loading

- (1) Laboratory and on-site tests on structures subjected to explosive loads have shown a better behavior with the AFRP system in comparison to the CFRP and GFRP systems. Test on full-scale buildings have demonstrated the technique of alternating layers of AFRP characterized by different modulus of elasticity and impregnated with epoxy matrix. Layers of the elastomeric resin (polyuria) allow the dissipation of energy generated from the impact or explosion, while containing the deflagration and preventing the penetration of debris within the structures.

3.5.4 Vandalism

- (1)P FRP composite materials are particularly sensitive to cuts and incisions produced by cutting tools.
- (2) If FRP materials are installed on members located in areas with public access, particular protection systems need to be considered to prevent damages of the FRP system due to act of vandalism. The safety of the structural member shall be checked, assuming that the FRP system is no longer in place. The ULS shall be verified using *quasi-permanent loads* with material partial factors of *exceptional loading*.

3.6 STRENGTHENING LIMITATIONS IN CASE OF FIRE

- (1)P FRP materials are particularly sensitive to high temperatures that may occur during a fire. When the room temperature exceeds the glass transition temperature of the resin (or the melting

temperature in the case of semi-crystalline materials), both strength and stiffness of the installed FRP system are reduced. In case of applied FRP as external reinforcement to concrete or masonry members, exposure to high temperatures produces an accelerated degradation of the bond between the FRP system and the substrate. As a result, debonding of FRP composite may take place as well as degradation of the effectiveness of strengthening.

(2) With regard to fire exposure, the mechanical properties of FRP strengthened members may be improved by the use of adequate layers of protective coatings. It is suggested to employ a coating capable of reducing the spreading of flames as well as the production of smoke. It is also recommended to employ a protective coating system having official certificates. Further specifications regarding the application of protective coating systems are reported in Sections 4.8.2.3 and 5.8.2.3.

(3) In the case of fire, the strengthened structures shall be complied with the situations listed below, in which the symbol E_d indicates the effect of indirect thermal loading:

- Exceptional loading with FRP strengthening still in place: $E_d \neq 0$ when the strengthening system has been designed to withstand fire exposure. Applied loads shall be considered for the SLS and load factors in compliance with exceptional loading conditions. In this case, all loads acting on the structure for the various combinations are to be considered. The member capacity, which is reduced to take into account the duration of fire exposure, shall be computed using the partial factors corresponding to exceptional situations, indicated by the current building code.
- Given a situation following an exceptional event: $E_d = 0$ when the strengthening system is no longer in place. Applied loads need to be considered for quasi-permanent loading conditions. The member capacity, which is reduced to take into account the duration of fire exposure, shall be computed as stated in the previous item.

4 STRENGTHENING OF REINFORCED AND PRESTRESSED CONCRETE STRUCTURE

4.1 DEBONDING MECHANISMS

4.1.1 Failure mechanisms due to debonding

(1)P When strengthening reinforced concrete members with FRP composites, the role of the bond between the concrete and FRP is of great relevance due to the brittle failure mechanism associated with debonding (loss of adhesion). According to the capacity design criteria, failure due to debonding shall not precede flexural or shear failure of the strengthened member.

(2)P The loss of adhesion between FRP and concrete may concern both the laminates or sheets applied to reinforced concrete beams for flexural and/or shear strengthening. As shown in Figure 4-1, debonding may take place within the adhesive, between the concrete and the adhesive, in the concrete itself, or within the FRP reinforcement (e.g. at the interface between two adjacent layers bonded each other). When proper installation is performed, the adhesive strength is typically much higher than the concrete tensile strength, therefore failure occurs within the concrete itself in the form of removal of a layer of material (thickness may range from few millimeters to the whole concrete cover).

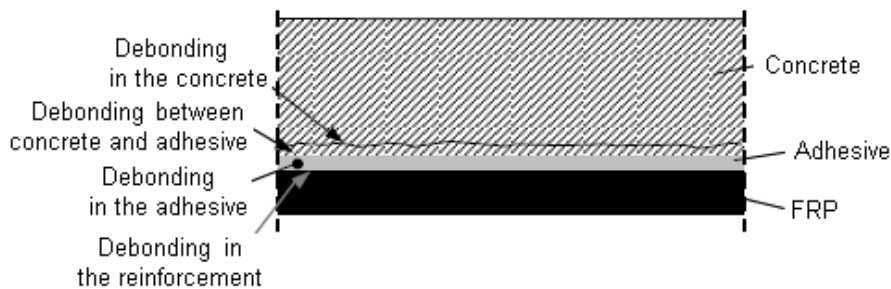


Figure 4-1 – Debonding between FRP and concrete.

(3)P Debonding failure modes for flexural strengthening are schematically represented in, Figure 4-2 and may be classified in the following four categories.

- Mode 1 (Laminate/sheet end debonding)
- Mode 2 (Intermediate debonding, caused by flexural cracks)
- Mode 3 (Debonding caused by diagonal shear cracks)
- Mode 4 (Debonding caused by irregularities and roughness of concrete surface)

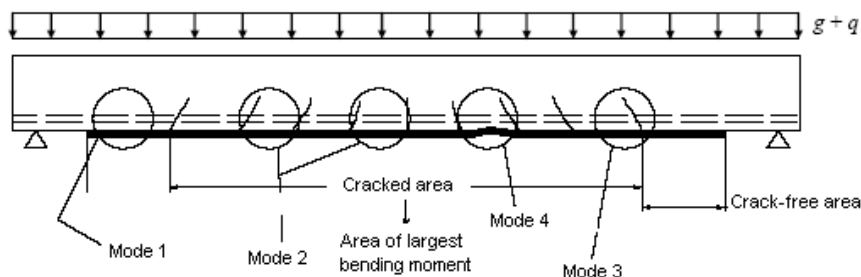


Figure 4-2 – FRP flexural strengthening: debonding failure modes.

(4) The following section discusses only Modes 1 and 2, since they are the most frequent in ordinary situations. To mitigate the risk of the remaining failure modes, recommendations reported in this document for both support control and preparation (Section 4.8), can be followed.

(5) Further details on debonding and design criteria for failure modes 1 and 2 are provided in Appendix D.

4.1.2 Fracture energy

(1)P Before designing for flexural and shear, the evaluation of the maximum force transferred from the concrete to the FRP, as well as the evaluation of shear and normal stresses at the concrete-FRP interface, is required. The former is necessary when designing for ULS and the latter when designing for SLS.

(2)P Figure 4-3 represents a typical bond test. The ultimate value of the force transferred to the FRP system before debonding depends on the length, l_b , of the bonded area. The optimal bond length, l_e , is defined as the length, if exceeded, having no increase in the force transferred between concrete and FRP.

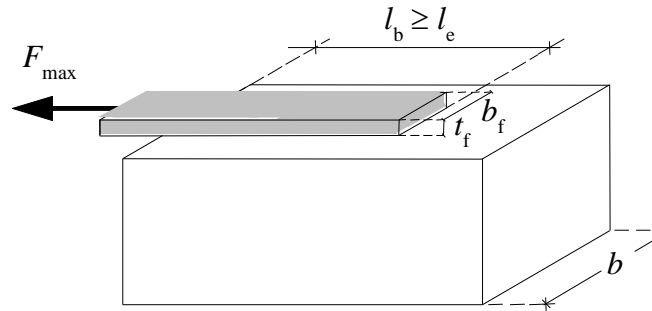


Figure 4-3 – Maximum force transferred between FRP and concrete.

(3) The optimal bond length, l_{ed} , may be estimated as follows:

$$l_{ed} = \max \left\{ \frac{1}{\gamma_{Rd} \cdot f_{bd}} \sqrt{\frac{\pi^2 \cdot E_f \cdot t_f \cdot \Gamma_{Fd}}{2}}, 200 \text{ mm} \right\}, \quad (4.1)$$

where:

- E_f and t_f are the modulus of elasticity in the direction of force and the thickness of the FRP, respectively;
- Γ_{Fd} is the design value of the specific fracture energy;
- $f_{bd} = \frac{2 \cdot \Gamma_{Fd}}{s_u}$, with $s_u = 0.25 \text{ mm}$ is the design bond strength between FRP and concrete (further details can be found in Appendix C);
- $\gamma_{Rd} = 1.25$ is a corrective factor.

The design fracture energy is computed as follow:

$$\Gamma_{Fd} = \frac{k_b \cdot k_G}{FC} \cdot \sqrt{f_{cm} \cdot f_{ctm}} \quad (4.2)$$

where:

- f_{cm} e f_{ctm} are the mean values of the concrete compressive and tensile strengths, respectively, evaluated on-site. If experimental data is not available, the average concrete tensile strength can be computed using f_{cm} in accordance with the Building code specification.
- FC is the confidence factor;
- k_b is the geometrical corrective factor and function of the ratio between the FRP and concrete width, b_f/b . k_b is defined with the following equation:

$$k_b = \sqrt{\frac{2 - b_f/b}{1 + b_f/b}} \geq 1, \quad (4.3)$$

with value of $b_f/b \geq 0.25$ (if $b_f/b < 0.25$, k_b is equal to 1.18).

- k_G is an additional corrective factor calibrated from experimental results and equal to 0.023 mm or 0.037 mm for pre-cured and wet lay-up systems, respectively.

When FRP is used for the flexural strengthening of slab elements and applied using different sheets placed side by side, each having a width equal to b_f , k_b can be computed by equation (4.3) assuming the width b is the center to center distance between two sheets.

4.1.3 Ultimate design strength for laminate/sheet end debonding (mode 1)

(1) For laminate/sheet end debonding, the provided bond length is equal to or larger than the optimal bond length. The ultimate design strength, f_{idd} , is defined as the maximum allowed strength before debonding of the ends (Figure 4-3) and can be calculated as follows::

$$f_{idd} = \frac{1}{\gamma_{f,d}} \cdot \sqrt{\frac{2 \cdot E_f \cdot \Gamma_{Fd}}{t_f}}, \quad (4.4)$$

where $\gamma_{f,d}$ is the partial factor indicated in Section 3.4.1 and Γ_{Fd} is the fracture energy indicated in (4.2), respectively.

(2) For a bond length (l_b) shorter than the design optimal bond length (l_{ed}), the ultimate design strength shall be reduced according to the following equation:

$$f_{idd,rid} = f_{idd} \cdot \frac{l_b}{l_{ed}} \cdot \left(2 - \frac{l_b}{l_{ed}} \right). \quad (4.5)$$

(3) When special anchoring devices are used (FRP transverse bars, U-wrap with FRP sheets, etc.), the maximum load F_{max} (Figure 4-3) must be directly evaluated with ad-hoc experimental tests in order to use higher values of f_{idd} in comparison to the value computed by using equations (4.4) e (4.5).

4.1.4 Ultimate design strength for intermediate debonding (mode 2)

(1)P To prevent failure from intermediate debonding mechanism, the stress variation $\Delta\sigma_f$, in the FRP system between two subsequent cracks should not exceed the limit $\Delta\sigma_R$. The latter value typically depends on the bond characteristics between the concrete and FRP (see Appendix D), the distance between transverse cracks in the concrete, and the level of stress, σ_f , in the FRP reinforcement.

(2) Alternatively, a simplified procedure may be used. The maximum strength calculated in the FRP system at ULS shall be less than $f_{idd,2}$ computed as follows:

$$f_{idd,2} = \frac{k_q}{\gamma_{f,d}} \cdot \sqrt{\frac{E_f}{t_f} \cdot \frac{2 \cdot k_b \cdot k_{G,2}}{FC} \cdot \sqrt{f_{ctm} \cdot f_{ctm}}}, \quad (4.6)$$

where, $k_{G,2}$ is a corrective factor calibrated on experimental results and equal to 0.10 mm irrespective of the type of reinforcement, k_q is a coefficient that considers load distributions and is equal to 1.25 for distributed loads and 1.0 for all other load configurations.

Consequently, the maximum design strain value is:

$$\varepsilon_{idd} = \frac{f_{idd,2}}{E_f} \geq \varepsilon_{sy} - \varepsilon_0, \quad (4.7)$$

where ε_{sy} is the design yield strain of steel reinforcement, computed by using the average divided the factor of confidence FC (Section 3.3.3(6)), and ε_0 is the maximum tensile strain present before the FRP is applied and is computed in accordance to Section 4.2.2.2.

4.1.5 Interfacial stress for serviceability limit state

(1)P For FRP-strengthened beams, stress concentrations (shear and normal stresses) occur at the concrete and FRP interface close to transverse cracks in the concrete or at the ends of FRP reinforcement. Stress concentrations may cause cracking at the interface.

(2) Under service conditions, interfacial cracks should be avoided, especially when the strengthened member could be subject to fatigue and freeze/thaw cycles. For the analysis, a linear elastic behavior for both concrete and steel can be considered.

(3) For rare or frequent loading conditions, the “equivalent” shear stress, $\tau_{b,e}$, at the adhesive-concrete interface, shall be smaller than the design bond strength, f_{bd} , between the FRP reinforcement and concrete according to the following equation:

$$\tau_{b,e} \leq f_{bd}. \quad (4.8)$$

(4) The design bond value between FRP and concrete, f_{bd} , is a function of the characteristic tensile strength of the concrete, f_{ctm} , as follows:

$$f_{bd} = 0.21 \cdot \frac{k_b}{\gamma_b} \cdot \frac{f_{ctm}}{FC}, \quad (4.9)$$

where γ_b is equal to 1.0 for rare loading conditions or 1.2 for frequent loading conditions, whereas

k_b can be obtained from Equation (4.3).

(5) The “equivalent” shear stress, $\tau_{b,e}$, is defined as follows:

$$\tau_{b,e} = k_{id} \cdot \tau_m \quad (4.10)$$

where k_{id} represents a coefficient (≥ 1), accounting for shear and normal stress close to the anchorage ends (Appendix D):

$$k_{id} = \left(k_\sigma^{1.5} + 1.15 \cdot k_\tau^{1.5} \right)^{2/3}, \quad (4.11)$$

where:

- $k_\sigma = k_\tau \cdot \beta \cdot t_f$,
- $k_\tau = 1 + \alpha \cdot a \cdot \frac{M_{(z=a)}}{V_{(z=a)} \cdot a}$,
- $M_{(z=a)}$ is the flexure moment acting on the section where FRP strengthening ends (Figure 4-4),
- $V_{(z=a)}$ is the shear force acting on the section where FRP strengthening ends,
- $\alpha = \sqrt{\frac{K_1}{E_f \cdot t_f}}$,
- $\beta = \left(\frac{b_f \cdot 2.30 \cdot K_1}{4 \cdot E_f \cdot I_f} \right)^{1/4}$,
- $K_1 = \frac{1}{t_a/G_a + t_c/G_c}$,
- G_a and G_c are the adhesive and concrete shear modulus, respectively,
- t_a is the nominal thickness of the adhesive,
- t_c is the effective thickness of the concrete (typical values for t_c are 20 ÷ 30 mm).

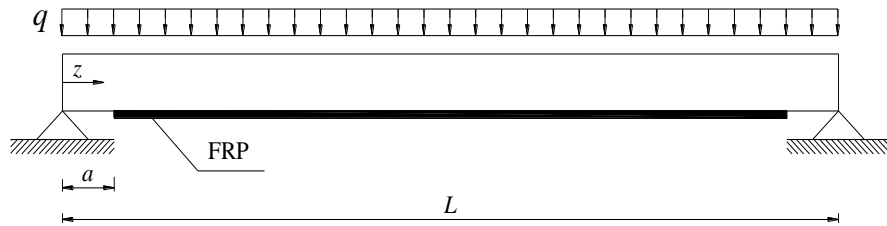


Figure 4-4 – Definition of beam geometrical parameters.

- τ_m is the average shear stress according to the Jourawski theory:

$$\tau_m = \frac{V_{(z=a)} \cdot t_f \cdot (h - x)}{I_c / n_f}, \quad (4.12)$$

- h is the height of the section,

- x is the distance from the extreme compression fiber to the neutral axis,
- I_c is the moment of inertia of the transformed section,
- E_c is the Young modulus of elasticity for the concrete,
- $n_f = E_f/E_c$ is the modular ratio corresponding to the considered load combination (rare or frequent).

(5) If end anchorage is provided using a U-wrap, the normal stress effects can be neglected and the coefficient k_σ can be assumed equal to zero.

(6) When computing anchorage stress at the SLS, reference can be made to the stress corresponding to the increased load following the application of FRP reinforcement.

4.2 FLEXURAL STRENGTHENING

4.2.1 Introduction

(1)P Flexural strengthening is necessary for structural members subjected to a bending moment larger than the corresponding flexural capacity. Only the case of uniaxial bending (*e.g.*, when the moment axis coincides with a principal axis of inertia of the cross-section, in particular a symmetry axis) is addressed.

(2) Flexural strengthening with FRP materials may be done by applying one or more laminates or one or more sheets to the tension side of the member to be strengthened.

4.2.2 Analysis at ultimate limit state

4.2.2.1 Introduction

(1)P Flexural design at the ULS of FRP strengthened members requires that both the flexural capacity, M_{Rd} , and factored ultimate moment, M_{Sd} , satisfy the following equation:

$$M_{Sd} \leq M_{Rd} . \quad (4.13)$$

(2)P ULS analysis of RC members strengthened with FRP relies on the following fundamental assumptions:

- Plane sections remain plane.
- Perfect bond exists between FRP and concrete, and steel and concrete.
- Concrete does not carry tension.
- Constitutive laws for concrete and steel are accounted for according to the current building code.
- FRP is considered to be a linear-elastic material up until failure.

(3) FRP strengthening is effective for low steel reinforcement ratios. The rules hereafter reported refer exclusively to this situation.

(4) It is assumed that flexural failure occurs when one of the following conditions is met:

- The maximum concrete compressive strain, ε_{cu} , as defined by the current building code is reached.
- The maximum FRP tensile strain, ε_{fd} , is reached and is calculated as follows:

$$\varepsilon_{fd} = \min \left\{ \eta_a \cdot \frac{\varepsilon_{fk}}{\gamma_f}, \varepsilon_{fdd} \right\}, \quad (4.14)$$

where ε_{fk} is the characteristic strain at failure of the adopted strengthening system, γ_f and η_a are the coefficients defined in Section 3.4.1 (1) and in Table 3-2 of Section 3.5.1, respectively, ε_{fdd} is the maximum strain due to intermediate debonding as defined in (4.7) (generally the minimum value in Equation (4.14) corresponds to ε_{fdd}).

- (5) The shear capacity of the strengthened member shall be larger than the shear demand corresponding to the examined case. If deemed necessary, shear capacity shall be increased according to the provisions of Section 4.3.

4.2.2.2 Strain in the structure prior to FRP strengthening

(1)P Strain in the structure prior to FRP strengthening shall be considered when the FRP is applied.

(2) When the applied moment due to the existing load, M_0 , is smaller than the cracking moment, the strain in the structure prior to strengthening can be neglected.

(3)P Strain in the structure prior to the installation of FRP can be computed assuming the elastic behavior of concrete and steel and, assuming that the concrete does not carry tension.

4.2.2.3 Flexural capacity of FRP-strengthened members

(1)P Member flexural capacity is analyzed in Section 4.2.2.1. The flexural analysis of FRP strengthened members can be performed by using strain compatibility and force equilibrium methods. The stress at any point in the member must correspond to the strain at that point; the internal forces must balance the external load effects.

(2) With reference to the simple situation shown in Figure 4-5, two types of failure can be observed, depending on whether the ultimate FRP strain (region 1) or the ultimate concrete compressive strain (region 2) is reached.

(3) If the design falls in region 1, failure occurs due to the rupture of the FRP system. Any strain diagram corresponding to such a failure mode has a fixed point at the FRP strain value, ε_{fd} , as defined in Equation (4.14).

The distribution of strains over the depth of the member must be linear in order to satisfy the fundamental hypotheses presented earlier in this chapter. They shall be calculated as follows:

- (FRP) $\varepsilon_f = \varepsilon_{fd}$,
- (concrete in compression) $\varepsilon_c = (\varepsilon_{fd} + \varepsilon_0) \cdot \frac{x}{(h-x)} \leq \varepsilon_{cu}$,
- (steel in compression) $\varepsilon_{s2} = (\varepsilon_{fd} + \varepsilon_0) \cdot \frac{x-d_2}{(h-x)}$,

- (steel in tension)
$$\varepsilon_{s1} = (\varepsilon_{fd} + \varepsilon_0) \cdot \frac{d-x}{(h-x)},$$

where all the symbols are shown in Figure 4-5. In particular, the position of the neutral axis, x , is identified by its distance from the extreme compression fiber of the member cross-section; ε_{fd} calculated as per Equation (4.14); ε_{cu} represents the ultimate concrete compressive strain (design strain); ε_0 is the strain prior to FRP strengthening on the tension side and is calculated according to Section 4.2.2.2.

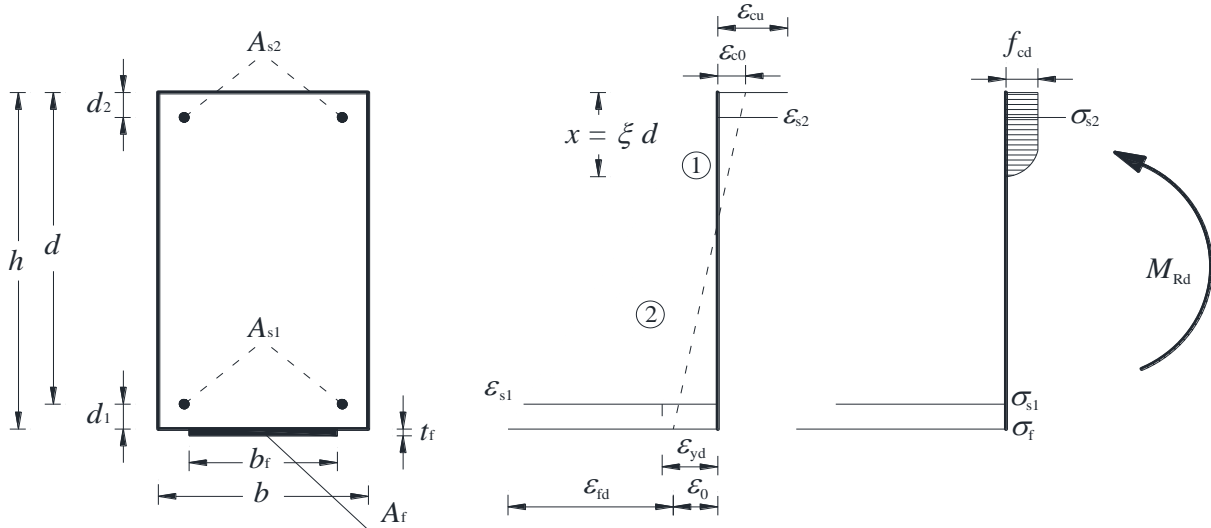


Figure 4-5 – Failure mode of a RC member Strengthened with FRP.

It is typically unnecessary to check the ultimate steel strain value because typical FRP systems present values of ultimate strain significantly smaller compared to that of steel. If the ultimate strain for steel according to the current building code is exceeded, this shall be taken into account when computing the position of the neutral axis and thus the member flexural capacity.

(4) When design falls in region 2, failure due to concrete crushing (strain equal to ε_{cu}) occurs with the yielding of steel in traction, while the FRP strain has not reached its ultimate value. The distribution of strains over the depth of the member must be linear to satisfy the fundamental hypotheses presented earlier in this chapter. They shall be calculated as follows::

- (FRP)
$$\varepsilon_f = \frac{\varepsilon_{cu}}{x} \cdot (h-x) - \varepsilon_0 \leq \varepsilon_{fd},$$

- (concrete in compression)
$$\varepsilon_c = \varepsilon_{cu},$$

- (steel in compression)
$$\varepsilon_{s2} = \varepsilon_{cu} \cdot \frac{x-d_2}{x},$$

- (steel in tension)
$$\varepsilon_{s1} = \varepsilon_{cu} \cdot \frac{d-x}{x}.$$

(5) For both failure modes, the position of the neutral axis, x , is using the translational equilibrium equation along the beam axis as follows:

$$0 = \psi \cdot b \cdot x \cdot f_{cd} + A_{s2} \cdot \sigma_{s2} - A_{s1} \cdot \sigma_{s1} - A_f \cdot \sigma_f, \quad (4.15)$$

where f_{cd} is equal to the design concrete compressive strength as per Section 3.3.3(6). When strengthening a fairly new structure, f_{cd} can be reduced to account for probable creep phenomena. The flexural capacity, M_{Rd} , of the strengthened member can be calculated using the following rotational equilibrium equation:

$$M_{Rd} = \frac{1}{\gamma_{Rd}} \cdot [\psi \cdot b \cdot x \cdot f_{cd} \cdot (d - \lambda \cdot x) + A_{s2} \cdot \sigma_{s2} \cdot (d - d_2) + A_f \cdot \sigma_f \cdot d_1], \quad (4.16)$$

where the partial factor γ_{Rd} is equal to 1.00 (Table 3-1, Section 3.4.2).

In Equations (4.15) and (4.16), the non-dimensional coefficients ψ and λ represent the resultant of the compression stresses divided by $b \cdot x \cdot f_{cd}$ and the distance from the extreme compression fiber divided by x .

(6) Because FRP materials have a linear elastic behavior up to the point of failure, the stress shall be taken as the product of the Young modulus of elasticity and the calculated strain.

4.2.2.4 Flexural capacity of FRP-strengthened members subjected to bending moment and axial force

(1)P The principles introduced in Section 4.2.2.1, from (1) through (5), still apply. However, the presence of an axial force, N_{Sd} , needs to be considered when determining the member flexural capacity, M_{Rd} .

(2)P The effectiveness of strengthening close to the beam-column intersections shall be guaranteed by providing suitable construction details in which FRP anchoring and the transfer of tensile stresses from FRP to the beam-column intersection are described. Moreover, debonding shall be prevented. This condition can be obtained by using cross-sectional confinement. Experimental tests shall be performed to validate this behavior.

(3) Items (2) through (6) of Section 4.2.2.3 still apply to this case. Equation (4.15) is no longer equal to zero and is equal to the design factored axial load, N_{Sd} .

(4) Alternatively, it is possible to determine the member flexural capacity due to combined axial load and bending according to the provisions of Appendix E.

4.2.2.5 Failure by laminate/sheet end debonding

(1)P Laminate/sheet end debonding depends on several parameters such as crack location, type of cracks (shear or flexural cracks), uneven concrete surface, and stress concentration near the anchorage zone.

(2) In the case of flexural strengthening, once the starting point of the application of the FRP laminate/sheet is located, the tensile stress under ULS in the cross section shall be limited to the maximum stress in the end debonding. This value is a function of the bonded length which depends on the distance a^* (Figure 4-6). For $a^* \geq l_{ed}$ it is recommended to use bonded length $l_b \geq l_{ed}$ where the allowed maximum tensile stress in the FRP is equal to f_{fid} (Equation (4.4)). If $a^* < l_{ed}$, the bonded length is $l_b < l_e$ and the allowed maximum tensile stress is equal to $f_{fid,rid}$ (Equation (4.5)).

(3) When the end of the FRP system is close to the member supports, and shear forces may induce inclined cracking, the design moment item (2) increases and is determined as follows:

$$M = V_{sd} \cdot a_1, \quad (4.17)$$

where V_{sd} is the factored shear force, $a_1=0.9 \cdot d \cdot (1-\cot\alpha)$, α is the angle of existing transverse steel reinforcement, and d is the effective depth of the member (Figure 4-6).

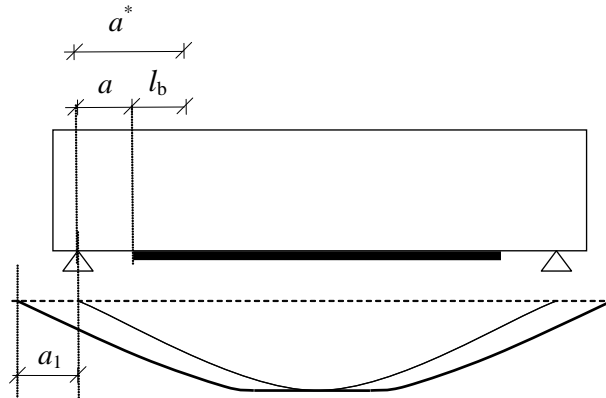


Figure 4-6 – Shifting of bending moment diagram.

(4) When special anchoring devices are used to avoid debonding of the FRP at the termination points, previous provisions shall be neglected. Such anchoring devices shall be guaranteed and based on proper experimental tests. Experimental tests shall be conducted for the material intended for such application (adhesives and reinforcing fibers), for the specific system used (transverse bars embedded in concrete, U-wrap with FRP sheets, etc.), for construction procedures recommended by the manufacturer/supplier, for surface preparation, and for the expected environmental conditions.

(5) When negative moment is present at the ends of the strengthening member, unless further data or adoption of special anchoring devices are available, the FRP application shall be limited to the area of positive moment, with a^* starting from the point of zero moment in the section.

4.2.3 Analysis at serviceability limit state

4.2.3.1 Assumptions

(1)P This section deals with the following serviceability limit states:

- Stress limits (Section 4.2.3.2);
- Deflection control (Section 4.2.3.3);
- Crack control (Section 4.2.3.4).

Other serviceability limit states may be relevant in particular situations, although they are not listed in this guide.

(2)P At SLS the following items shall be checked:

- Stresses shall be controlled to avoid yielding of the tensile steel and creep phenomena in both the concrete and FRP.
- Excessive deflection should not occur to prevent the normal use of the structure, induced damage to non-structural members, and potential harm to the users.
- Excessive cracking could significantly reduce the durability of a structure, its functionality, aspect, and consequentially decrease the bond performance of the FRP-concrete interface.

(3)P Design at SLS can be implemented considering the strain at the time of FRP installation.

The principle of superposition can be used for design. Design assumptions are as follows

- Cross sections remain plain.
- Linear-elastic behavior of the steel reinforcement and FRP.
- Linear-elastic behavior of concrete under compression and limited capacity to carry tensile stress, *tension stiffening* effect can be considered.
- Perfect bond exists between steel and concrete, and between concrete and FRP.

(4)P The first assumption allows for the use of a constant value for the Young modulus of elasticity for each material. The second implies the linearity of the strain diagram. The third, along with the first, uses the definition of the modular ratios ($\sigma_s/\sigma_c = E_s/E_c = n_s$) and ($\sigma_f/\sigma_c = E_f/E_c = n_f$). Such modular ratios are used to transform the actual beam into homogeneous concrete section.

Modular ratio values shall be set to account for creep as well as short and long-term conditions.

(5)P If deemed necessary, service stress due to thermal loads, creep, shrinkage, etc., shall be added to the stress induced by the applied loads.

4.2.3.2 Stress limitation

(1)P Stress at service in the FRP system, computed for the quasi-permanent loading condition, shall satisfy the limitation $\sigma_f \leq \eta \cdot f_{fk}$, where f_{fk} is the FRP characteristic strength at failure and η is the conversion factor as suggested in Section 3.5

Service stresses in the concrete and steel shall be limited according to the current building code.

(2) Assuming that M_0 is the bending moment prior to FRP strengthening, and assuming that M_1 is the bending moment after FRP strengthening, the stress due to the combined moment $M=M_0+M_1$ can be evaluated as follows

- Stress in the concrete: $\sigma_c = \sigma_{c0} + \sigma_{c1}, \quad \sigma_{c0} = M_0 / W_{0,c}^s, \quad \sigma_{c1} = M_1 / W_{1,c}^s;$
- Stress in the steel: $\sigma_s = \sigma_{s0} + \sigma_{s1}, \quad \sigma_{s0} = n_s \cdot M_0 / W_{0,s}^i, \quad \sigma_{s1} = n_s \cdot M_1 / W_{1,s}^i;$
- Stress in the FRP: $\sigma_f = n_f \cdot M_1 / W_{1,f}^i.$

where (see Figure 4-5):

- $W_{0,c}^s = I_0 / x_0$: modulus of resistance for RC members related to extreme concrete compression fiber;
- $W_{0,s}^i = I_0 / (d - x_0)$: modulus of resistance for RC members related to tension steel;
- $W_{1,c}^s = I_1 / x_1$: modulus of resistance for RC strengthened members related to extreme concrete compression fiber;
- $W_{1,s}^i = I_1 / (d - x_1)$: modulus of resistance for RC strengthened members related to tension steel;
- $W_{1,f}^i = I_1 / (h - x_1)$: modulus of resistance for RC strengthened members related to FRP system.

When the existing applied moment, M_0 , produces cracking in the concrete member, neutral axis determination as well as values of the moment of inertia I_0 e I_1 shall be calculated with respect to the

cracked transformed section for unstrengthened and strengthened conditions, respectively.

4.2.3.3 Deflection control

(1)P Deflections exhibited by FRP strengthened structures shall comply with current building code requirements.

(2)P The adopted deflection model shall simulate the real behavior of the structure. If deemed necessary, cracking shall be accounted for.

(3)P The adopted deflection model should take into account the following:

- Creep and shrinkage of concrete.
- Concrete stiffening between cracks.
- Existing cracks prior to FRP strengthening.
- Thermal loads.
- Static and/or dynamic loads.
- Appropriate concrete Young modulus of elasticity depending upon aggregate type and concrete curing at the time of loading.

(4) Deflections for FRP strengthened beams can be determined by integration of the curvature diagrams. Such diagrams can be computed with non-linear analyses by taking into account the tension stiffening of concrete.

Alternatively, simplified analyses are possible, similar to what is used for traditional RC beams, provided that they are supported by suitable experimental support.

4.2.3.4 Crack control

(1)P For SLS, the crack width shall be checked to guarantee proper use of the structure and protect the internal steel reinforcement.

(2) Crack width limitations for FRP strengthened structures shall satisfy the requirements of the current building code requirements.

(3) Presently there are no accurate and reliable models available for crack width computation of FRP strengthened concrete structures. Several experimentally-based formulations are available in the literature. Such formulations modify the expressions used for traditional RC sections to consider the presence of the external strengthening. Experimental evidence shows that members strengthened with FRP have smaller, closely spaced cracks.

(4) More refined and accurate models can be adopted when supported by ad-hoc experimental results.

4.2.4 Ductility

(1)P For flexural members, ductility is a measure of the member capability of evolving to the plastic range. It depends on both the section behavior and actual failure modes of the overall structural member. Ductility increases with steel yielding and curvature of the strengthened member at failure initiation. It can be considered totally absent if debonding starts prior to any other failure mechanism.

4.3 SHEAR STRENGTHENING

4.3.1 Introduction

- (1)P Shear strengthening is necessary when the applied factored shear force is greater than the corresponding member shear capacity. The latter shall be determined considering the contributions of both the concrete and transverse steel reinforcing bars when available.
- (2) Shear strengthening shall be verified at ULS only.
- (3) This guide contains specific configurations where FRP shear strengthening is considered. Other solutions are also possible, provided their effectiveness is proven and their contribution to the shear capacity is quantified.

4.3.2 Strengthening configurations

Shear strengthening is achieved by applying one or more layers of FRP material externally bonded to the surface of the member to be strengthened (Figure 4-7). External monodirectional or bidirectional (i.e., fabric) FRP reinforcement can be applied in a discontinuous fashion, with gaps between successive strips, or continuously, with strips adjacent each other.

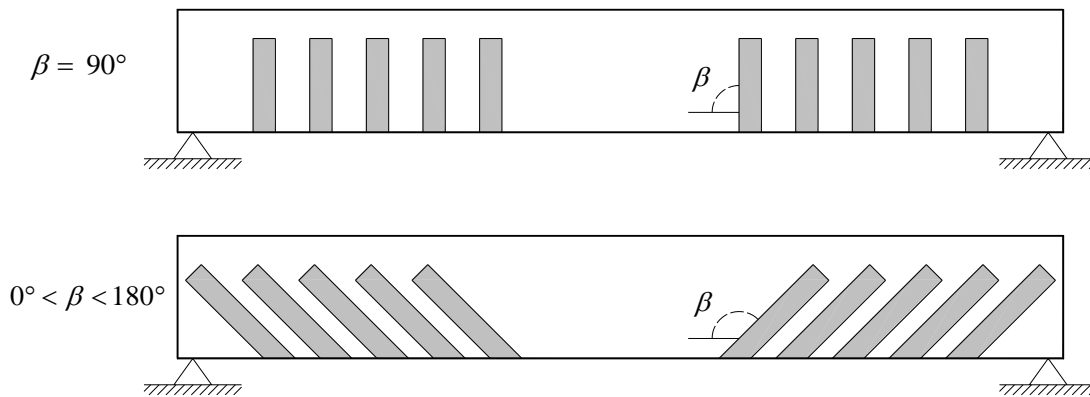


Figure 4-7 – Lateral view of FRP shear strengthening.

- (2) Design of FRP strengthening depends on both geometry (FRP thickness, width, and spacing) and the fiber's angle with respect to the longitudinal axis of the member.
- (3) Figure 4-8 shows the FRP strengthening configurations: U-wrapped and completely wrapped beams.

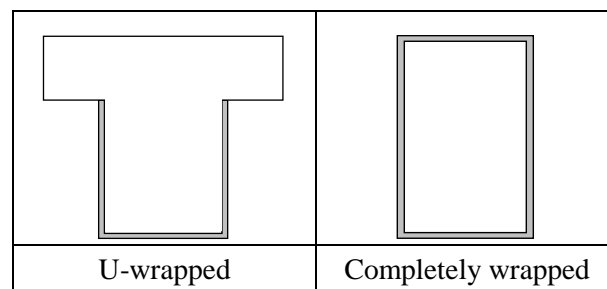


Figure 4-8 – Cross section of FRP strengthened members.

- (4) For the U-wrap strengthening of rectangular or T-sections, delamination of the end portions of FRP reinforcement can be avoided by using laminates/sheets and/or bars installed in the direction

of the members longitudinal axis. In such a case, the behavior of U-wrap strengthening can be considered equivalent to that of a completely wrapped member, provided the effectiveness offered by these devices is proven.

(5) Shear strengthening may also be achieved through the installation of FRP bars in dedicated slots made on the outer surface of the member to be strengthened as near-surface mounted reinforcement. This strengthening is addressed in this document. If used, its effectiveness shall be supported by experimental results.

4.3.3 Shear capacity of FRP strengthened members

4.3.3.1 Shear capacity

(1) The shear capacity shall be evaluated as follows:

$$V_{Rd} = \min \{ V_{Rd,s} + V_{Rd,f}, V_{Rd,c} \}, \quad (4.18)$$

where $V_{Rd,s}$, $V_{Rd,f}$ and $V_{Rd,c}$ are the steel, FRP and concrete contributions to the shear capacity, respectively. Steel and concrete shear contributions shall be calculate according to (2) and (4) as well as the current building code.

(2) In the case of a RC member with a rectangular cross-section and FRP side bonding configuration, the FRP contribution to the shear capacity, $V_{Rd,f}$, shall be calculated as follows:

$$V_{Rd,f} = \frac{1}{\gamma_{Rd}} \cdot 0.9 \cdot d \cdot f_{fed} \cdot 2 \cdot t_f \cdot (\cot \theta + \cot \beta) \cdot \frac{b_f}{p_f}, \quad (4.19)$$

where (Figure 4-9):

- d is the distance from the extreme compression fiber to the centroid of tension steel reinforcement.
- f_{fed} is the effective design strength of the FRP shear reinforcement, as stated in Section 4.3.3.2.
- t_f is the thickness of FRP shear reinforcement.
- b_f and p_f are respectively the width and the spacing of FRP strips, measured orthogonal to the direction of fibers ($b_f/p_f = 1.0$ when FRP strips are placed adjacent to one another or in case of bidirectional FRP elements).
- γ_{Rd} is evaluated as per Table 3-1, Section 3.4.2.

In Equation (4.19), p_f can be substituted with $\bar{p}_f \cdot \sin \beta$, where \bar{p}_f is the FRP strip spacing measured along the element (Figure 4-9).

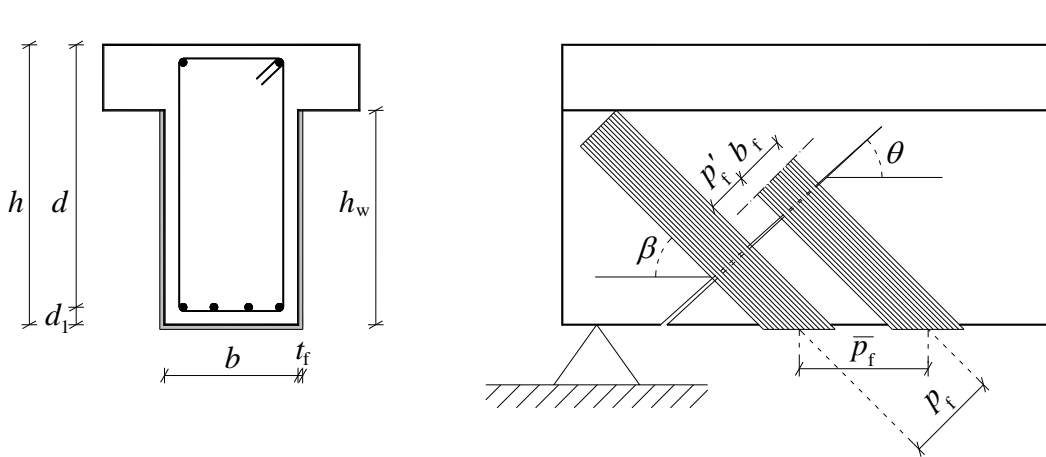


Figure 4-9 – Notation for shear strengthening using FRP strips.

(3) For external FRP reinforcement in the form of discrete strips, strips width, b_f (mm), and center-to-center spacing between strips, p_f (mm) shall not exceed the following limitations: $50 \text{ mm} \leq b_f \leq 250 \text{ mm}$, and $b_f \leq p_f \leq \min\{0.5 \cdot d, 3 \cdot b_f, b_f + 200 \text{ mm}\}$.

The external FRP reinforcement shall be substituted with a different system in terms of geometry or mechanical characteristics when $\min\{0.5 \cdot d, 3 \cdot b_f, b_f + 200 \text{ mm}\} < b_f$.

(4) For completely wrapped members having a circular cross-section with diameter D and when fibers are placed orthogonal to the axis of the member ($\beta = 90^\circ$), the FRP contribution to shear capacity, $V_{\text{Rd,f}}$, shall be calculated as follows:

$$V_{\text{Rd,f}} = \frac{1}{\gamma_{\text{Rd}}} \cdot D \cdot f_{\text{fed}} \cdot \frac{\pi}{2} \cdot t_f \cdot \cot \theta. \quad (4.20)$$

4.3.3.2 Effective FRP design strength

(1) Debonding of FRP may be caused by stress concentrations at the concrete-FRP interface close to shear cracks (Section 4.1.3). A simplified procedure considering such phenomenon requires the introduction of the “effective FRP design strength” defined as the FRP tensile strength when debonding begins.

(2) For FRP side bonding to a rectangular cross section, the effective FRP design strength, f_{fed} , can be calculated as follows:

$$f_{\text{fed}} = f_{\text{fid}} \cdot \left[1 - \frac{1}{3} \cdot \frac{l_{\text{ed}} \cdot \sin \beta}{\min\{0.9 \cdot d, h_w\}} \right], \quad (4.21)$$

where f_{fid} is the design debonding strength of FRP computed according to Equation (4.4) and follow the guidelines in the following point (4). l_{ed} is the design bond length given in Equation (4.1), β is the angle between fibers and the longitudinal axis of the member, d is effective depth and h_w is the web depth completely impregnated with U-wrap.

Particular attention shall be given to the case of cantilever applications (Figure 4-10), where it is recommended to use anchoring or mechanical devices for the U-wrap. In this configuration, f_{fed} can be computed using Equation (4.21) neglecting the following point (3).

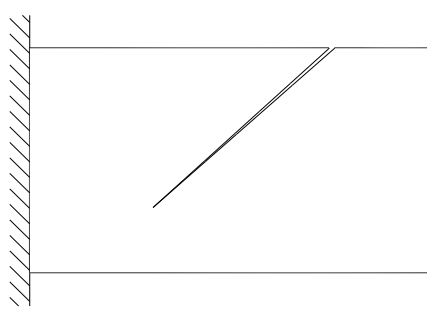


Figure 4-10 – Cantilever configuration.

(3) For completely wrapped members having rectangular cross sections, the effective FRP design strength can be calculated as follows:

$$f_{\text{fed}} = f_{\text{fdd}} \cdot \left[1 - \frac{1}{6} \cdot \frac{l_e \cdot \sin \beta}{\min\{0.9 \cdot d, h_w\}} \right] + \frac{1}{2} (\phi_R \cdot f_{\text{fd}} - f_{\text{fdd}}) \cdot \left[1 - \frac{l_e \cdot \sin \beta}{\min\{0.9 \cdot d, h_w\}} \right], \quad (4.22)$$

where f_{fdd} is the FRP design strength to be evaluated as in Equation (4.4), moreover:

$$\phi_R = 0.2 + 1.6 \cdot \frac{r_c}{b}, \quad 0 \leq \frac{r_c}{b} \leq 0.5, \quad (4.23)$$

where r_c is the corner radius of the section to be wrapped, and, b is the width of the member. The second term of Equation (4.22) shall be considered only when it is greater than zero.

(4) When calculating k_b from Equation (4.3):

- $b = p_f$ for discrete FRP strip application,
- $b = b_f = \min\{0.9 \cdot d, h_w\} \cdot \sin(\theta + \beta) / \sin \theta$ for FRP systems installed continuously along the length of the member.

(5) When special devices used to anchor the end portions of U-wrapped FRP systems are proven to be equally effective as the completely wrapped strengthening configuration, the effective FRP design strength can be computed from Equation (4.22). If this is not the case, the effective FRP design strength shall be calculated according to Equation (4.21).

(6) For completely wrapped members having a circular cross-section of diameter D and when the fibers are placed orthogonal to the axis of the member ($\beta = 90^\circ$), the effective FRP design strength shall be calculated as follows:

$$f_{\text{fed}} = E_f \cdot \varepsilon_{f,\text{max}}, \quad (4.24)$$

where E_f is the FRP Young modulus of elasticity, and $\varepsilon_{f,\text{max}}$ represents the maximum allowable strain in the FRP set equal to $5 \cdot 10^{-3}$, unless a more detailed calculation is performed.

4.4 TORSIONAL STRENGTHENING

4.4.1 Introduction

- (1)P Torsional strengthening is necessary when the applied factored torsional moment is greater than the corresponding torsional capacity. The latter shall be determined considering the contributions of both the concrete and transverse steel reinforcement when available.
- (2) Torsional strengthening shall be verified at ULS only.
- (3) The following sections of this document contain specific configurations of FRP torsional strengthening applications. Other solutions are also possible, provided the effectiveness is proven and contribution to the shear capacity is quantified.

4.4.2 Strengthening configurations

- (1) Strengthening for torsion is achieved by applying one or more layers of externally bonded FRP material to the surface of the member to be strengthened (Figure 4-7). External FRP reinforcement can be applied in a discontinuous manner with gaps between strips, or continuously with strips adjacent to one another.
- (2) Design of FRP reinforcement depends on FRP thickness, width, and spacing. Fibers shall be arranged with an angle $\alpha = 90^\circ$ with respect to the longitudinal axis of the member.
- (3) FRP shall be placed around the cross section specifically as a completely wrapped system (Figure 4-8).
- (4) Strengthening for torsion may also be achieved through near surface mounted reinforcement defined as the installation of FRP bars in dedicated slots made to the outer surface of the member being strengthened. This type of strengthening is not addressed in this document. If used, its effectiveness shall be supported by experimental results.

4.4.3 Torsional capacity of FRP strengthened members

- (1)P The following applies to prismatic members where an ideal ring-shaped resisting area can be identified and where the lack in torsional capacity is not generated by defects of the steel longitudinal reinforcement. The following shall be verified:

$$T_{Rd,l} > \min \{ T_{Rd,s}, T_{Rd,c} \}, \quad (4.25)$$

where $T_{Rd,l}$, $T_{Rd,s}$, $T_{Rd,c}$ are the existing longitudinal steel, vertical steel, and concrete contributions to the torsional capacity, respectively, according to the current building code.

4.4.3.1 Torsional capacity

- (1) Torsional capacity of FRP strengthened members can be evaluated as follows:

$$T_{Rd} = \min \{ T_{Rd,s} + T_{Rd,f}, T_{Rd,l}, T_{Rd,c} \}, \quad (4.26)$$

where $T_{Rd,s}$, $T_{Rd,l}$, $T_{Rd,c}$ are previously stated. The quantity $T_{Rd,f}$ is the FRP's contribution to the torsional capacity, evaluated by the following condition.

(2) If Equation (4.26) is $T_{Rd}=T_{Rd,s}$, $T_{Rd,f}$ shall be calculated as follows:

$$T_{Rd,f} = \frac{1}{\gamma_{Rd}} \cdot 2 \cdot f_{fed} \cdot t_f \cdot b \cdot h \cdot \frac{b_f}{p_f} \cdot \cot \theta, \quad (4.27)$$

where the partial factor γ_{Rd} is equal to 1.20 (Table 3-1, Section 3.4.2), f_{fed} is the FRP design effective strength evaluated in Section 4.3.3.2, t_f is the thickness of the FRP strip or sheet, b and h are the section width and depth, respectively. θ is the angle of the compressed struts with respect to the member longitudinal axis ($22^\circ \leq \theta \leq 45^\circ$), b_f and p_f are the width and center-to-center spacing of FRP strips measured orthogonally to the fiber direction, respectively. For FRP strips applied adjacent to each other, the ratio b_f/p_f shall be equal to 1.0.

(3) For external FRP reinforcement in the form of discrete strips, the strips width, b_f (mm), and center-to-center spacing between strips, p_f (mm), shall not exceed the following limitations: $50 \text{ mm} \leq b_f \leq 250 \text{ mm}$, and $b_f \leq p_f \leq \min\{0.5 \cdot d, 3 \cdot b_f, b_f + 200 \text{ mm}\}$.

External FRP reinforcement shall be substituted with different systems in terms of geometry or mechanical characteristics when $\min\{0.5 \cdot d, 3 \cdot b_f, b_f + 200 \text{ mm}\} < b_f$.

(4) In case of combined torsion, T_{Sd} , and shear, V_{Sd} , the following limitation shall be met:

$$\frac{T_{Sd}}{T_{Rd,c}} + \frac{V_{Sd}}{V_{Rd,c}} \leq 1. \quad (4.28)$$

where $T_{Rd,c}$ and $V_{Rd,c}$ are previously stated.

Strengthening for shear and torsion shall be calculated separately. The overall strengthening area is given by the sum of the area deemed necessary for shear and torsional FRP strengthening. The angle of the concrete compressed struts, θ , shall be considered equal to 45° for both shear and torsion.

4.5 CONFINEMENT

4.5.1 Introduction

(1)P Appropriate confinement of reinforced concrete members may improve structural performance. In particular, it allows the increase of the following:

- Ultimate capacity and strain for members under concentric or slightly eccentric axial loads;
- Ductility and capacity under combined bending and axial load, when FRP reinforcements are present with fibers lying along the longitudinal axis of the member (Section 4.2.2.4 and Appendix F).

(2) Confinement of RC members can be achieved with FRP sheets arranged along the member perimeter as both continuous and discontinuous external wrapping.

(3)P Increase in the axial capacity and ultimate strain of FRP-confined concrete depends on the applied confinement pressure. The latter is a function of the member cross section and FRP stiffness.

(4)P The redistribution of vertical loads cannot depend on the ductility of members under concentric or slightly eccentric axial load.

(5)P FRP-confinement (FRP is linear-elastic up to failure), unlike steel confinement (steel has an elastic-plastic behavior), exerts a lateral pressure on confined members that increases with the transversal expansion of the confined members.

(6) A typical stress-strain (σ - ε) diagram for compression tests performed on FRP-confined specimens is reported in Figure 4-11.

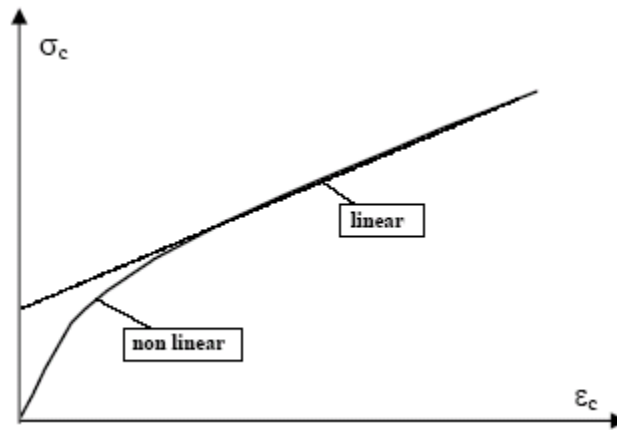


Figure 4-11 – Stress-strain relationship for FRP-confined concrete.

(7) For axial strain values, ε_c , up to 2‰, the stress in the confined concrete is only slightly greater than that exhibited by unconfined concrete.

(8) For axial strain values larger than 2‰, the stress-strain diagram is non linear and the slope of the corresponding stress vs. strain curve gradually decreases and approaches a nearly constant value. In the linear section of the graph, the confined concrete gradually loses its integrity due to widespread cracking.

(9) Failure of a RC confined member is attained by fiber rupture. However, beyond a critical value of the axial strain, the FRP-confined member may be linked to a recipient with very flexible walls filled with incoherent material. Beyond that threshold it loses its functionality because can only carry small or negligible transverse forces. As a result, failure of the FRP-confined RC member is reached when the FRP strain equal to 4‰ is attained.

(10) Confined elements shall be verifies using only USL.

4.5.2 Axial capacity of FRP-confined members

(1) Proper confinement can only be achieved by installing FRP fibers positioned orthogonally to the member axis.

(2) When FRP reinforcement is spirally arranged around the member perimeter, the confinement effectiveness shall be properly evaluated.

(3)P If the adopted FRP system is not initially prestressed, it exerts a passive confinement on the compressed member. The confinement action becomes significant only after cracking of the concrete and yielding of the internal steel reinforcement due to the increased lateral expansion.

(4)P Design at ULS of FRP confined members requires that both factored design axial load, N_{sd} , and factored axial capacity, $N_{Rcc,d}$, satisfy the following condition:

$$N_{Sd} \leq N_{Rcc,d}, \quad (4.29)$$

(5) For non-slender FRP confined members, the factored axial capacity can be calculated as follows:

$$N_{Rcc,d} = \frac{1}{\gamma_{Rd}} \cdot A_c \cdot f_{ccd} + A_s \cdot f_{yd}, \quad (4.30)$$

where:

- γ_{Rd} is the partial factor equal to 1.10 (Table 3-1, Section 3.4.2),
- A_c and f_{ccd} represent the member cross-sectional area and design strength of confined concrete as indicated in item (6), respectively,
- A_s and f_{yd} represent area and yield design strengths of existing steel reinforcement (as per Section 3.3.3(6)), respectively.

(6) The design strength, f_{ccd} , of confined concrete shall be evaluated as follows:

$$\frac{f_{ccd}}{f_{cd}} = 1 + 2.6 \cdot \left(\frac{f_{l,eff}}{f_{cd}} \right)^{2/3}, \quad (4.31)$$

where:

- f_{cd} is the design strength of unconfined concrete as per Section 3.3.3(6),
- $f_{l,eff}$ is the effective confinement lateral pressure as defined in the following section.

The Equation (4.31) shall be used also to attain the second objective mentioned in Section 4.5.1(1)P.

(7) The confinement is effective if $f_{l,eff} / f_{cd} > 0.05$.

4.5.2.1 Confinement lateral pressure

(1)P The effectiveness of FRP-confined members only depends on a fraction of confinement lateral pressure, f_l , exerted by the system, namely the effective confinement lateral pressure $f_{l,eff}$.

(2) The effective confinement lateral pressure, $f_{l,eff}$, is a function of member cross section and FRP configuration as indicated in the following equation:

$$f_{l,eff} = k_{eff} \cdot f_l, \quad (4.32)$$

where k_{eff} is a coefficient of efficiency (≤ 1), defined as the ratio between the volume of the effectively confined concrete, $V_{c,eff}$, and the volume of the concrete member, V_c , neglecting the area of existing internal steel reinforcement.

(3) The confinement lateral pressure shall be evaluated as follows:

$$f_1 = \frac{1}{2} \cdot \rho_f \cdot E_f \cdot \varepsilon_{fd,rid}, \quad (4.33)$$

where ρ_f is the geometric strengthening ratio as a function of section shape (circular or rectangular) and FRP configuration (continuous or discontinuous wrapping), E_f is Young modulus of elasticity of the FRP in the direction of fibers, and $\varepsilon_{fd,rid}$ is a reduced FRP design strain.

(4) The coefficient of efficiency, k_{eff} , shall be expressed as:

$$k_{eff} = k_H \cdot k_V \cdot k_\alpha. \quad (4.34)$$

(5) The coefficient of horizontal efficiency, k_H , depends on the cross-section shape.

(6) The coefficient of vertical efficiency, k_V , depends on FRP configurations.

For RC confined members with continuous FRP wrapping, it is assumed $k_V = 1$.

For RC confined members with discontinuous FRP wrapping (Figure 4-12), such as FRP strips installed with a center-to-center spacing of p_f and clear spacing of p'_f , reduction in the confinement effectiveness due to the diffusion of stresses (approximately at 45°) between two subsequent wrappings shall be considered.

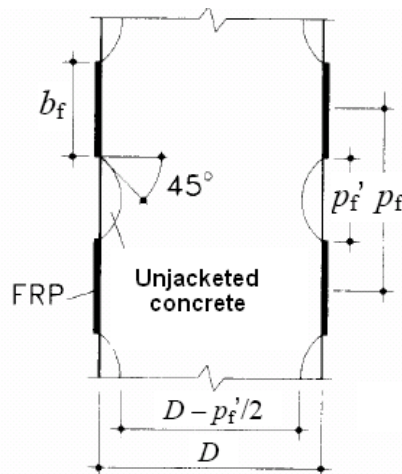


Figure 4-12 – Elevation view of circular member confined with FRP strips.

Irrespective of the section shape, the coefficient of vertical efficiency, k_V , shall be assumed as follows:

$$k_V = \left(1 - \frac{p'_f}{2 \cdot d_{min}} \right)^2, \quad (4.35)$$

where d_{min} is the minimum cross-section of the member.

(7) In case of discontinuous wrapping the net distance between strips shall satisfy the limitation $p'_f \leq d_{min}/2$.

(8) Irrespective of the section shape, the efficiency coefficient, k_α to be used when fibers are

spirally installed with an angle α_f with respect to the member cross-section, shall be expressed as follows:

$$k_\alpha = \frac{1}{1 + (\tan \alpha_f)^2} \quad (4.36)$$

(9) The reduced FRP design strain, $\varepsilon_{fd,rid}$, shall be computed as follows:

$$\varepsilon_{fd,rid} = \min\{\eta_a \cdot \varepsilon_{fk} / \gamma_f; 0.004\}, \quad (4.37)$$

where η_a and γ_f represent the environmental conversion factor and partial factor suggested in Table 3-2 and Section 3.4.1 respectively; the maximum allowed strain is 0.004 as per item (9) on Section 4.5.1.

4.5.2.1.1 Circular sections

(1)P FRP-confinement is particularly effective for circular cross sections subjected to both concentric and slightly eccentric axial loads.

(2)P Fibers installed transversely to the longitudinal axis of the strengthened member induce a uniform pressure that opposes the radial expansion of the loaded member.

(3) The geometric strengthening ratio, ρ_f , to be used for the evaluation of the effective confinement pressure in Equation (4.33) shall be expressed as follows:

$$\rho_f = \frac{4 \cdot t_f \cdot b_f}{D \cdot p_f}, \quad (4.38)$$

where (Figure 4-12) t_f , b_f and p_f represent FRP thickness, width, and spacing, respectively, and D is the diameter of the circular cross section.

In the case of continuous wrapping, ρ_f becomes $4 \cdot t_f / D$.

(4) For circular cross sections, the coefficient of horizontal efficiency, k_H , is equal to 1.0.

(5) For circular sections, the dimension d_{min} , introduced in Equation (4.35) for the computation of the coefficient of vertical efficiency, is defined as the section diameter.

4.5.2.1.2 Square and rectangular sections

(1)P FRP-confinement of members with square or rectangular cross sections produces a marginal increase of the members compressive strength. Therefore such applications shall be carefully validated and analyzed.

(2) The strengthening geometric ratio, ρ_f , to be used for the evaluation of the effective confinement pressure shall be expressed as follows:

$$\rho_f = \frac{2 \cdot t_f \cdot (b+h) \cdot b_f}{b \cdot h \cdot p_f}, \quad (4.39)$$

where t_f , b_f and p_f represent FRP thickness, width, and spacing, respectively, and b and h are the cross sectional dimensions of the rectangular member.

In the case of continuous wrapping ρ_f in Equation (4.39) becomes $2 \cdot t_f \cdot (b + h) / (b \cdot h)$.

(3) For rectangular cross sections, the effectively confined concrete area may be considered to be only a fraction of the overall concrete cross section (Figure 4-13). The reason for this behavior is due to the “arch effect” that forms within the concrete cross section. Such an effect depends on the values of the corner radius r_c (Section 4.8.2.2).

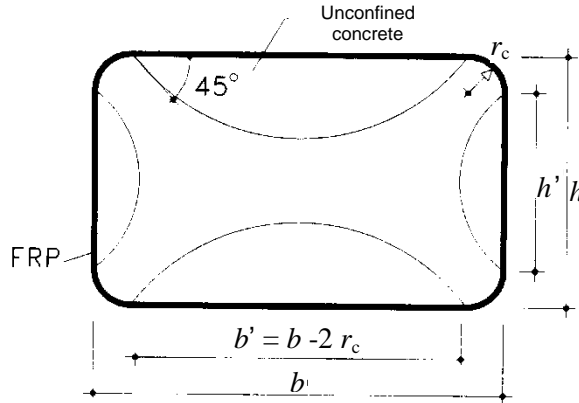


Figure 4-13 – Confinement of rectangular sections.

(4) For rectangular cross sections, the coefficient of horizontal efficiency, k_H , which takes into account the arch effect shall be expressed as follows:

$$k_H = 1 - \frac{b'^2 + h'^2}{3 \cdot A_g}, \quad (4.40)$$

where b' and h' are the dimensions indicated in Figure 4-13 and A_g is the cross section area.

(5) The effect of FRP confinement shall not be considered for rectangular cross sections having $b/h > 2$, or $\max\{b, h\} > 900\text{mm}$ unless otherwise proven by suitable experimental tests.

4.5.3 Ductility of FRP-confined members under combined bending and axial load

(1)P FRP-confinement may also be achieved in concrete members under combined bending and axial load (axial load with large eccentricity). Confinement will result in a ductility enhancement while the member axial capacity can only be slightly increased.

(2) Unless a more detailed analysis is performed, the evaluation of the ultimate curvature of a FRP confined concrete member under combined bending and axial load may be accomplished by assuming a parabolic-rectangular approximation for the concrete stress-strain relationship, characterized by an ultimate strain ϵ_{ccu} , computed as follows:

$$\epsilon_{ccu} = 0.0035 + 0.015 \cdot \sqrt{\frac{f_{l,eff}}{f_{cd}}}, \quad (4.41)$$

where f_{cd} is the design strength of the unconfined concrete and $f_{l,eff}$ is the effective confinement

pressure. In Equation (4.41), the effective pressure is computed assuming a reduced FRP design strain as follows:

$$\varepsilon_{fd,rid} = \eta_a \cdot \frac{\varepsilon_{fk}}{\gamma_f} \leq 0.6 \cdot \varepsilon_{fk} \quad (4.42)$$

(3) More accurate evaluation of ultimate curvature and flexural capacity of FRP strengthened members may be obtained with suitable concrete-confined models (Appendix F) capable of capturing the behavior described in Section 4.5.1 and Figure 4-11.

4.6 FLEXURAL STRENGTHENING OF PRESTRESSED CONCRETE MEMBERS

4.6.1 Use of FRP for prestressed concrete members

(1)P Flexural capacity of a prestressed concrete (PC) structure can be achieved by the application to non-prestressed FRP systems.

4.6.1.1 Design at ultimate limit state

(1)P The evaluation of the flexural capacity of PC members subjected to a bending moment shall be carried out in the following procedures similar to those described in Section 4.2.2 for RC members, with the following changes:

- The strain of prestressed reinforcement is equal to the algebraic sum of the strain of the concrete surrounding the tendon and the strain at the decompression limit, $\bar{\varepsilon}_p$; The latter represents the strain exhibited by existing tendons for an appropriate combination of internal forces producing zero stress in the concrete surrounding the tendons (Figure 4-14).
- If the concrete age is such to consider to have exhausted all long-term phenomena, the initial concrete strain, ε_0 is equal to the strain at the time of FRP installation.
- If long-term phenomena in the concrete can not be considered, the value of ε_0 is the algebraic sum of the previously computed value and the long-term strain developed in the concrete substrate after FRP strengthening takes place. For the evaluation of a long-term strain, as well as any prestress loss, the presence of the strengthening system can be neglected.

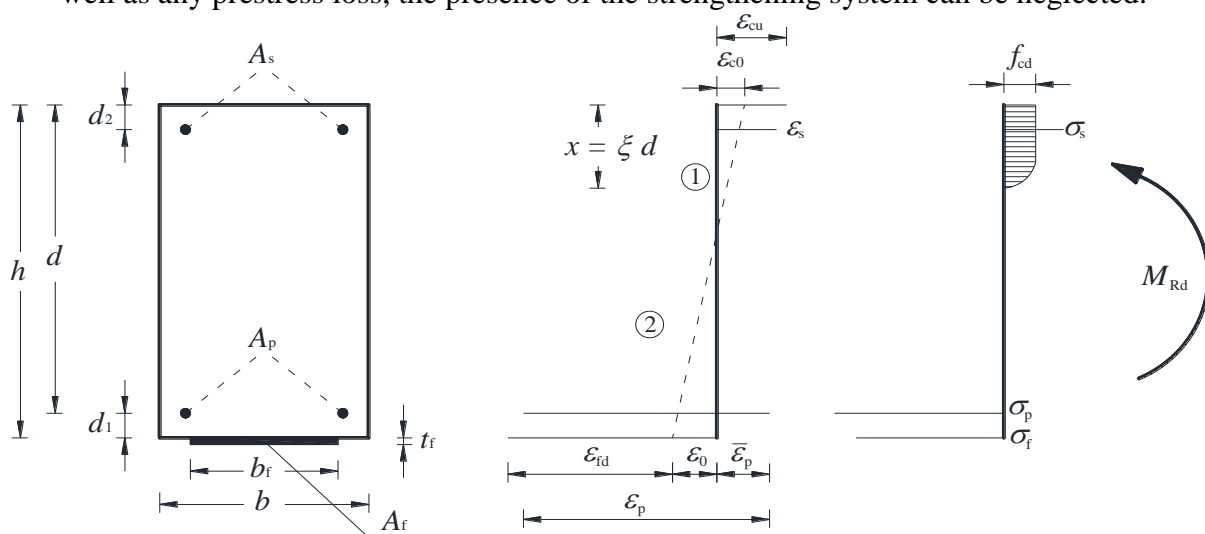


Figure 4-14 – Failure mode of PC member strengthened with FRP.

(2)P Achieving the ultimate limit state shall be preceded by the yielding of existing prestressing steel tendons.

- (3) For debonding-failure mechanisms, refer to Sections 4.1 and 4.2.

4.6.1.2 Design at serviceability limit state

(1)P Service stress limitations for concrete and steel shall satisfy the requirements of the current building code. Service stress limitations for FRP material shall comply with Section 4.2.3.2.

- (2) FRP strengthening shall be neglected if FRP is temporarily compressed (*e.g.*, due to creep of concrete).

4.7 DESIGN FOR SEISMIC APPLICATIONS

4.7.1 Introduction

(1)P It shall be permitted to strengthen RC and PC members with FRP composites when the structure fails to meet the seismic requirements specified in the current building code.

This section recognizes the provisions of the current building code as well as indications provided by updated literature related to seismic constructions; particular importance is given to the following:

- Evaluation of seismic safety.
- Safety requirements (verification of limit states).
- Levels of seismic protection (magnitude of the associated seismic action).
- Methods of analysis.
- Verification criteria (distinction between ductile and brittle members).
- Material characteristics to be used for design.

4.7.2 Selection criteria for FRP strengthening

(1)P When using FRP material for the strengthening of RC members, the following principles shall be considered:

- Removal of all brittle collapse mechanisms (Section 4.7.2.1).
- Removal of all story collapse mechanisms (“soft story”) (Section 4.7.2.2).
- Enhancement of the overall deformation capacity of the structure through one of the following mechanisms (Section 4.7.2.3.1):
 - Increasing the rotational capacity of the potential plastic hinges without changing their position (Section 4.7.2.3.1).
 - Relocating the potential plastic hinges following the design capacity criteria (hierarchy of resistance) (Section 4.7.2.3.2).

(2) Type and size of selected FRP systems as well as the urgency of FRP installation shall take into account the following:

- Major building irregularities (in terms of capacity and/or stiffness) can not be eliminated using FRP as a strengthening technique.
- A better resistance regularity can be obtained by strengthening a limited number of members.
- Enhancement of local ductility is always advantageous.
- Localized strengthening shall not reduce the overall ductility of the structure.

4.7.2.1 Prevention of all brittle collapse mechanisms

(1)P Brittle collapse mechanisms to be prevented as well as FRP strengthening methodologies are as follows:

- Shear failures.
- Failure due to loss of bond in steel overlapping areas into columns.
- Failure due to buckling of longitudinal steel bars into the columns.
- Failure due to tensile stresses on the beam-column joint.

4.7.2.1.1 Shear failure

(1)P Increase in shear capacity shall be achieved by installation of FRP systems with the fibers oriented perpendicular to the member axis ($\beta = 90^\circ$) and, if applicable, also in other directions .

4.7.2.1.2 Failure of columns due to loss of bond in steel reinforcement

(1) Slipping of existing steel reinforcement in RC columns at the locations of lap splice may be avoided by confining the member cross section with FRP.

(2) For circular cross sections with diameter D , the thickness of the FRP confining the member cross section shall be evaluated as follows:

$$t_f = \frac{D \cdot (f_1 - \sigma_{sw})}{2 \cdot 0.001 \cdot E_f}, \quad (4.43)$$

where:

- σ_{sw} represents the stirrup's tensile stress corresponding to a 1 % strain or the mortar injection pressure between the FRP reinforcement and the RC column, if present;
- f_1 represents the confinement pressure at the lap splice location with a length, L_s , equal to:

$$f_1 = \frac{A_s \cdot f_{yd}}{\left[\frac{u_e}{2 \cdot n} + 2 \cdot (d_b + c) \right] \cdot L_s}, \quad (4.44)$$

where f_{yd} is design yield strength of longitudinal steel reinforcement (Section 3.3.3(6)), u_e is the perimeter of the cross section within the polygon circumscribing the longitudinal bars having average diameter d_b , n is the number of bars spliced along u_e and c is the concrete cover.

(3) For rectangular sections b and h , Equation (4.43) and (4.44) shall be determined by substituting D with $\max\{b, h\}$ and reducing the effectiveness of FRP confinement by the use of k_H as defined in Section 4.5.2.1.2.

4.7.2.1.3 Failure due to buckling of longitudinal steel bars into the columns.

- (1) Buckling of existing vertical steel reinforcement of RC columns may be avoided by confining the member cross section with FRP.
- (2) The thickness of such FRP confinement shall be evaluated as follows:

$$t_f = \frac{0.45 \cdot n \cdot f_{yd}^2 \cdot d}{4 \cdot E_{ds} \cdot E_f} \approx \frac{10 \cdot n \cdot d}{E_f}, \quad (4.45)$$

where:

- n , represents the total number of existing steel longitudinal bars subjected to buckling;
- f_{yd} , is the design strength of longitudinal steel reinforcement (Section 3.3.3(6));
- d , size of the cross section parallel to the bending plane;
- E_f , Young modulus of elasticity of FRP reinforcement in the direction of existing steel vertical bars;
- E_{ds} , suitable “reduced modulus” defined as follows:

$$E_{ds} = \frac{4 \cdot E_s \cdot E_i}{(\sqrt{E_s} + \sqrt{E_i})^2}, \quad (4.46)$$

where E_s and E_i are the initial Young modulus and the tangent modulus of elasticity of existing vertical steel bars after yielding, respectively.

4.7.2.1.4 Failure due to tensile stresses on the beam-column joint.

- (1) Beam-column joints of RC members can be effectively strengthened with FRP only when FRP reinforcement is applied with the fibers running in the direction of principal tensile stresses and provided the FRP reinforcement is properly anchored. In any case, the maximum tensile strain for FRP reinforcement shall not be larger than 4%. When FRP reinforcement is not properly anchored, FRP strengthening is not considered effective.

4.7.2.2 Removal of all story collapse mechanisms

- (1)P Story collapse mechanisms usually begin after the formation of plastic hinges at column top and bottom locations of structures with no vertical walls. In this case, FRP strengthening is performed to enhance the column’s flexural capacity with the intent of precluding the formation of plastic hinges. In no case is the removal of the story collapse mechanisms allowed with the sole intent of increasing story displacements.

4.7.2.3 Enhancement of the overall deformation capacity of a structure

- (1)P The ultimate deformation capacity of a structure is a measure of its ability to resist seismic forces and depends on the plastic deformation capacity of each single resisting member (beams, columns, and walls).

4.7.2.3.1 Increasing of the local rotational capacity of RC members

- (1) The deformation capacity of beams and columns can be measured through the rotation θ of the end section in comparison to the line generated between the section of zero moment and the end section (chord rotation) at a distance equal to the shear span: $L_v = M/V$. This rotation is also equal

to the ratio of the relative displacement between the two above mentioned sections to the shear span.

(2)P The deformation capacity of RC members in the plastic range is limited by the failure of concrete in compression. FRP confinement increases the ultimate deformation capacity of compressed concrete and enhances the ductility of the strengthened member.

4.7.2.3.2 Strategic relocation of plastic hinges – Capacity design criterion

(1)P The application of the capacity design criteria (hierarchy of resistance) implies the adoption of mechanisms such to prevent the formation of all potential plastic hinges in the columns. In the “weak column-strong beam” case, typical for structures designed for vertical loads only, the columns are under-designed due to the lack of longitudinal reinforcement. In this case, it is necessary to increase the column capacity under combined bending and axial load toward a “strong column-weak beam” situation.

(2)P When FRP reinforcement is used to increase the flexural capacity of a member, it is important to verify that the member is capable of resisting the shear forces associated with the increased flexural strength. If necessary, shear strengthening shall be taken into account to avoid premature brittle failures.

4.7.2.3.3 Ultimate rotation of strengthened elements

(1) Evaluation of the ultimate chord rotation, θ_u , of a member strengthened with FRP confinement, shall be evaluated imposing the ultimate strain of confined concrete, ε_{ccu} , as stated in Section 4.5.3.

4.8 INSTALLATION, MONITORING, AND QUALITY CONTROL

(1)P Several aspects influence the effectiveness of FRP material used as externally bonded systems for strengthening RC members. In addition to those discussed in previous chapters, surface preparation and FRP installation will be discussed in this section.

4.8.1 Quality control and substrate preparation

(1) Quality control of the support implies the determination of concrete conditions, removal of any deteriorated or loose concrete, cleaning and protection from corrosion of existing steel reinforcement, and finally substrate preparation for receiving the selected FRP reinforcement.

(2) When special devices are used to properly anchor the selected FRP system, testing of such devices shall be conducted in compliance with available standardization documents. Anchoring devices shall be installed according to the manufacturer/supplier specifications regarding both the material used and surface preparation, environmental conditions, and sequence of each phase. The investigation shall also evaluate the effects of such parameters on the final result.

4.8.1.1 Evaluation of substrate deterioration

(1) Prior to FRP application, the designer and construction manager shall verify the quality of the concrete substrate following the prescription of Chapter 6. In any case, the concrete compressive strength shall not be less than 15 N/mm^2 .

(2) It is suggested to perform quality control tests on the entire area to be strengthened.

4.8.1.2 Removal of defective concrete, restoring of concrete substrate and protection of existing steel reinforcement

- (1) Concrete substrate may have undergone physical-chemical, physical-mechanical, or impact-causing deterioration. Deteriorated concrete shall be removed from all damaged areas.
- (2) Removal of unsound concrete allows for the assessment of existing reinforcing steel bars. Corroded steel bars shall be protected against further corrosion so as to eliminate a possible source of deterioration of the restored concrete.
- (3) Once all deteriorated concrete has been removed, and suitable measures have been taken to prevent further corrosion of existing steel reinforcement and other phenomena causing concrete degradation (*e.g.*, water leakage), concrete restoration using shrinkage-free cement grouts shall be performed.
Concrete surface roughness larger than 10 mm shall be leveled with a compatible epoxy paste; specific filling material shall be used for unevenness larger than 20 mm. Also, cracks wider than 0.5 mm within solid concrete in the substrate shall be stabilized using epoxy injection methods before FRP strengthening can take place.

4.8.1.3 Substrate preparation

- (1) Once the quality control of the substrate has been performed, the deteriorated concrete has been removed, the concrete cross section has been restored, and the existing steel reinforcement has been properly treated, sandblasting of the concrete surface shall be performed. Sandblasting shall provide a roughness degree of at least 0.3 mm; and the level of roughness can be measured using suitable instruments (*e.g.*, a laser profilometer or an optical profile-measuring device)
- (2) Poor concrete surfaces that do not require remedial work before FRP application, should be treated with a consolidating agent before *primer* application takes place.
- (3) Cleaning of the concrete surface shall remove any dust, laitance, oil, surface lubricants, foreign particles, or any other bond-inhibiting material.
- (4) All inside and outside corners and sharp edges shall be rounded or chamfered to a minimum radius of 20 mm.

4.8.2 Recommendations for the installation

- (1) FRP strengthening of RC members is highly dependent upon environmental temperature and humidity as well as the characteristics of the concrete substrate.

4.8.2.1 Humidity and temperature conditions in the environment and substrate

- (1) It is suggested not to install FRP material when the environment is very moist. A high degree of humidity may delay the curing of resin and affect the overall performance of the strengthening system specifically for wet lay-up applications.
- (2) FRP systems shall be installed in humidity and temperature conditions as defined by the materials data sheet.
- (3) If curing of the FRP reinforcement takes place in rainy conditions, heavy insulation, large thermal gradients, or in the presence of dust, protective measures can be employed to ensure proper curing.

4.8.2.2 Construction details

- (1) Anchorage (bond) length of at least 200 mm shall be provided for the end portion of FRP systems used for strengthening RC members. Alternatively, mechanical connectors may be used.
- (2) In shear, torsional and confinement installations and prior to FRP application, the cross section edges shall be rounded to avoid stress concentrations that could result in a premature failure of the system. The corner radius shall be at least 20 mm.
- (3) Proper fibers alignment shall be provided for in-situ wet lay-up application. Waving of FRP reinforcement shall also be avoided during installation.
- (4) When carbon fiber reinforcement is used for strengthening RC members and there is potential for direct contact between the carbon and existing steel reinforcement, layers of insulating material shall be installed to prevent the occurrence of galvanic corrosion.
- (5) When semi-destructive tests are performed, it is suggested to provide additional strengthening areas (“witness areas” or “test areas”) in selected parts of the structure having dimensions of at least $500 \times 200 \text{ mm}^2$, with a minimum extension of 0.1 m^2 but not less than 0.5% of the overall strengthened area. Test areas shall be realized at the same time of the main FRP installation, using the same materials and procedures in areas where removal of FRP strengthening system does not imply alteration of the failure mechanisms. In addition, witness areas shall be exposed to the same environmental conditions as the main FRP system and shall be uniformly distributed on the strengthened structure.

4.8.2.3 Protection of the FRP system

- (1) For outdoor FRP applications, it is recommended to protect the FRP system from direct sunlight, which may produce chemical-physical alterations in the epoxy matrix. This can be achieved by using protective acrylic paint provided that cleaning of the composite surface with a sponge and soap is performed.
- (2) Alternatively, better protection can be achieved by applying a layer of plaster or mortar (preferably cement-based) to the installed strengthening system. The plaster, whose thickness is recommended by the FRP manufacturer/supplier, is to be laid on the strengthening system after treating the surface by means of epoxy resin applications with subsequent quartz dusting green-on-green.
- (3) For fire protection, two different solutions may be adopted: the use of intumescent panels or the application of protective plasters. In both cases, the manufacturer/supplier shall indicate the degree of fire protection as a function of the panel/plaster thickness. The panels, generally based on calcium silicates, are applied directly to the FRP system provided the fibers will not be cut during installation. Protective plasters represent the most widely adopted solution for fire protection and shall be applied as indicated in item (2).

4.9 NUMERICAL EXAMPLES

Some numerical examples concerning the FRP strengthening of RC structures are reported in Appendix G.

5 STRENGTHENING OF MASONRY STRUCTURES

5.1 INTRODUCTION

5.1.1 Scope

(1)P This chapter specifies design recommendations for masonry structural members strengthened with FRP.

(2)P The primary objective of FRP strengthening is to increase the capacity of each member as well as the overall capacity of the masonry structure. Whenever possible, the enhancement of structural displacement at failure is also recommended.

5.1.2 Strengthening of historical and monumental buildings

(1)P Strengthening of historical and monumental buildings shall be justified and carefully detailed. Adopted strengthening technique shall be in compliance with the theory of restoration (see Section 3.1(3)).

5.1.3 FRP strengthening design criteria

(1) Strengthening methodologies addressed in this document consist of the application of FRP materials in the form of laminates, sheets, grids, and bars installed on the members by adhesion or by means of mechanical anchorage devices. FRP reinforcement may be applied to the external surfaces of the masonry structure as well as in slots or grooves cut in the masonry itself.

(2) FRP strengthening can be employed for the following reasons:

- Enhancement of capacity in panels, arches or vaults.
- Column confinement in order to increase compressive capacity and ductility.
- Connection between members (vault and wall ties, connections between orthogonal walls, etc.).
- Transformation of non-structural elements in a structural element providing additional stiffness and capacity.
- Crack width limitation.

(3)P Strengthening applications shall always be related to the overall behavior of the consolidated structure.

(4) Design of FRP reinforcement shall ensure that the selected FRP system is always in tension. In fact, FRP in compression is unable to increase the performance of the strengthened masonry member due to its small area compared to that of compressed masonry. Moreover, FRP in compression may be subjected to debonding due to local instability.

(5) For masonry structures strengthened with FRP and subjected to cyclic loads (*e.g.*, seismic, thermal variations), the bond between masonry and FRP may degrade remarkably during the structure's lifetime. In such a case, it could be necessary to properly anchor the FRP system to the masonry by either inserting FRP reinforcement in suitable grooves to prevent local instability or applying mechanical anchoring devices.

(6) FRP strengthening shall be applied to structural members having suitable mechanical prop-

erties. If the masonry is damaged, not uniform, or cracked, it shall be repaired with appropriate techniques to ensure a proper sharing of loads between support and FRP. The selection of the appropriate strengthening material (carbon, glass, or aramid FRP) shall also take into account physical and chemical properties of the masonry (further details are discussed in Section 5.8).

(7) FRP reinforcement that completely encases the strengthened member may prevent moisture absorption. Such FRP systems shall not be applied continuously on extended areas of the wall surface to ensure moisture absorption.

5.2 DESIGN ASSUMPTIONS

5.2.1 Structural modeling

(1)P Design of FRP reinforcement shall be based on a structural scheme representing the behavior of the building for the expected future use.

(2) The structure can be modeled through proven non linear models capable of simulating the inelastic behavior and the negligible tensile strength of the masonry. Linear elastic models can be also used if in compliance with the following item (3). Structural modeling shall be used to evaluate internal forces acting on the masonry.

(3) Simplified schemes can also be used to describe the behavior of the structure. For example, provided that tensile stresses are directly taken by the FRP system, the stress level may be determined by adopting a simplified distribution of stresses that satisfies the equilibrium conditions but not necessarily the strain compatibility. The use of simplified stress distributions should be carefully chosen because a statically satisfactory stress level may have caused the structure to collapse due to the brittle nature of the FRP-masonry system.

(4) In the case of structures with regular or repetitive parts, partial structural schemes may be identified to allow for a rapid evaluation of the overall behavior of the strengthened structure.

(5) Simplified models may be adopted for verifications of local failure mechanisms, provided that their use is correctly motivated.

In these cases method of limit analysis shall be used.

5.2.2 Failure modes

(1)P Possible failure modes of masonry walls strengthened with FRP systems can be summarized as follows:

- Excessive cracking due to tensile stresses in the wall;
- Crushing of masonry.
- Shear-slip of masonry.
- FRP rupture.
- FRP debonding.

Failure modes of FRP strengthened masonry structures usually involve a combination of the above mentioned mechanisms.

5.2.3 Design requirements

(1)P Masonry can be considered an anisotropic material exhibiting a non-linear behavior. The

stress-strain relationship may vary quite significantly depending whether the structure is built with artificial or natural blocks as well as the type of mortar employed.

(2) Masonry exhibits a brittle behavior when subjected to tensile loading, therefore the corresponding tensile strength is negligible compared to its compressive strength. For design purposes, it is accepted to neglect the tensile strength of masonry.

(3)P Laboratory tests show that the stress-strain diagram of masonry blocks subjected to compressive loads can be described as follows:

- Linear for low strain values.
- Non-linear as the load increases up to the ultimate value.
- Non-linear softening after the load at ultimate has been reached.

(4)P The masonry behavior for compressive loading also depends on the availability of transverse confinement. By increasing the transverse confinement, the strength and ductility of the material is improved.

(5)P Masonry shear strength depends on the applied axial load because it usually depends on the cohesion and friction of the material.

(6) On-site masonry is characterized by average values of mechanical properties (Section 3.3.3(6)). The characteristic values for strength are as follows:

- Vertical compressive strength, f_{mm} ;
- Horizontal compression strength, f_{mm}^h ;
- Shear strength, f_{vm} .

A reference value of f_{mm}^h can be assumed as 50% of f_{mm} .

(7) Values of mechanical properties shall be in compliance with Section 3.3.3.

(8) For most engineering applications, the stress-strain constitutive law of masonry under uniaxial loads may be simplified as follows:

- tensile stress: shall be neglected;
- compression: linear behavior with the slope equals to the secant modulus of elasticity up to both the design strength of f_{md} , and design strain of $\bar{\varepsilon}_m$. The design strength is equal to f_{md} for strain between $\bar{\varepsilon}_m \leq \varepsilon \leq \varepsilon_{mu}$, and zero strength for strain larger than ε_{mu} .

(9) Unless experimental data is available, the masonry ultimate design strain, ε_{mu} , is equal to 3.5‰.

(10) Alternatively, appropriate stress-strain diagrams embracing the behavior described in (3)P may be used, provided that their performance is validated on the basis of experimental investigations.

(11) The maximum design strain allowed to the FRP system shall be expressed as follows:

$$\varepsilon_{fd} = \min \left\{ \eta_a \cdot \frac{\varepsilon_{fk}}{\gamma_f}, \varepsilon_{fdd} \right\}, \quad (5.1)$$

where ε_{fk} represents the FRP characteristic strain at failure, and ε_{fdd} is the maximum FRP strain after FRP debonding takes place (Section 5.3, Equation (5.10)).

The values assigned to the conversion factor η_a , and the partial factor, γ_f are indicated in Table 3-2 and Section 3.4.1 respectively.

In the presence of high level of humidity, η_a shall be evaluated with caution.

(12) Design recommendations are based on limit-states-design principles.

For an ultimate limit states analysis, two possible approaches may be recognized depending on the type of structural analysis performed. If non linear models are used, the member's load carrying capacity shall be greater than the factored applied load. The latter is computed according to the current building code. Care shall be taken to ensure that the proposed solution is not affected by the particular discretization adopted for the computation.

If linear elastic models or simplified schemes adopting a balanced distribution of stresses that satisfy equilibrium conditions but not necessarily compatibility of strain are used, the resulting stress on each structural member shall be verified. In particular, for bi-dimensional members (slabs, shells), the unit stress shall be considered (*e.g.*, those evaluated per unit length of the member). Assuming that a plane section before loading remains plane after loading, the design criteria is met when factored shear forces and bending moments due to the applied loads are smaller than the corresponding design factored shear and flexural capacities. The latter shall be evaluated as a function of the applied axial force, considering the non-linear behavior of the material represented by the simplified stress-strain diagram introduced in item (8)P.

5.3 EVALUATION OF DEBONDING STRENGTH

(1)P The bond between masonry and FRP is of great relevance because debonding yields to undesirable, brittle failure modes. When designing according to the capacity design criterion, FRP debonding shall always follow the post-elastic behavior of compressed masonry.

(2) Due to the wide variety of existing masonry structures (*e.g.*, artificial clay, concrete masonry blocks, squared or non-squared stones, etc.), debonding may occur at the interface between different materials. Moreover, in masonry structures with irregular faces, a layer of mortar may be used to create a suitable surface for FRP application. The same strengthening system may then be linked to different materials characterized by different interface properties.

(3) If the tensile strength of the adhesive used to install FRP reinforcement is larger than that of the substrate, debonding between FRP and masonry will occur at the masonry face-level.

5.3.1 General considerations and failure modes

(1)P Debonding between FRP reinforcement applied in isolated strips along straight lines and the masonry may occur in the following failure modes: plate end debonding or intermediate crack debonding. In masonry structures strengthened with FRP and loaded to tensile stresses in FRP reinforcement both at laminate ends as well as close to the locations of existing cracks, the FRP-masonry interface undergoes high stresses localized within 150 to 200 mm from the discontinuity section.

(2)P Shear debonding occurs close to FRP reinforcement ends (anchorage sections) and may be followed by removal of a significant portion of brick (rip-off failure), specifically when shear

stresses at the FRP end are combined with normal tensile stresses. This failure mode appears with the formation of cracks due to spreading of anchorage stresses that may be accompanied by tensile stresses in the masonry responsible for its fracture (Figure 5-1).

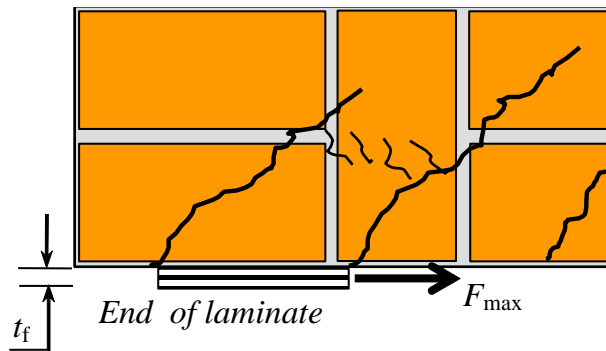


Figure 5-1 – Failure due to rip-off of the anchorage brick.

(3)P Combined stresses reduce the bond strength. In particular, when FRP strengthening is applied to curved surfaces or when high flexural stiffness FRP reinforcement is used, significant tensile stresses perpendicular to the masonry-FRP interface (peeling stresses) arise, and reduce the force that may be transferred.

(4) P The effectiveness of FRP systems is maximum with respect to cracks opening and propagation when applied fibers are inclined in the orthogonal direction of the crack. Stresses around cracks generated by relative movements produce a stress concentration at the masonry-FRP interface

5.3.2 Design strength for laminate/sheet end debonding

(1)P Experimental bond tests in **Figure 5-2** show that the ultimate value of the force transferred from FRP reinforcement to the support prior to FRP debonding depends on the length, l_b , of the bonded area.

This value grows with l_b up to a maximum corresponding length, l_e : further increase of the bond area does not increase the force that it is possible to transfer.

The length l_e is called optimal bond length and corresponds to the minimal bond length able to carry the maximum anchorage force.

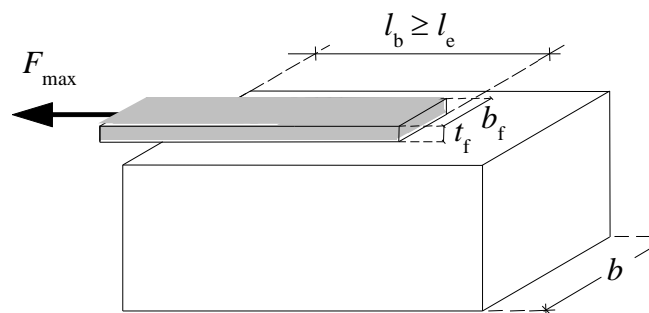


Figure 5-2 – Maximum force transferred between FRP and concrete.

(2) The optimal bond length, l_{ed} , shall be estimated as follows:

$$l_{ed} = \max \left\{ \frac{1}{\gamma_{Rd} \cdot f_{bd}} \sqrt{\frac{\pi^2 \cdot E_f \cdot t_f \cdot \Gamma_{Fd}}{2}}; 150 \text{ mm} \right\}. \quad (5.2)$$

Where E_f and t_f are the Young modulus of elasticity of FRP reinforcement and the FRP thickness, respectively. Γ_{Fd} is the design value of specific fracture energy, γ_{rd} is a corrective factor equal to 1.5 for tuff and perforated stones, and 1.25 for calcarenite masonry and Lecce stones. f_{bd} is the design bond strength between FRP and masonry and is calculated as follows:

$$f_{bd} = \frac{2 \cdot \Gamma_{Fd}}{s_u} \quad (5.3)$$

If experimental data are not available, s_u in Equation (5.3) is equal to 0.4 mm for tuff stones and perforated bricks, and 0.3 mm for calcarenite masonry and Lecce stones (see Appendix D).

The design value of the specific fracture energy is computed as follows:

$$\Gamma_{Fd} = \frac{k_b \cdot k_G}{FC} \cdot \sqrt{f_{bm} \cdot f_{btm}} \quad (5.4)$$

The symbols in Equation (5.4) assume the following meanings:

- k_b is a geometrical corrective factor.
- k_G is a corrective factor, expressed in mm and dependent on the type of masonry (for wet-lay up systems):
 - for perforated bricks masonry: $k_G = 0.031$ mm;
 - for tuff masonry: $k_G = 0.048$ mm;
 - for calcarenite and Lecce stones masonry: $k_G = 0.012$ mm;
- FC is a confidence factor.
- f_{bm} and f_{btm} are the average compressive and tensile strength of masonry blocks, respectively. In absence of experimental evidences, the average tensile strength can be computed as $0.10 f_{bm}$.

If experimental data are not available, k_b can be computed as follows:

$$k_b = \sqrt{\frac{3 - b_f / b}{1 + b_f / b}} \quad (5.5)$$

where b and b_f are the width of the strengthened element and FRP, respectively. The value of b can be computed as a sum of the quantity b_f and the width of the bond strength distribution area, b_d . In the case of masonry with irregular shaped stones, b_d can be considered equal to the average diameter of the stones (Figure 5-3).

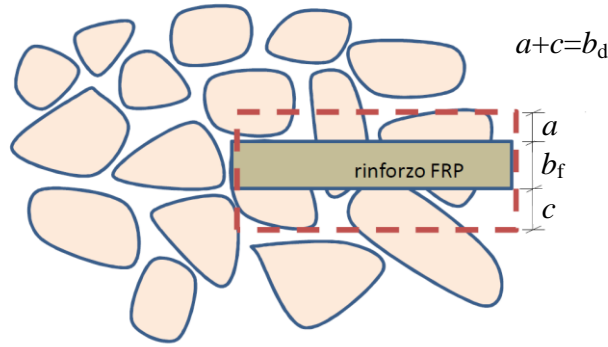


Figure 5-3 – Bond strength distribution for irregular shapes stones.

In the case of masonry with regular shaped stones, b_d is equal to the support block dimension in the perpendicular direction of the FRP principal axis (Figure 5-4).

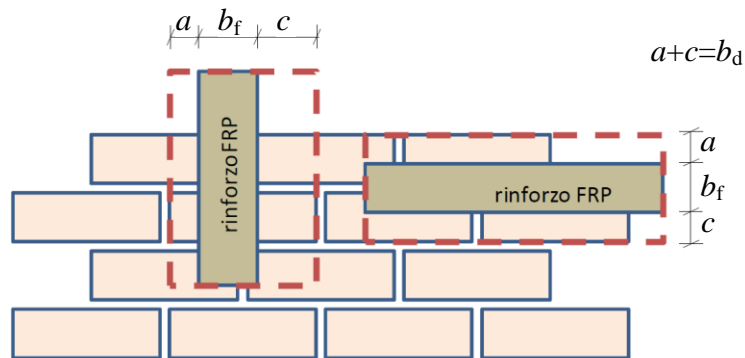


Figure 5-4 –Bond strength distribution for regular shaped stones.

For pre-cured systems, the values of k_G previously stated shall be reduced to 40%. Equations reported in item (2) are considered valid when using low viscosity epoxy resin in order to ensure the penetration through the pores present in the masonry block. High viscosity epoxy and low porosity supports shall be used carefully.

(3) When debonding involves the first masonry layers and the bond length is longer or equal to the optimal bond length, the design bond strength shall be expressed as follows:

$$f_{fd} = \frac{1}{\gamma_{f,d}} \cdot \sqrt{\frac{2 \cdot E_f \cdot \Gamma_{Fd}}{t_f}}, \quad (5.6)$$

where $\gamma_{f,d}$ is the partial factor as per Section 3.4.1.

In case of application to masonry with a joint distance smaller than the optimal bonding length, the design bond strength from Equation (5.6) shall be reduced to 85% of its value.

(4) For bond lengths, l_b , smaller than l_{ed} , the design bond strength shall be reduced as follows:

$$f_{fd,rid} = f_{fd} \cdot \frac{l_b}{l_{ed}} \cdot \left(2 - \frac{l_b}{l_{ed}} \right) \quad (5.7)$$

(5) When special anchorage devices (FRP transverse bars, FRP end wrapping) are used, the maximum bond force shall be evaluated with experimental investigations.

(6) When FRP systems are applied in intermediate epoxy layer due to irregularity on the masonry surface, debonding strength shall be evaluated at the interface between the layer of regularization and the masonry, provided that the simultaneous curing of the epoxy resin on the mortar and the FRP resin is ensured. In this case Equations (5.2)-(5.7) are still applicable unless there are more stringent requirements. The thickness, t_h , and Young's modulus of elasticity, E_h , of the homogeneous system made of FRP and layer of regularization shall be calculated as follows:

$$t_h = t_f + t_r, E_h = \frac{E_f \cdot t_f + E_r \cdot t_r}{t_h} \quad (5.8)$$

where t_f and E_f are the thickness and Young modulus of elasticity of the regularization layer, respectively. The thickness t_f can be estimated knowing the volume of material applied to the masonry surface and assuming the layer equivalent to a cylindrical solid. Bonding strength capacity shall be computed by using Equations (5.2)-(5.7) where $b_h = b_f + 2 \cdot t_f$.

5.3.3 Design strength for intermediate debonding

(1) In absence of more accurate indications, the intermediate debonding shall be performed by limited the debonding strength of FRP to the design value:

$$f_{\text{idd},2} = \alpha \cdot f_{\text{idd}} \quad (1.0 \leq \alpha \leq 2.0). \quad (5.9)$$

In particular, if the distance from the free end is smaller than $3 \cdot l_e$, then $\alpha = 1.5$.

Assuming in Equation (5.1):

$$\varepsilon_{\text{idd}} = \frac{f_{\text{idd},2}}{E_f}, \quad (5.10)$$

where E_f is the Young's modulus of elasticity of FRP, the code requirements are implicitly met. However, debonding strength capacity shall be verify as per Section 5.3.2.

5.3.4 Bond strength with stresses perpendicular to the bond surface

(1) Experimental data carried out on FRP strengthened masonry structures should be used for the determination of the bond strength in case of stresses occurring perpendicular to the bonding surface.

(2) The same procedure can be used for slightly curved profile FRP systems.

5.3.5 Mechanical anchorage devices

(1)P Bond capacity can be increased up to FRP failure by using mechanical anchorage devices.

(2) Mechanical anchorage devices shall be tested in order to provide experimental evidences of the functionality of the system.

(3) Mechanical anchorage devices are described as follows:

- Clamping of the external FRP reinforcement by means of steel plates tied to the masonry by means of dowels.
- Anchoring of the external FRP reinforcing by means of dowels, strengths and FRP nails inserted orthogonally.
- After grooving the masonry in a direction perpendicular to the direction of the reinforcement, insert a bar into the groove over the external FRP reinforcement.
- Addition of an FRP strip bonded perpendicular to the direction of the reinforcement.

(4) When mechanical anchoring devices are used in combination with a pre-cured laminate, prestressed behavior is generated within the FRP system. In this case, the strength design shall include the prestressed behavior of the laminate.

5.4 SAFETY REQUIREMENTS

(1) Principles as stated in Section 5.2 are hereafter referred to as practical applications.

5.4.1 Strengthening of masonry panels

(1) Masonry panels may be strengthened with FRP to increase their load carrying capacity and/or ductility for in-plane or out-of-plane loading. In the following sections, simple requirements to control the degree of safety of the strengthened masonry panel are suggested. Such requirements are not exhaustive and should be integrated with further analysis suitable to the complexity of the case studied.

5.4.1.1 Strengthening for out-of-plane loads

(1) Out-of-plane collapse of masonry panels is one of the most frequent types of failure for masonry structural masonry members. This failure mode is primarily due to seismic actions and secondary horizontal forces created by the presence of arches and vaults. Out-of-plane collapse can appear as any of the following:

- Simple overturning (Section 5.4.1.1.1);
- Vertical flexure failure (Section 5.4.1.1.2);
- Horizontal flexure failure (Section 5.4.1.1.3).

5.4.1.1.1 Simple overturning

(1) Kinematic motion is represented by an overturning about a hinge at the bottom of the masonry panel. Due to the small tensile strength of the masonry, the hinge is usually located on the outer surface of the panel.

Collapse by overturning may occur in the presence of walls not connected to the orthogonal walls nor restrained at their top. Collapse by overturning may depend on several factors, such as boundary conditions, slenderness of the wall, and geometry of the masonry member.

A possible retrofitting technique may consist of the use of FRP applied to the top portion of the masonry panel and then properly anchored to the orthogonal walls. When orthogonal pilasters are present within the masonry panel, FRP can be modeled to conform to surface irregularities. However, this solution may lead to tensile stresses within the support and possible debonding. Mechanical anchoring devices shall be used to mitigate the risk of localized failure.

An optimal solution from a performance point of view, is embracing the entire perimeter of the building with the selected FRP system. Particular care shall be taken in the rounding of masonry corners to avoid stress concentration in the FRP, as indicated in Section 5.8.2.2.

As an example, a masonry panel subjected to the following loads (design values) is considered:

- P_d panel self weight,
- N_d axial force acting at the top of the panel,
- α_s ratio between vertical and horizontal loads,
- F_d force exerted on the masonry panel by the FRP system.

Other loads may be applied at the top end of the wall.

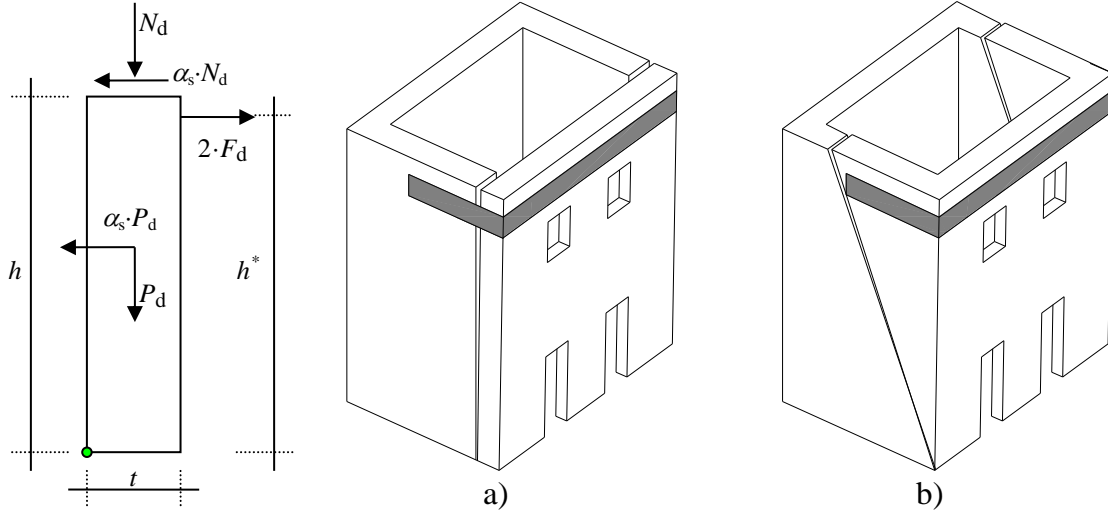


Figure 5-5 – Collapse mechanisms by simple overturning.

Assuming that floors and walls perpendicular to the panel being studied provide negligible restraint to the panel itself (Figure 5-5a), a tensile force in the FRP reinforcement can be calculated using the moment equilibrium equation as follows:

$$F_d = \frac{1}{2 \cdot h^*} \cdot \left[\alpha_s \cdot \left(P_d \cdot \frac{h}{2} + N_d \cdot h \right) - (P_d + N_d) \cdot t \right], \quad (5.11)$$

where h^* is the distance between FRP and the bottom portion of the masonry panel. To prevent simple overturning of the masonry panel, the two following conditions shall be met:

- FRP tensile strength:

$$F_d \leq F_{Rd} . \quad (5.12)$$

where: $F_{Rd} = A_f \cdot f_{fd}$, $f_{fd} = E_f \cdot \varepsilon_{fd}$ and A_f is the FRP reinforcement area.

- Rip-off of FRP from orthogonal walls:

$$F_d \leq F_{pd} . \quad (5.13)$$

where: $F_{pd} = A_f \cdot f_{idd}$ represents the maximum anchorage force of the FRP applied to one of the two orthogonal walls.

Usually, the rip-off is more demanding than the tensile strength in the FRP.

If the structure is not fully wrapped, the installation of FRP shall be extended to the orthogonal walls in order to avoid mechanisms of failure as in Figure 5-5 b). This calculation can be performed using a limit analysis and neglecting the contribution of masonry internal cohesive strength. The

collapse mechanism of Figure 5-5 b) identifies the failure surface that goes from the plastic hinge to the two terminal sections of FRP.

(2) Additionally, determination of stresses due to the combined bending moment and axial load as well as determination of shear force on panel horizontal sections, shall be performed according to the current building code.

5.4.1.1.2 Vertical flexural failure

(1) For masonry panels restrained at both top and bottom and subjected to horizontal loading, failure may occur due to flexure with the formation of three hinges: one at the bottom of the panel, one at the panel top and the last at a certain panel height.

Flexural collapse may occur in high masonry panels and/or panels restrained or far apart from orthogonal walls.

In the case of seismic loading, masonry panels loaded from opposite sides by floors located at different heights are particularly sensitive to flexural collapse. This type of masonry panels may be strengthened with FRP having fibers running in the vertical direction.

For example, a unit strip of masonry panel is strengthened with FRP and subject to the following external loading (design values) (Figure 5-6):

- $P_d^{(s)}$ weight of the upper side of the panel.
- $P_d^{(i)}$ weight of the lower side of the panel.
- N_d axial force acting on the panel.
- α_s ratio between vertical and horizontal loads.
- Q_d load due to horizontal loading.

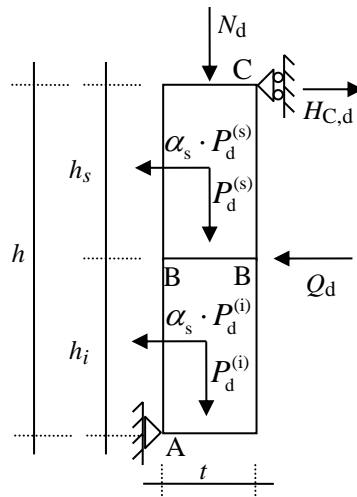


Figure 5-6 – Collapse mechanism by vertical flexure.

By force equilibrium around A, the horizontal reaction in C may be calculated as follows:

$$H_{C,d} = \frac{h_i \cdot (2 \cdot Q_d + \alpha_s \cdot P_d^{(i)}) + \alpha_s \cdot P_d^{(s)} \cdot (2 \cdot h - h_s) - t \cdot (N_d + P_d^{(s)} + P_d^{(i)})}{2 \cdot h} \quad (5.14)$$

The masonry panel at section B-B, where the FRP is applied to prevent formation of the hinge, is subject to an axial force and bending moment equal to the following:

$$\begin{aligned} N_{sd} &= N_d + P_d^{(s)}, \\ M_{sd} &= H_{C,d} \cdot h_s - \alpha_s \cdot P_d^{(s)} \cdot \frac{h_s}{2}. \end{aligned} \quad (5.15)$$

The masonry panel flexural capacity is verified when the following relationship is satisfied:

$$M_{sd} \leq M_{Rd}. \quad (5.16)$$

The flexural capacity of the strengthened masonry panel, M_{Rd} , may be determined as a function of the mechanical characteristics of the masonry and FRP (Section 5.2.3), the thickness of the masonry panel, t , the value of the applied axial force and the partial factor for resistance models, γ_{Rd} , that is equal to 1.00 (Table 3-1 in Section 3.4.2).

(2) The compressive stress-strain relationship for masonry is assumed to be rectangular with a uniform compressive stress of $0.85 f_{md}$, distributed over an equivalent compression zone bounded by the edges of the cross section and a straight line located parallel to the neutral axis, x , at a distance of $0.6 \div 0.8 x$.

(3) The factored shear force, V_{sd} , shall not exceed the shear capacity:

$$V_{Rd,m} = 1 \cdot x \cdot f_{vd}, \quad (5.17)$$

where f_{vd} is the design shear strength of masonry computed in accordance with the building code.

(4) Design strength for FRP end debonding shall be also verified.

(5) FRP vertical reinforcement shall be placed at a center-to-center distance, p_f , such that:

$$p_f \leq 3 \cdot t + b_f, \quad (5.18)$$

where b_f is the FRP width. Larger center-to-center spacing can be used only if adequately justified.

5.4.1.1.3 Horizontal flexural failure

(1) Figure 5-7 shows kinematic mechanisms for masonry panels firmly connected with transverse walls but not restrained with connections at the top. In this configuration, the resistance to horizontal forces is ensured by the arching effect of the top strip as illustrated in Figure 5-8. The value of the maximum uniformly distributed horizontal load, q_d , which can be carried by the arch mechanism can be expressed as follows:

$$q_d = \frac{2 \cdot t^2}{3 \cdot L^2} \cdot f_{md}^h, \quad (5.19)$$

where L is the panel width, and f_{md}^h represents the design compressive strength of the masonry in the horizontal direction.

FRP systems can help to increase the value of q_d .



Figure 5-7 – Collapse by horizontal flexure.

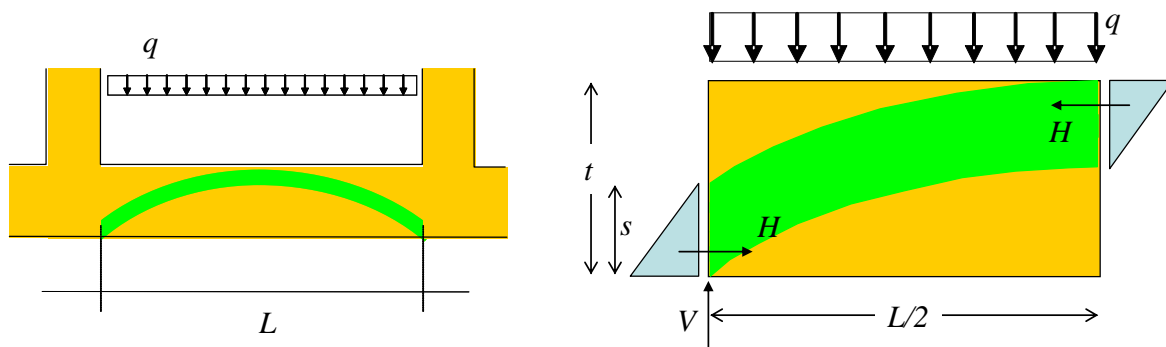


Figure 5-8 – Collapse by horizontal inflection.

For a masonry beam to be strengthened, the use of adequately bonded FRP prevents such mechanisms from failure by providing flexural capacity to the mentioned unit strip. The height of the horizontal masonry strip to be strengthened with FRP shall be taken as half of the entire panel height unless further evaluations are available.

In the example, the applied bending moment, M_{Sd} , is considered due to earthquake loads or wind pressure with respect to the wall inertia.

- (2) The horizontal FRP strip shall be verified also for the floor and ceiling that interact with the panel. In such cases, the thickness of the horizontal FRP strip can be computed considering a stress distribution of 45° .
- (3) Flexural safety of the masonry panel is satisfied when Equation (5.16) is met, and may be determined as a function of the mechanical characteristics of masonry and FRP and the thickness, t , of the masonry panel. Unless a more detailed analysis is available, the horizontal force due to the presence of transversal walls may be considered equal to zero.
- (4) An additional shear check shall be carried out on the connection joints between the masonry panel and transverse walls, as per Section 5.4.1.1.2 (3), assuming f_{vd} equal to zero.
- (5) Design strength for FRP end debonding shall be also verified.
- (6) Verification of the magnitude of tensile loads on transverse walls close to the main masonry panel shall also be performed

5.4.1.2 Strengthening for in-plane loads

(1) The following checks shall be carried out for masonry panels subjected to in-plane loading:

- In-plane combined bending and axial load,
- Shear force.

5.4.1.2.1 In-plane combined bending and axial load

(1) Vertical FRP systems, symmetrically installed on both panel sides and adequately bonded at the surface, can be used to enhance the combined bending and axial load currying capacity.

(2) A simplified procedure to evaluate the combined bending and axial capacity can be performed as indicated in Section 5.4.1.1.2 (2).

(3) In particular, the capacity of panel end sections delimited by the foundation and the first level or between two consecutive floors shall be computed. FRP contribution is neglected if mechanical anchorage devices are not present.

5.4.1.2.2 Shear capacity

(1)P The shear capacity of masonry panels strengthened with FRP applied to both sides of the panel can be incremented by further applying FRP to both sides with fibers placed parallel to the shear direction. By using this system, the shear capacity can be observed as the combination of two resisting mechanisms: (1) shear forces due to friction in presence of compression loads, and (2) for elements capable of resisting tensile stress a truss mechanism becomes active, and shear forces are determined by equilibrium.

(2) When formation of truss mechanism is ensured, the design shear capacity V_{Rd} , of the FRP strengthened masonry panel is computed as the sum of the masonry contribution, $V_{Rd,m}$, and the FRP contribution, $V_{Rd,f}$, up to the maximum value $V_{Rd,max}$ inducing failure of the compressed strut of the truss:

$$V_{Rd} = \min \{ V_{Rd,m} + V_{Rd,f}; V_{Rd,max} \}. \quad (5.20)$$

If shear strengthening is placed parallel to the mortar joints, the above defined variables may be evaluated as follows:

$$V_{Rd,m} = x \cdot t \cdot f_{vd}, \quad (5.21)$$

$$V_{Rd,f} = \frac{1}{\gamma_{Rd}} \cdot 0.6 \cdot d \cdot (E_f \cdot \varepsilon_{fd}) \cdot 2 \cdot t_f \cdot \frac{b_f}{p_f}, \quad (5.22)$$

where:

- x is the distance of the neutral axis from the extreme compression fiber.
- t is the masonry panel thickness.
- f_{vd} is the design shear strength of the masonry, as per the building code, equal to the ratio of the sum of the compressive forces and the area between extreme compression member and neutral axis, $x \cdot t$.
- E_f is the FRP Young's modulus of elasticity in the fiber direction.
- ε_{fd} is the FRP ultimate strain as per Equation (5.1).

- t_f is the thickness of FRP.
- b_f and p_f , are the width and center-to-center spacing of FRP strips measured orthogonally to the fiber direction, respectively. For FRP strips applied adjacent to one another, the ratio b_f/p_f is equal to 1.0.

The partial factor for resistance model, γ_{Rd} , is equal to 1.20 (Table 3-1 of Section 3.4.2). If the angle of friction, φ , of mortar joints is smaller than 45° , the value of $V_{Rd,f}$ provided by Equation (5.22) shall be reduced by a multiplicative factor equal to $\cotg(90^\circ - \varphi)$. The angle φ can be computed from the compressive and tensile strength of mortar.

(3) In the vertical direction, FRP shall be placed in order to ensure the formation of the truss mechanism as an element in tension. Moreover, the shifting of the bending moment diagram shall be also taken into account.

(4) The design shear capacity of the masonry panel, $V_{Rd,max}$, corresponding to the failure of the compressed strut of the truss can be calculated as follows:

$$V_{Rd,max} = 0.3 \cdot f_{md}^h \cdot t \cdot d, \quad (5.23)$$

where f_{md}^h is the design compressive strength of the masonry parallel to the mortar joints.

(5)P When only vertical fibers of FRP are installed, the shear capacity of the masonry panel still improves due to the increase in compressive strength from the flexure acting within the masonry. The shear capacity of masonry shall be computed as follows:

$$V_{Rd,m} = x \cdot t \cdot f_{vd}, \quad (5.24)$$

where f_{vd} is the design shear strength of the masonry, as per the building code, equal to the ratio between the sum of the compressive forces and the area between extreme compression member and neutral axis, $x \cdot t$.

(6) Walls comprised of several panels delimited by structural floors can be shear strengthened using FRP located diagonally on the single panel. This FRP application requires the presence of bond beams or cables in the floor capable of resisting a uniform horizontal displacement at the panel ends. Couples of diagonal FRP are applied symmetrically to both sides of the panel.

(7) The shear capacity of the panel in Figure 5-9, strengthened with FRP inclined of an angle α , can be evaluated neglecting the contribution of the FRP under compression, as in the following.

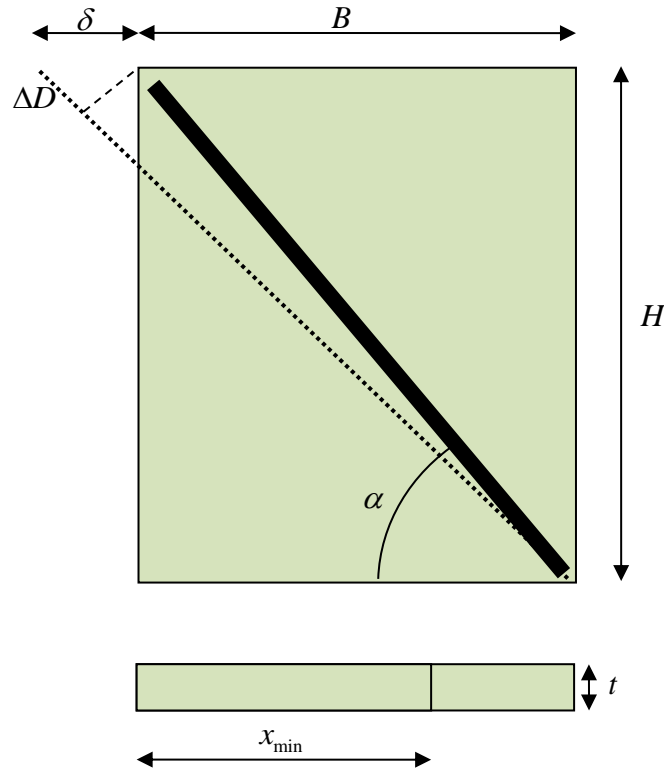


Figure 5-9 – Panel strengthened with FRP inclined by an angle α

Referring to Figure 5-9, the horizontal displacement of the top cross section is equal to:

$$\delta_{Rd,1} = 0.005 \cdot H . \quad (5.25)$$

In this section, the shear capacity of the panel is:

$$V_{Rd,m} = x_{min} \cdot t \cdot f_{vd} , \quad (5.26)$$

where x_{min} is the minimum distance between the neutral axis and the extreme compression fiber of the section, f_{vd} is the shear strength computed in accordance to the building code and equal to the ratio between the sum of the compressive load and the area $x_{min} \cdot t$.

Moreover, the maximum horizontal displacement compatible with design strain of FRP is equal to:

$$\delta_{Rd,2} = \frac{\Delta D_{fdd}}{\cos \alpha} = \varepsilon_{fdd} \frac{H}{\sin \alpha \cos \alpha} = \frac{f_{fdd} \cdot H}{E_f \cdot \sin \alpha \cos \alpha} . \quad (5.27)$$

Therefore:

$$\frac{\delta_{Rd}}{H} = \frac{1}{H} \min \{ \delta_{Rd,1}, \delta_{Rd,2} \} = \min \left\{ 0.005, \frac{f_{fdd}}{E_f \cdot \sin \alpha \cos \alpha} \right\} , \quad (5.28)$$

and, the shear capacity becomes:

$$V_{Rd} = \frac{\delta_{Rd}}{H} \left(\frac{V_{Rd,m}}{0.005} + \sin \alpha \cos^2 \alpha \cdot E_f \cdot A_f \right), \quad (5.29)$$

where $\frac{\delta_{Rd}}{H} (\sin \alpha \cos^2 \alpha \cdot E_f \cdot A_f)$ is the horizontal component of the FRP corresponding to a displacement equal to δ_{Rd} .

(8) When only FRP in the configuration of Figure 5-9 is used, the combined bending and axial load capacity of the panel shall be computed neglecting the FRP contribution.

5.4.2 Lintel and tie areas

(1)P The areas connecting different wall bays within a masonry panel are named tie areas. Their function is twofold: (1) restrain the adjoining wall to assume deformed shapes compatible with the applied horizontal load, and (2) support the masonry wall located above openings.

(2) Due to the presence of vertical loads, two effects in the areas above the openings are displayed: (1) The portion of masonry wall above the opening can not withstand its own weight and shall be supported by a lintel functioning as a beam and (2) when the wall bays surrounding the openings are slender and can not withstand the horizontal load due to the presence of the opening itself, the lintel shall provide adequate strength to carry the tensile stresses to ensure the overall equilibrium of the wall.

(3) In the next two sections, three methods for designing both lintels and tie areas subject to seismic loads are presented (see Figure 5-10).

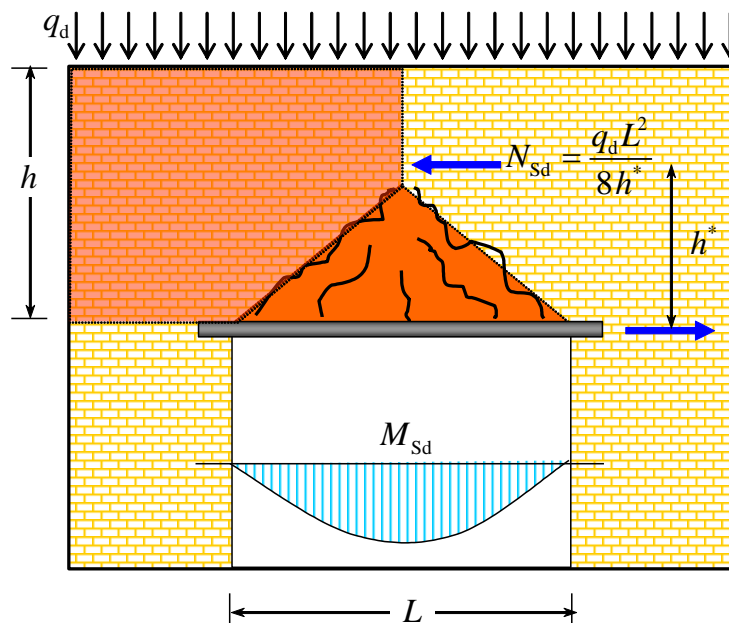


Figure 5-10 – Lintels design subjected to combined bending and axial loads.

5.4.2.1 Design of lintels

(1) Lintels may be designed using structural elements having both axial and flexural capacity. Alternatively, lintels having only axial capacity can be employed. In the former case, lintels are capable of functioning as a beam carrying tensile stresses to ensure the overall equilibrium of the wall.

(2) Support to the wall above the opening shall be ensured by formation of a reinforced masonry member located just above the opening where tensile stresses are resisted by the applied FRP strengthening system. Design can be performed using the indications in Section 5.4.1.1.3 and considering the compressive strength of the masonry in the horizontal direction, f_{md}^{h} .

(3) The portion of the FRP strengthened lintel shall have a flexural capacity, M_{Rd} , larger than the applied moment, and is calculated as follows:

$$M_{\text{sd}} = \gamma_{\text{G}} \cdot \frac{1}{24} \cdot g \cdot t \cdot L^3, \quad (5.30)$$

where g is the masonry weight per cubic meter, t is the thickness of the masonry, L is the net span of the opening, and γ_{G} is the partial factor for self weight at ultimate limit state.

FRP shall also be capable of withstanding the following force:

$$N_{\text{sd}} = \frac{q_{\text{d}} \cdot L^2}{8 \cdot h^*}, \quad (5.31)$$

where q_{d} is the design vertical load at ultimate limit state acting on the lintel (sum of factored dead and live loads), and h^* is the internal lever arm, to be assumed no larger than the span L of the opening or the height h of the tie area.

5.4.2.2 Design of tie areas

(1) FRP strengthened tie areas shall be verified for bending moment, shear, and axial loads acting at the vertical masonry walls connection. Flexural and shear capacity shall be calculated according to the requirements for the masonry wall panels by tacking into account the compressive strength of the masonry f_{md}^{h} parallel to the mortar joints.

(2) FRP strengthening of tie areas may be achieved by installing reinforcement with fibers in the horizontal direction at floor level, located above and below the tie area itself. FRP reinforcement may be continuous or discontinuous and is preferably applied symmetrically to both the internal or external face of the masonry wall. In particular, FRP reinforcement used as wrapping of the building may function as a strengthening of the external face of the masonry wall.

(3) To ensure proper behavior with respect to the applied shear force, FRP reinforcement with fibers in the diagonal direction could also be applied to tie areas. FRP reinforcement shall install symmetrically on both the internal and external sides of the strengthened masonry wall.

5.5 STRENGTHENING OF STRUCTURAL MEMBERS WITH SINGLE OR DOUBLE CURVATURE

(1)P Structural members with single or double curvature generally lose their functionality due to the formation of hinges generated by the negligible tensile strength of the masonry.

(2)P FRP strengthening systems can improve the structural member capacity with single or double curvature. Design can be performed in these members by using the limit state criteria.

(3)P The design capacity evaluated using ULS shall be incremented in analogy with the prescriptions for masonry panels (Section 5.4.1). In the case of bidirectional elements, structural capacity is

determined using the unit length.

(4)P FRP reinforcement shall be used as external strengthening of a structure to prevent the formation of certain hinges and failure mechanisms. At first, the hinges are considered to be located at the intrados or extrados of the structural element. Consequentially, the normal stress transferred from the hinges is eccentric compared to the mean surface of the structure. Therefore, the eccentricity is equal to half of the structural thickness.

(5)P FRP reinforcement delays both the opening of cracks and formation of hinges within the masonry panel. Therefore, FRP reinforcement can be used to prevent the formation of hinges on the opposite side to the one where the FRP system is installed

(6)P FRP reinforcement is not recommended when collapse is controlled by shear failure or crushing of the masonry, unless in the second case, FRP is formed by pre-cured laminates placed as an internal arch and is well anchored to the masonry.

(7) FRP strengthening systems can also improve the capacity and stability of non structural vaults.

5.5.1 Arches

(1) Two structural schemes can be taken into consideration:

- Arch scheme: for arches resting on fixed and/or hinged supports.
- Arch-pier scheme: known as a frame scheme, for arches resting on piers.

(2)P Generally, an arch or arch-pier structure tends to collapse due to the formation of at least four hinges.

(3) Hinges can be classified as real and pseudo-hinge. In particular, a possible mechanism may be due to the formation of three (real) hinges and a double pendulum (pseudo-hinge) leading to a shear failure of only a portion of the arch.

5.5.1.1 Arch scheme

(1)P To prevent the mechanism characterized by the formation of four hinges, FRP reinforcement may be bonded either to the extrados or the intrados of the masonry arch.

(2)P Hinges can be formed both at the intrados and the impost of the arch. Hinges at the impost can be eliminating only by the use of specific systems.

(3) Experimental evidence shows that application of FRP reinforcement on the side surface of the arch does not provide significant improvement of the structural behavior. In such a case, a premature debonding of the FRP reinforcement from the masonry face takes place. Such debonding is localized in the arch compressed region and caused typical FRP instability, followed by a rapid degradation of the bond between masonry and FRP.

(4) FRP reinforcement may also be applied to both extrados and intrados of the masonry arch to prevent the formation of a first and second type-hinge. However, this application is not common.

(5) Partial FRP strengthening carried out on a portion of the extrados or intrados does not prevent the possibility of formation of hinges responsible for the activation of a kinematic mechanism

of the structure. However, when FRP strengthening is properly designed and achieved, it may enhance the structure's ultimate capacity.

(6) It shall be preferable to do the following:

- Carry out complete FRP strengthening on the extrados or intrados of the arch.
- Anchor the FRP with the vertical structures.
- Choose FRP fabric over laminate, to better fit the geometry of the masonry arch.

5.5.1.2 Arch-pier scheme

(1) For arch-pier structures, application of FRP reinforcement to the arch intrados or extrados may be insufficient to prevent relative displacements of the pier-arch connections. In such a case, it is preferable to act on the piers.

(2) Checks to be carried out are identical to those considered for the arch scheme.

5.5.2 Single curvature vaults: barrel vaults

(1) In most situations, the study of barrel vaults is similar to that of a unit depth arch. Consequently, barrel vaults may be strengthened with FRP applied both on the extrados and intrados. To satisfy safety the requirements, FRP strengthening shall be applied along the entire longitudinal length of the vault. For this reason, FRP reinforcement shall be placed at a center-to-center distance, p_f , calculated as follows:

$$p_f \leq 5 \cdot t + b_f \quad b_f \leq 2t, \quad (5.32)$$

where t is the vault thickness and b_f is the FRP width. In case of ribbed vaults the thickness shall be considered equal to that of the webbing and not the one of the rib.

(2) Longitudinal FRP strengthening has the secondary importance of bridging the ideal arches forming the barrel vault. This mechanism is particularly important in cases of horizontal loading.

(3) Typically, it is suggested to install, in the longitudinal direction, at least 10 % of the FRP reinforcement applied in the transversal direction. It shall be increased to 25 % for FRP strengthening in seismic areas.

(4) If vaults are used in cellular buildings with small-size rooms, FRP strengthening should be performed on the building walls rather than the vault.

5.5.3 Double curvature vaults: domes

(1)P Domes exhibit membrane-type and flexural-type stresses.

5.5.3.1 Membrane-type stresses

(1)P In a dome subjected to vertical loads, normal tensile stresses directed along the dome parallels are displayed. Typical cracking pattern with cracks located along the meridians, is primarily due to the negligible tensile strength of the masonry. The mentioned crack pattern modifies the equilibrium condition of the dome while enhancing the horizontal forces where the dome connects to the supporting structure. The use of FRP reinforcement applied in a circle manner around the lower portion of the dome's perimeter may help prevent the opening of cracks as well as reduce the magnitude of the horizontal force acting on the supporting structure.

- (2) The degree of safety of a masonry dome shall be performed by checking the following:
- Tensile stress in FRP reinforcement;
 - FRP debonding according to Section 5.3.4.

5.5.3.2 Flexural-type stresses

(1)P Flexural-type stress is typically localized where the dome meets the supporting structure or at the edge of skylight, when available. In particular, flexural related stress may cause collapse of portions of the dome delimited by meridian cracks. If the load carrying capacity of such portions is controlled by failure of the region connecting the dome to the supporting structure, the dome may be strengthened by applying FRP reinforcement in a circle manner around the lower portion of the dome perimeter. If the dome supporting structure does not exhibit any displacement, the above mentioned FRP circular strengthening is inactive. In this case, FRP reinforcement shall be applied along the dome meridians.

- (2) The degree of safety of a masonry dome shall be performed by checking the following:
- Combined bending and axial force.
 - Shear.
 - FRP debonding.

For combined bending and axial loads as well as shear, the internal forces shall be evaluated on a unit dome element according to Sections 5.4.1.2.1 and 5.4.1.2.2. Possible strength reduction for the loading carrying capacity of the strengthened dome shall be considered due to the complexity of the internal forces associated with the analysis of dome structures. Precautions shall be taken in the case of combined bending and axial load when the tensile zone in one direction corresponds to a compression zone in the opposite direction. In such a case, unless a more rigorous analysis is performed, the ratio of the absolute value of the design applied moment to the nominal moment calculated under the applied axial load shall not be larger than 1. On the contrary, unless a more rigorous analysis is performed, the specific flexural capacity in each plane can be assumed equal to the 1, resulting from a monoaxial loading condition.

Planar shear design can be performed according to the first two cases previously mentioned.

It is to be noted that flexural and shear capacity shall be calculated with respect to the design compressive strength of the masonry by considering differences due to loading perpendicular or parallel to the masonry texture (Section 5.2.3(6)P).

Orthogonal shear design can not take into account the presence of FRP reinforcement and shall be performed in the case of unreinforced masonry, considering the complexity of the existing internal forces. Checks for FRP debonding shall consider tensile stresses acting perpendicular to the FRP reinforcement according to Section 5.3.4.

- (3) To ensure proper behavior of the FRP system applied in a circular manner around the lower portion of the dome perimeter, FRP reinforcement shall be accurately anchored to the dome porting structure by means of mechanical anchorage.

5.5.4 Double curvature vaults on a square plane

(1) FRP strengthening of double curvature vaults resting on a square plane shall primarily be performed on the masonry walls of the room that supports the vault itself. For vertically loaded structures, integrity and stiffness of the supporting masonry walls ensure that the vault is primarily subjected to compression stresses. If this is not the case, FRP strengthening may be performed with-

in the corner region of the vaults where tensile stress in a direction orthogonal to the room diagonals, is expected to occur.

5.6 CONFINEMENT OF MASONRY COLUMNS

(1)P FRP reinforcement is typically installed by wrapping of the member, where such wrapping exerts a beneficial effect on the lateral strain of the column by providing tri-axial confinement. FRP strengthening may be employed either in the case of rehabilitation of deteriorated structures or for seismic upgrade.

(2) Confinement with composites may be performed by using FRP sheets or bars. FRP sheets are applied as external reinforcement along the perimeter of the member to be strengthened in the form of continuous or discontinuous wrap. Instead, FRP bars are inserted in spread holes drilled through the member that requires upgrade.

(3) FRP bars are inserted in the holes drilled along two directions orthogonal to the member transversal cross section. Each set of two bars inserted in either of the two directions represents a “layer of bars” (Figure 5-11).

Such reinforcement can effectively contrast the transverse strain of the masonry. To ensure continuity between FRP bars and surrounding masonry, each hole is filled with epoxy paste or, alternatively, the FRP bar ends are mechanically fastened to the masonry.

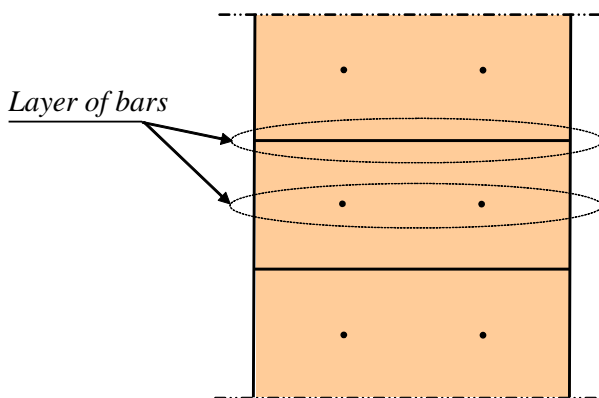


Figure 5-11 – Lateral view of a column with FRP bars arranged along two orthogonal directions.

(4) When FRP sheets and bars are used in the same application for strengthening masonry columns, it is recommended that such FRP materials exhibit similar mechanical characteristics.

(5) Provisional confinement prior to the installation of vertical bars is suggested when columns show vertical cracks. An L-shape profile that is eventually wood made, can be used columns with rectangular cross-section along with belt-bearing devices.

(6) Confinement of masonry structures with FRP shall be performed using design mechanical parameters in compliance with the current building code.

5.6.1 Design of axially loaded confined members

1) Design of FRP confined masonry columns is based upon the appropriateness of the FRP system as a function of the member geometry.

(2) It is recommended to install FRP reinforcement with fibers running in the orthogonal direction with respect to the vertical axis of the strengthened member. Effectiveness of spiral FRP reinforcement shall be adequately proven.

(3) The axial capacity of the FRP strengthened member, N_{Sd} , shall exceed the design axial force due to the applied loads calculated according to the current building code, $N_{Rmc,d}$, as follows

$$N_{Sd} \leq N_{Rmc,d}, \quad (5.33)$$

(4) $N_{Rmc,d}$, is given as follows:

$$N_{Rmc,d} = \frac{1}{\gamma_{Rd}} \cdot A_m \cdot f_{mcd} \geq A_m \cdot f_{md}, \quad (5.34)$$

where the partial factor, γ_{Rd} , shall be equal to 1.10. In the case of non-circular cross section columns, internally confined with bars only, $\gamma_{Rd} = 1.25$ (Table 3-1, Section 3.4.2). A_m represents the cross sectional area of the FRP confined member, f_{md} represents the design compressive strength of unconfined masonry, and f_{mcd} is the design compressive strength of the FRP confined member.

(5) The design compressive strength, f_{mcd} , for members confined with FRP subjected to a lateral confining pressure, f_1 , can be written as follows: $f_{l,eff}$, called “effective confinement pressure”:

$$f_{mcd} = f_{md} \cdot \left[1 + k' \cdot \left(\frac{f_{l,eff}}{f_{md}} \right)^{\alpha_1} \right], \quad (5.35)$$

where k' is a non-dimensional coefficient, $f_{l,eff}$ represents the effective confining pressure, and α_1 is a coefficient equal to 0.5 if further experimental data is not available.

(6) Unless a more detailed analysis is performed, k' may be calculated as follows:

$$k' = \alpha_2 \cdot \left(\frac{g_m}{1000} \right)^{\alpha_3}, \quad (5.36)$$

where g_m is the masonry mass-density expressed as kg/m^3 , and, α_2 and α_3 are coefficients equal to 1.0 if further experimental data is not available.

(7) The effective confining pressure, $f_{l,eff}$, is a function of cross-sectional shape and the FRP system.

Defining V_m as the volume of the masonry member to be strengthened, and $V_{c,eff}$ as the portion of the effectively confined volume, the following coefficient of efficiency can be written:

$$k_{eff} = \frac{V_{c,eff}}{V_m}. \quad (5.37)$$

The effective confining pressure may be defined as a function of the coefficient of efficiency. In turn, this may be expressed as the product of a horizontal and vertical coefficient of efficiency, k_H

and k_v , respectively:

$$f_{1,\text{eff}} = k_{\text{eff}} \cdot f_1 = k_H \cdot k_v \cdot f_1. \quad (5.38)$$

(8) When spiral FRP sheets are used, the effectiveness of FRP confinement is penalized by fiber inclinations. α_f indicates the FRP fiber inclination with respect to the horizontal plane of the member cross section. The following coefficient can be defined:

$$k_\alpha = \frac{1}{1 + \text{tg}^2 \alpha_f}. \quad (5.39)$$

This coefficient penalizes the lateral confining pressure, f_1 , reported in Equation (5.38). FRP strengthening performed with FRP bars inserted in the holes shall not be affected by this coefficient.

(9) To mitigate axial deformation and prevent damage at the serviceability limit state, the increased axial capacity due to FRP confinement shall not be larger than 50 % of the design compressive strength, f_{md} , of the unconfined member.

5.6.2 Confinement of circular columns

(1) The geometric ratio of FRP confined members when both FRP sheets and bars are employed can be defined as follows (Figure 5-12):

$$\rho_f = \frac{4 \cdot t_f \cdot b_f}{D \cdot p_f}, \quad (5.40)$$

where:

- t_f is the FRP thickness.
- b_f is the FRP strip width.
- D is the masonry cross-section diameter.
- p_f is the center-to-center spacing of FRP strips.

In the case of continuous FRP wrapping, the ratio ρ_f becomes equal to $4 \cdot t_f / D$.

(2) Via equilibrium, the confining pressure, f_1 , can be calculated as follows:

$$f_1 = \frac{1}{2} \cdot \rho_f \cdot E_f \cdot \varepsilon_{\text{fd,rid}}, \quad (5.41)$$

where E_f is the Young modulus of elasticity of FRP sheets, and $\varepsilon_{\text{fd,rid}}$ represents the reduced design value of the FRP strain measured at column collapse.

(3)P The reduced design strain for FRP reinforcement can be written as follows:

$$\varepsilon_{\text{fd,rid}} = \min\{\eta_a \cdot \varepsilon_{\text{fk}} / \gamma_f; 0.004\}, \quad (5.42)$$

where η_a is the environmental conversion factor (Table 3-2), ε_{fk} and γ_f , represent ultimate strain

the partial factors of FRP sheets, respectively (Section 3.4.1), and 0.004 is a conventional strain limit (see Section 4.5.1).

(4) For a circular cross section strengthened with FRP sheets, the horizontal coefficient of efficiency, k_H , is equal to 1. The coefficient of vertical efficiency, k_V , is also assumed equal to 1 only for continuous confinement.

(5) A reduction of the confined volume (Figure 5-12) is observed in case of non-continuous confinement. In such a case, the coefficient of vertical efficiency, k_V , can be computed as follows:

$$k_V = \left(1 - \frac{p_f'}{2 \cdot D}\right)^2, \quad (5.43)$$

where p_f' is the center-to-center distance between two consecutive strips.

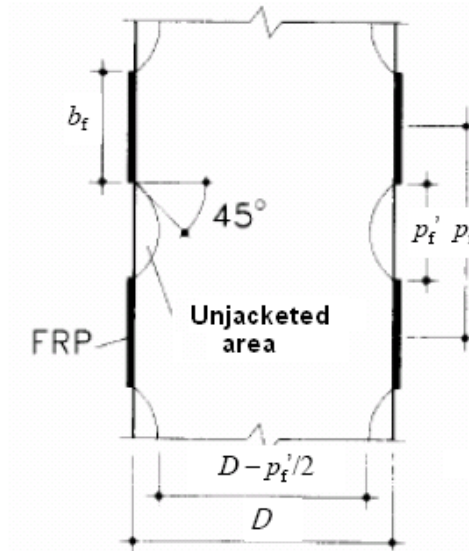


Figure 5-12 – Front view of circular masonry member confined with discontinuous FRP strips.

(6) The center-to-center distance, p_f , shall not be greater than $D/2$.

5.6.3 Confinement of prismatic columns

(1)P FRP confinement of non-circular cross sections shows only a slight increase in the load carrying capacity. Therefore such applications shall be carefully analyzed.

(2) The external confinement on prismatic columns shall not be considered when $b/h > 2$ or $\max\{b, h\} > 900\text{mm}$, unless experimental data is available (Figure 5-13).

(3) As per Section 5.6.2(1), the confining pressure, f_1 , of a rectangular member having dimension $b \times h$ can be calculated as follows:

$$f_1 = \frac{1}{2} \cdot \min \left\{ \rho_{f,x} \cdot E_f + 2 \cdot \rho_{b,x} \cdot E_b ; \rho_{f,y} \cdot E_f + 2 \cdot \rho_{b,y} \cdot E_b \right\} \cdot \varepsilon_{fd,rid}, \quad (5.44)$$

where the non-dimensional parameters $\rho_{f,x}$, $\rho_{f,y}$, $\rho_{b,x}$, $\rho_{b,y}$ are defined by (Figure 5-13):

$$\rho_{f,x} = \frac{4 \cdot t_f \cdot b_f}{h \cdot p_f}, \quad \rho_{f,y} = \frac{4 \cdot t_f \cdot b_f}{b \cdot p_f}, \quad \rho_{b,x} = \frac{n_{b,x} \cdot A_b}{p_b \cdot h}, \quad \rho_{b,y} = \frac{n_{b,y} \cdot A_b}{p_b \cdot b}, \quad (5.45)$$

where $n_{b,x}$ and $n_{b,y}$ represent the number of bars in the x and y direction, respectively, A_b is the bar cross circular area, and p_b the distance between two consecutive bars layers placed along the same direction.

For continuous wrapping, $\rho_{f,x}$ and $\rho_{f,y}$ become (Equation (5.45)):

$$\rho_{f,x} = \frac{4 \cdot t_f}{h}, \quad \rho_{f,y} = \frac{4 \cdot t_f}{b}. \quad (5.46)$$

In the case of a rectangular cross section, Equation (5.44) becomes:

$$f_1 = 2 \cdot \frac{t_f \cdot E_f}{\max\{b, h\}} \cdot \varepsilon_{fd,rid}, \quad f_1 = \frac{2t_f b_f E_f}{\max\{b, h\} p_f} \quad (5.47)$$

for continuous and non-continuous FRP reinforcement, respectively. When only bars are used, the same equation becomes:

$$f_1 = \min\{\rho_{b,x} \cdot E_b; \rho_{b,y} \cdot E_b\} \cdot \varepsilon_{fd,rid}. \quad (5.48)$$

(4) Figure 5-13 shows a rectangular cross section confined with a continuous FRP reinforcement. Due to the arch-effect shown in the figure, the confined section is only a portion of the total area of the masonry column. The extension of the confined area depends on the adopted rounding radius.

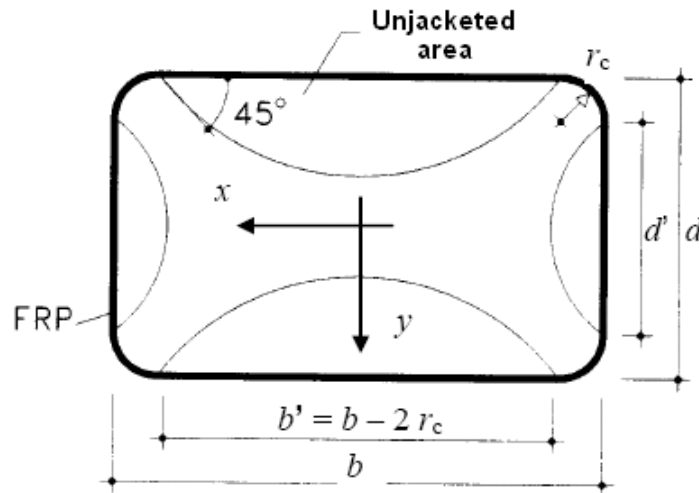


Figure 5-13 – Confinement of rectangular sections externally wrapped with FRP.

The horizontal coefficient of efficiency is given by the ratio between the confined area and the total area of the masonry column, A_m , as follows:

$$k_H = 1 - \frac{b'^2 + h'^2}{3 \cdot A_m}, \quad (5.49)$$

where b' and h' are the dimensions indicated in Figure 5-13.

(5) If the FRP strengthening system of (4) is non-continuous, the vertical coefficient of efficiency is equal to (Figure 5-12):

$$k_v = \left(1 - \frac{p_f}{2 \cdot \min\{b, h\}}\right)^2 \quad (5.50)$$

For a continuous confinement, k_v is equal to 1.

(6) The center-to-center distance, p_f , shall comply with Equation (5.51):

$$p_f \leq \frac{1}{2} \cdot \min\{b, h\} \quad (5.51)$$

(7) Unless a more appropriate determination of the portion of the effective confined volume is made, the coefficient of efficiency, k_{eff} , can be assumed only when FRP bars are used and equal (Figure 5-14):

$$k_{\text{eff}} = k_H \cdot k_v = \left[1 - \frac{1}{3 \cdot b \cdot h} \cdot \left(c_x^2 \cdot (n_{bx} - 1) + c_y^2 \cdot (n_{by} - 1) + 6 \cdot c_{xs} \cdot c_{ys}\right)\right] \cdot \left(1 - \frac{p_b}{2 \min\{b, h\}}\right)^2 \quad (5.52)$$

In case of prismatic columns with one side equal to b , Equation (5.52) becomes:

$$k_{\text{eff}} = k_H \cdot k_v = \left[1 - \frac{1}{3 \cdot b^2} \cdot \left(2 \cdot c_b^2 \cdot (n_b - 1) + 6 \cdot c_{bs}^2\right)\right] \cdot \left(1 - \frac{p_b}{2 \cdot b}\right)^2 \quad (5.53)$$

where $n_{bx} = n_{by} = n_b$, $c_x = c_y = c_b$, $c_{xs} = c_{ys} = c_{bs}$.

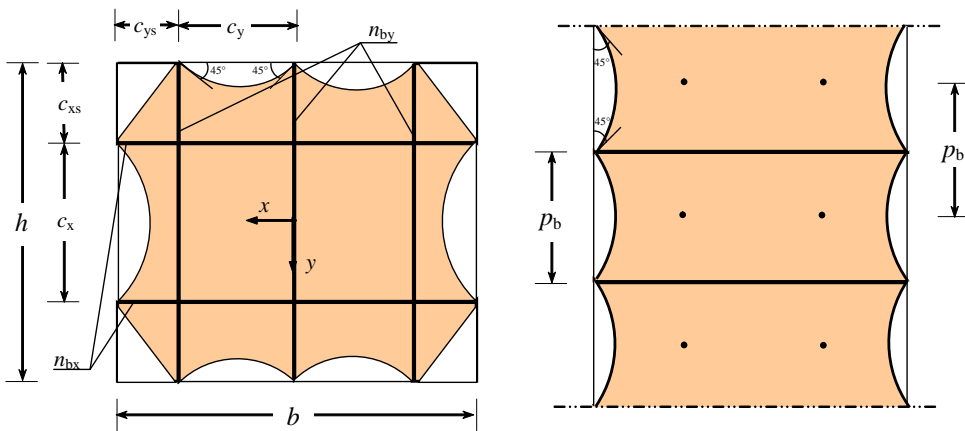


Figure 5-14 – Plan and lateral view of confinement with FRP bars.

(8) The distance between the member edge and the FRP bar closer to the edge itself shall not be greater than 1/4 of the member width. In addition:

$$c_x \leq \frac{h}{5}, c_y \leq \frac{b}{5}. \quad (5.54)$$

The center-to-center distance, p_b , shall satisfy $p_b \leq \max \{c_x, c_y\}$.

(9) FRP bars inserted in holes drilled through the strengthened masonry member shall be anchored for a length equal to at least 10 times the FRP bar diameter. When this length is greater than 1/5 of the FRP bar length, the anchorage force should be adequately distributed at the two bar ends.

(10)P The combined use of external FRP wrapping and internal FRP bars inserted in holes drilled through the member cross section may increase the area effectively confined for square, rectangular, or more complex cross sections (Figure 5-15).

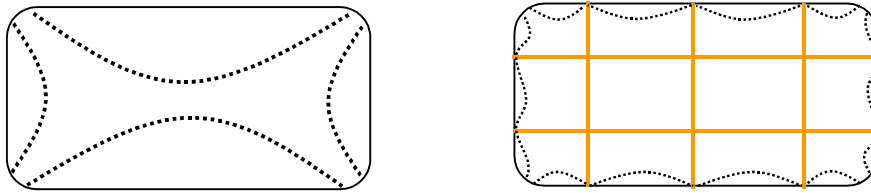


Figure 5-15 – Confinement of masonry members with FRP sheets and bars.

(11) When using a combination of external FRP wrapping and internal FRP bars, the coefficient of efficiency, k_{eff} , as per Equations (5.37) and (5.38), can be computed as follows:

$$k_{\text{eff}} = k_H \cdot k_v = \left[1 - \frac{1}{3 \cdot b \cdot h} \cdot \left(c_x^2 \cdot (n_{bx} - 1) + c_y^2 \cdot (n_{by} - 1) + 2 \cdot (c_{xs} - r_c)^2 + 2 \cdot (c_{ys} - r_c)^2 \right) \right] \cdot 1. \quad (5.55)$$

In the particular case of square section:

$$k_{\text{eff}} = k_H \cdot k_v = \left[1 - \frac{1}{3 \cdot b \cdot h} \cdot \left(2 \cdot c_b^2 \cdot (n_b - 1) + 4 \cdot (c_{bs} - r_c)^2 \right) \right] \cdot 1, \quad (5.56)$$

where $n_{bx} = n_{by} = n_b$, $c_x = c_y = c_b$, $c_{xs} = c_{ys} = c_{bs}$ and r_c is the circular corner radius.

5.7 DESIGN FOR SEISMIC APPLICATIONS

5.7.1 Design objectives

(1)P FRP strengthening of masonry structures subjected to seismic loads can be performed when the unstrengthened member does not satisfy one or more limit states according to the current building code.

This part of the document recognizes the provisions of the current building code as well as the indications provided in the most updated literature related to seismic constructions. Particular importance is given to the following:

- Evaluation of seismic safety.
- Safety requirements (verification of limit states).

- Levels of seismic protection (magnitude of the associated seismic action).
- Methods of analysis.
- Verification criteria (distinction between ductile and brittle members).
- Material characteristics to be used for design.

5.7.2 Selection criteria for FRP strengthening

(1)P Type and size of selected FRP systems shall consider the following:

- Masonry structures unable to withstand vertical and horizontal loads shall be strengthened or replaced.
- Walls ending on masonry T-junctions or masonry edges shall be appropriately connected.
- Unsatisfactory connections between floors/roof and vertical walls shall be made effective.
- Horizontal forces generated from roofs, arches, and vaults shall be taken by appropriate structural members.
- Floors effectively connected to vertical walls shall be properly stiffened in their plane to be able to transfer horizontal forces to the vertical walls located in the direction of seismic loading. They shall also provide restraint to the movement of vertical walls located in the orthogonal direction.
- Weak members for which strengthening is not suitable shall be eliminated.
- In the case of strongly irregular buildings (in term of resistance and/or stiffness), FRP strengthening is usually unable to provide relief to the structure. It may be used for few structural members to grant a minimum regularity to the structure.
- FRP strengthened members that enhance local ductility are always recommended.
- Local FRP strengthening shall never reduce the overall ductility of the structure.

(2)P FRP retrofitting is typically aimed at the following:

- Total or partial strengthening, replacing, or rebuilding of structural members;
- Modifying the overall structural behavior by means of connection of different structural members.

(3)P Design of FRP reinforcement shall include the following:

- Rational selection of the retrofitting technique.
- Selection of the appropriate technique and/or material.
- Preliminary dimensioning of FRP reinforcement.
- Structural analysis, taking into account the FRP strengthened structure.
- Safety checks of the strengthened structure performed on strengthened and newly added members (for existing, repaired, or strengthened members safety checks shall be performed according to this guide. For newly added members, safety checks shall be in compliance with the current building code).

5.8 INSTALLATION AND CONSTRUCTION DETAILS

(1)P Several aspects influence the effectiveness of FRP material used as externally bonded systems for the strengthening of masonry members. In addition to those discussed in previous chapters, surface preparation and FRP installation are also critical.

5.8.1 Quality control and substrate preparation

(1)P Quality control of the support implies the determination of masonry conditions, removal, and reconstruction of any deteriorated or loose masonry block, cleaning, and removal of a portion of masonry subjected to moisture, vegetation plants, or anything similar.

(2)P When special devices are used to properly anchor the selected FRP system, testing of these devices shall be conducted in compliance with available standardization documents. Anchoring devices shall be installed according to the manufacturer/supplier specifications regarding both the material used as well as the surface preparation, environmental conditions, and sequence of each phase. The investigation shall also evaluate the effects of such parameters on the final result.

5.8.1.1 Evaluation of substrate deterioration

(1) Prior to FRP application, tests on the homogeneity of the strengthened portion of the structure shall be performed to ensure proper quality of the masonry support.

(2) Mechanical characterization tests on masonry shall be performed for at least 1 every 100 m² of area to be strengthened, with a minimum of 2 tests for each homogeneous area. Tests shall be performed according to at least of one of the following:

- Compression test on a masonry specimen.
- Shear test on a masonry specimen.
- Flat jack test.
- Shear test by jacking.
- Dilatometer test.
- Ultrasonic test.

(3) When homogeneity tests are performed on the entire area to be strengthened, except for critical areas, they shall be distributed according to a square mesh spaced 1 m apart for areas smaller than 5 m², and proportionally increased for larger areas. Tests shall be performed as follows:

- Hand hammering of the interested area.
- X-ray analysis.
- Ultrasound speed in near-surface mode.
- Recording speed of sonic pulse (with instrumented hammer and accelerometers).
- Penetrometer.
- Thermography.
- Tomography.

5.8.1.2 Removal and reconstruction of defective masonry supports

(1) Masonry substrate may have undergone physical-chemical, physical-mechanical or impact-causing deterioration. Deteriorated masonry shall be removed from all damaged areas.

(2) Removal of defective masonry allows for the examination of characteristics of both natural and artificial masonry as well as mortar. When exfoliation, pulverization, cracking, or chemical attack processes occur, it is necessary to remove all defective areas and protect them with appropriate inhibitors.

(3) Once all deteriorated masonry has been removed, and suitable measures have been taken to

prevent further deterioration of the existing substrate as well as all other phenomena causing masonry degradation (*e.g.*, water leakage, vegetation), masonry restoration using masonry-compatible materials shall be performed. Masonry roughness between 10 and 20 mm shall be leveled with compatible epoxy paste; and specific filling material shall be used for unevenness larger than 20 mm. Crack widths wider than 0.5 mm shall be closed using epoxy injection methods before FRP strengthening can take place.

5.8.1.3 Substrate preparation

- (1) To improve the bond between the masonry support and FRP, sandblasting of the portion of masonry surface to be strengthened shall be performed. Sandblasting shall provide a roughness degree of at least 0.3 mm and level of the roughness can be measured by suitable instruments, such as a laser profilometer or an optical profile-measuring device.
- (2) Poor quality masonry surfaces that do not require remedial work prior to FRP application, should be treated with a reinforcing agent prior to the primer installation.
- (3) Cleaning of the surface to be strengthened shall remove any dust, laitance, oil, surface lubricants, foreign particles, or any other bond-inhibiting material.

5.8.2 Recommendations for the installation

- (1) FRP strengthening of masonry structures is highly dependent upon environmental temperature and humidity as well as the characteristics of the substrate.

5.8.2.1 Humidity and temperature conditions in the environment and substrate

- (1) It is suggested not to install FRP material when the environment is very moist. A high degree of humidity may delay the curing of the resin and affect the overall performance of the FRP system especially for wet lay-up applications.
- (2) FRP systems shall be installed in appropriate humidity and temperature conditions as defined by the materials data sheet.
- (3) If curing of FRP reinforcement takes place under rainy conditions, heavy insulation, large thermal gradients, or in the presence of dust, protective measures can be employed to ensure proper curing.

5.8.2.2 Construction details

- (1) An anchorage length of at least 150 mm shall be provided for the end portion of FRP systems used for strengthening RC members. Alternatively, mechanical connectors may be used.
- (2) Prior to FRP application, cross section edges shall be rounded to avoid stress concentrations that could cause a premature failure of the system. The corner radius shall be equal to at least 20 mm.
- (3) Proper fiber alignment shall be provided for in-situ wet lay-up application, and waving of FRP reinforcement shall be avoided during installation.
- (4) When semi-destructive tests are performed, it is suggested to provide additional strengthening areas (“witness areas”) in selected parts of the structure having dimensions of at least 500×300 mm², with a minimum extension of 0.15 m² but not less than 0.5 % of the overall area to be

strengthened. Witness areas shall be determined at the same time of the main FRP installation, using the same materials and procedures in areas where removal of FRP strengthening system does not imply alteration of the failure mechanisms. In addition, witness areas shall be exposed to the same environmental conditions as the main FRP system and shall be uniformly distributed on the strengthened structure.

5.8.2.3 Protection of FRP systems

(1) For outdoor FRP applications it is recommended to protect the FRP system from direct sunlight, which may produce chemical-physical alterations in the epoxy matrix. This can be achieved by using protective acrylic paint provided that cleaning of the composite surface with a sponge soaked in soap is performed.

(2) Alternatively, a better protection can be achieved by applying plaster or a layer of mortar (preferably cement-based) to the installed strengthening system. The plaster, whose thickness is recommended by the FRP manufacturer/supplier, is to be applied to the strengthening system after treating the surface by means of epoxy resin applications with subsequent quartz dusting green-on-green. The final layer is particularly suitable to receive any kind of plastering.

(3) For fire protection, two different solutions may be adopted: use of intumescent panels, or application of protective plasters. In both cases, the manufacturer/supplier shall indicate the degree of fire protection as a function of the panel/plaster thickness. The panels, generally based on calcium silicates, are applied directly to the FRP strengthening system, provided that fibers will not be cut during installation.

Protective plasters represent the most widely adopted solution for fire protection, and shall be applied to the FRP system as indicated before.

5.9 NUMERICAL EXAMPLES

Some numerical examples concerning the FRP strengthening of masonry structures are reported in Appendix H.

6 CONTROL AND MONITORING

- (1)P Acceptance and quality control shall be performed on FRP strengthening systems.
- (2)P After FRP installation, inspection and monitoring shall be performed by using non-destructive and semi-destructive tests. Tests shall be performed as indicated in Section 6.3.
- (3) In the same applications, such as a completely wrapped configuration and/or while using anchoring devices, tests on the substrate can be omitted.

6.1 QUALITY CONTROL ON THE CONSTRUCTION SITE

- (1)P Acceptance of FRP physical and mechanical characteristics shall be evaluated on the construction site, along with the adherence to the designer's requirements.
- (2) Quality control on the construction site shall be performed by using destructive evaluation tests on specimens. The number and type of tests shall be compliant with the *Guides for qualification and acceptance criteria of fiber reinforced composites for strengthening applications of existing structures*.

6.2 QUALITY CONTROL DURING INSTALLATION

- (1) Semi-destructive quality control during FRP installation is fundamental for the mechanical characterization of the installation itself. Installation uniformity and defects can be investigated through non-destructive tests.
- (2)P The number and type of tests shall be evaluated based on the importance of the installation and the relationship to the strengthened area versus the entire structure. In particular, greater attention shall be given to a building with public or strategic functions, as indicated by the Public Safety Agency in the event of a natural disaster.

6.2.1 Semi-destructive tests

- (1) Both pull-off tests and shear tearing tests may be performed. Semi-destructive tests shall be performed on witnesses (Sections 4.8 and 5.8) and, where possible, in non-critical strengthened areas at the rate of one test for every 30 m² for application to reinforced concrete structures, or 50 m² for application to masonry structures. In any case, no less than 3 of each type of test shall be performed.

- (2) Pull-off test.

The test is used for assessment of the properties of restored concrete substrate, whereas each test is performed by using a 20 mm thick circular steel plate with a diameter not less than 50 mm. After the steel plate is firmly attached to the FRP, it is isolated from the surrounding FRP with a core by using a drill bit not greater than 3 mm. Particular care shall be taken to avoid the heating of the FRP system while a 1-2 mm incision of the concrete substrate is achieved.

Devices, such as ball joint or spherical rod ends, shall be used to ensure the pull-force application perpendicular to the FRP.

FRP application may be considered acceptable if at least 80 % of the tests (both tests in case of only two tests) return a pull-off stress not less than 1.2 MPa for reinforced concrete elements or 10% of the substrate compressive strength for masonry, provided that failure occurs in the concrete substrate. If the failure occurs at the FRP-substrate interface, the construction manager shall evaluate the acceptance of the test.

(3) **Shear tearing test.** This test is particularly significant to assess the quality of bond between the FRP and concrete substrate. Figure 6-1 shows a possible test configuration. The preparation requires the FRP to be located close to an edge and detached from the concrete substrate, but in continuity with the bonded material. The force is applied on the same plane of the free FRP portion through a gripping mechanism by using the edge as a contrast device.

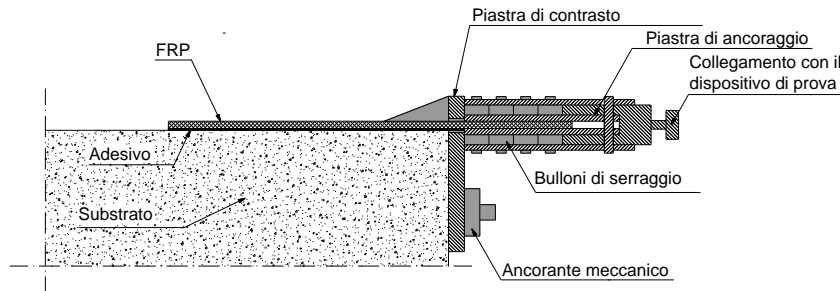


Figure 6-1 – Direct shear tearing test.

Figure 6-2 shows the same test when a free portion of FRP is not available. This procedure can be identified as indirect. The test area is still located close to an edge, where a steel plate is bonded to the surface. Part of the steel plate shall project from the edge to ensure the perfect grip of the testing device. The steel plate is 45 mm in width and 6 mm thick. The area of the steel plate in contact with the FRP can be treated to improve bonding.

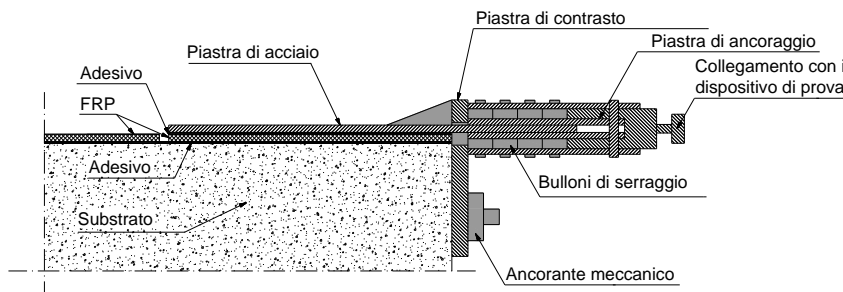


Figure 6-2 – “Indirect” shear tearing test.

In both Figure 6-1 and Figure 6-2, the length of bonded FRP portion shall not be less than 200 mm or 150 mm for reinforced concrete or masonry structures, respectively. In any case, the bonded portion shall not be less than 1.1 times the optimal bonding length of FRP (Sections 4.1.2 and 5.3.2). When using indirect shear tests, the portion of steel plate shall remain perfectly bonded to the FRP. FRP application may be considered acceptable if at least 80% of the tests (in the case of two tests) return a peak tearing force not less than 85% of the design strength computed by Equation (10.2), in which k_b is equal to 1.

6.2.2 Non destructive tests

(1) Acceptance criteria require that bonding defects shall not be greater than cylindrical imperfections with a height and diameter of 0.5 and 25 mm, respectively.

(2) Non-destructive tests may be used to characterize the uniformity of FRP application starting from a two-dimensional survey of the strengthened surface with different spatial resolution as a function of the strengthening area (Table 6-1).

Table 6-1 – Minimum resolution for defects thickness to be identified with non-destructive tests.

Shear stress transfer at interface	Type of application	Non-destructive test	Surface mapping grid (mm)	Minimum resolution for defects thickness (mm)
absent	wrappings, with the exception of the overlapping area in single-layer application	Optional	250	3
weak	central area of very extensive plane reinforcement	Optional	250	3
moderate	central area of longitudinal flexural strengthening	Suggested	100	0.5
critical	anchorage areas, overlapping areas between layers, stirrups for shear strengthening, interface areas with connectors, areas with large roughness or cracks in the substrate	Required	50	0.1

(3) Stimulated Acoustic testing. Similar to impact-echo testing, such tests rely on the different oscillatory behavior of the composite layer depending on the bond between the FRP layers and concrete substrate. In its most basic version, this test may be carried out by a technician hammering the composite surface and listening to the sound of the impact. More objective results may be obtained with automated systems.

(4) High-frequency ultrasonic testing. They should be carried out using reflection methods with frequencies no less than 1.5 MHz and probes with a diameter no greater than 25 mm, adopting a technique based on the first peak amplitude variation of localize defects.

(5) Thermography tests. They are effective only for FRP systems with low thermal conductivity and cannot be applied to carbon or metallic FRP strengthening systems unless specific precautions are taken. The heat developed during the test shall be lower than the glass transition temperature of the FRP system.

(6) Acoustic emission tests. The technique is based on the acoustic emission (AE) method and allows for the damage assessment inside a structural member, subject to loading by listening to and recording the sound generated by either formation of cracks or delamination phenomena that propagate as elastic waves.

6.3 PERSONNEL QUALIFICATION

(1) Personnel in charge of the tests shall have one of the three qualification levels specified in

Table **6-2** according to UNI EN 473 and UNI EN 45013.

Table 6-2 – Qualification levels to perform semi and non-destructive tests.

Level 1	Proper knowledge of testing equipment; performing tests; recording and classifying test results according to written criteria; writing a report on test results.
Level 2	Choosing the way of performing the test; defining the application limits of the test for which the level 2 technician is certified; understanding test specifications and translating them into practical test instructions suitable to the in-situ working conditions; adjusting and calibrating test equipment; performing and controlling the test; interpreting and evaluating test results according to the specifications to comply with; preparing written test instructions for level 1 personnel; performing and supervising all level 1 functions; training personnel of level 1; organizing test results and writing the final report.
Level 3	Be in charge of a laboratory facility; establishing and validating test techniques and procedures; interpreting specifications and procedures; having the skills to evaluate and understand test results according to existing specifications; having a sufficient practical knowledge of materials, production methods and installation technology of the system to be tested to be able to choose appropriate methods, establish techniques and collaborate in the definition of acceptance criteria when they are not pre-established; be knowledgeable in different application fields; being able to lead personnel of level 1 and 2.

6.4 MONITORING OF THE STRENGTHENING SYSTEM

(1) Due to the poor availability of data regarding long term behavior of FRP systems used for strengthening RC structures, it is recommended to accurately monitor the installed FRP system by means of semi and non-destructive tests periodically conducted on the strengthened structure. The aim of such a monitoring process is to keep the following parameters under control:

- Temperature of the installed FRP system.
- Environmental humidity.
- Measure of displacements and deformations of the strengthened structure.
- Potential damage of fibers.
- Extensions of defects and debonding in the installed FRP system.

(2) The type and number of tests to be performed shall be included in the maintenance manual.

7 APPENDIX A (CHARACTERISTICS OF COMPOSITES AND THEIR CONSTITUENTS)

7.1 INTRODUCTION

Composite materials exhibit the following characteristics:

- They are comprised of two or more materials (phases) different in nature and “macroscopically” distinguishable.
- At least two phases have physical and mechanical properties quite different from one another, such to provide FRP material with different properties than those of its constituents.

Fiber-reinforced composites with polymeric matrix satisfy both characteristics given above. In fact, they consist of both organic polymeric matrix and reinforcing fibers, whose main characteristics are summarized in Table 7-1.

Table 7-1 – Comparison between properties of fibers, resin, and steel (typical values).

	Young's modulus E	Tensile strength σ_r	Strain at failure ϵ_r	Coefficient of thermal expansion α	Density ρ
	[GPa]	[MPa]	[%]	[$10^{-6} \text{ }^\circ\text{C}^{-1}$]	[g/cm^3]
E-glass	70 – 80	2000 – 3500	3.5 – 4.5	5 – 5.4	2.5 – 2.6
S-glass	85 – 90	3500 – 4800	4.5 – 5.5	1.6 – 2.9	2.46 – 2.49
Carbon (high modulus)	390 – 760	2400 – 3400	0.5 – 0.8	-1.45	1.85 – 1.9
Carbon (high strength)	240 – 280	4100 – 5100	1.6 – 1.73	-0.6 – -0.9	1.75
Aramid	62 – 180	3600 – 3800	1.9 – 5.5	-2	1.44 – 1.47
Polymeric matrix	2.7 – 3.6	40 – 82	1.4 – 5.2	30 – 54	1.10 – 1.25
Steel	206	250 – 400 (yield) 350 – 600 (failure)	20 – 30	10.4	7.8

As it can be seen, carbon fibers may exhibit values of Young's modulus of elasticity much larger than those of typical construction materials. Therefore, they are considered more effective from a structural point of view. Designers and practitioners shall carefully evaluate potential problems with other materials used as support.

The matrix is considered an isotropic material, while the reinforcing phase (with the exception of glass fiber) is an anisotropic material (different properties in different directions). The defining characteristics of FRP materials are as follows:

- Geometry: shape and dimensions.
- Fiber orientation: the orientation with respect to the symmetrical axes of the material; when random, the composite characteristics are similar to an isotropic material (“quasi-

isotropic”). In all other cases the composite is considered an anisotropic material.

- Fiber concentration: volume fraction, distribution (dispersion).

Therefore, composites are in most cases a non-homogeneous and anisotropic material.

To summarize the FRP properties, it is convenient to classify fiber-reinforced composites in two categories, regardless of their production technology:

- Single-layer (lamina)
- Multi-layer (laminates)

Laminates are materials composed of stacked layers (the lamina) whose thickness is usually of some tenths of a millimeter. In the simplest case, fibers are embedded only in the lamina’s plane (there are no fibers arranged orthogonally to that plane). The size of laminates is intermediate between those of the fibers and those of engineering structures (Table 7-2). There is also a special class of multi-layer composites, called hybrid laminates, where each single lamina is comprised of both different fibers (*e.g.*, epoxy matrix composites with carbon and aramid fibers to maintain a stiff and tough composite) and different materials (*e.g.*, composites with alternate layers of epoxy resin with aramid and aluminum fibers).

The primary advantage of laminates is represented by the greater freedom of fiber arrangement.

Table 7-2 – Size of fiber composites with polymer matrix.

	representative dimensions					
	pm	nm	μm	mm	m	km
Atom	*	*				
Polymer molecules		*	*			
Biological polymers		*	*			
Crystallites			*	*		
Spheroids			*	*		
Diameter of fibers				*		
Thickness of FRP sheets				*	*	*
Thickness of FRP laminates					*	*
Length of laminates						*
Structures						*

Due to the anisotropic characteristics of FRP material, the mechanical properties depend on the choice of the reference system. The main axes are usually chosen to be concurred with the symmetrical axes of the material (natural axes). A unidirectional FRP material is illustrated in Figure 7-1.

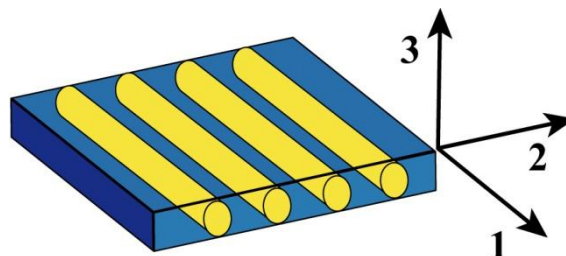


Figure 7-1 – Choice of axes for a unidirectional FRP material.

The ratio between values of the properties of composite materials in different directions is called on anisotropic ratio. Some values of the anisotropic ratio related to the main characteristics of interest in unidirectional laminates (E_i : Young modulus of elasticity; G_{ij} : shear modulus; σ_{fi} : failure

stress; α_i : coefficient of thermal expansion) are shown Table 7-3.

Table 7-3 – Anisotropic ratios of fiber-reinforced unidirectional laminates (typical values).

	E_1/E_2	E_1/G_{12}	σ_{r1}/σ_{r2}	α_1/α_2
Silicon carbide/ceramic	1.09	2.35	17.8	0.93
Boron/aluminum	1.71	5.01	11.6	0.30
Silicon carbide/aluminum	1.73	5.02	17.0	0.52
S-Glass/epoxy	2.44	5.06	28.0	0.23
E-Glass/epoxy	4.42	8.76	17.7	0.13
Boron/epoxy	9.27	37.40	24.6	0.20
Carbon/epoxy	13.60	19.10	41.4	-0.07
Aramid/epoxy	15.30	27.80	26.0	-0.07

Composite materials can be stronger and stiffer (carbon FRP) than traditional construction materials. As a result, composites may become very attractive when the weight of the structure becomes a concern. FRP specific values of tensile strength and Young's modulus of elasticity (calculated by dividing each quantity by the density of the material) can be up to four and two times that of traditional materials, respectively. Therefore, a composite material structure may weigh nearly half of a traditional construction material structure with equal stiffness.

The nature of the phases of the composite determines the final properties of FRP materials. To obtain a composite with high mechanical strength, using "strong" fibers is not sufficient. A good adhesion between the matrix and fibers used as a load-carrying component is also necessary. The adhesion is usually obtained with a third component applied in a very thin layer to the fiber surface that provides compatibility with the organic matrix. This surface treatment requires the presence of an intermediate phase between the matrix and the fibers, named interface, or interphase (Figure 7-2). The interphase is typically made of a very thin layer (often a single-atom) placed directly on the fiber that is required for determining the final properties of the material.

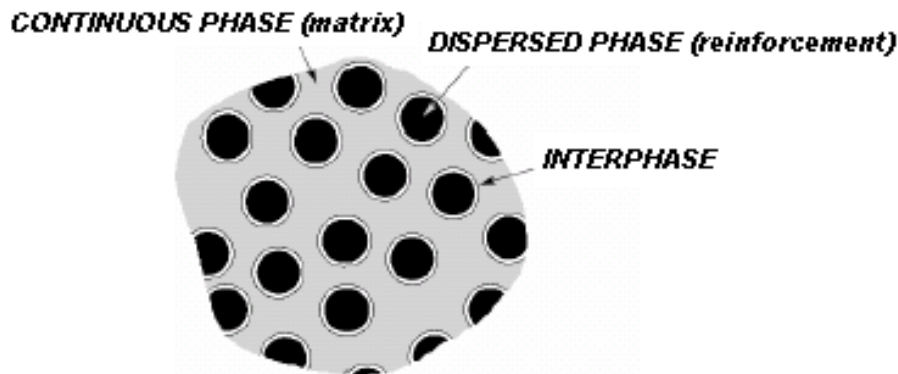


Figure 7-2 – Representation of phases in a FRP composite.

Structural failures of FRP composites are often due to lack of bond between the matrix and the fibers. Therefore, the FRP material manufacturer should take special care in selecting the most appropriate component to promote the bond.

7.2 FIBERS USED IN COMPOSITES

The most common fibers used in composites are glass, carbon, and aramid. Their unique monodimensional geometry, in addition to being particularly suitable for the realization of composites, provides FRP laminates with stiffness and strength higher than those of three-dimensional FRP

shapes. This is due to the lower number of defects of mono-dimensional configurations as opposed to three-dimensional members.

7.2.1 Types of fibers available in the market and their classification

Fibers are made of very thin continuous filaments, and therefore, are quite difficult to be individually manipulated. For this reason, they are commercially available in different shapes (Figure 7-3). A brief description of the most commonly used is summarized as follows:

- Monofilament: basic filament with a diameter of about 10 μm .
- Tow: untwisted bundle of continuous filaments.
- Yarn: assemblage of twisted filaments and fibers formed into a continuous length that is suitable for use in weaving textile materials.
- Roving: a number of yarn or tows collected into a parallel bundle with little or no twist.

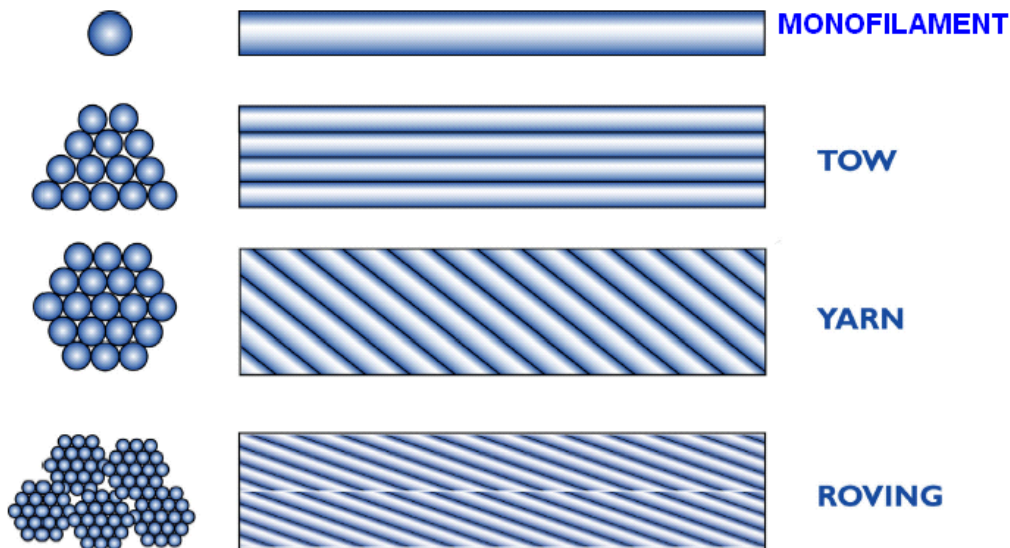


Figure 7-3 – Types of fibers.

By combining a number of tows or yarns together, a tape is obtained, where tows or yarns can be simply arranged side by side, or sewed or fastened on a bearing. The classification of fibers is directly taken from traditionally method used for textile fibers. The filaments used to produce yarns are characterized by their chemical composition or mass per unit length. The unit of linear mass or count (mass per unit length) according to ISO 2974:2000(E) is the TEX, equivalent to 1 g per km of fiber. Another unit of linear mass, now obsolete, is the denier, equivalent to 0.111 TEX.

The technical name of fiberglass follows the rule of ISO 1139:1973(E) and ISO 2078:1993(E) and includes the following members:

- A letter identifying the type of glass used
- A second letter identifying the type of fiber used
 - C (“Continuous”, for filaments)
 - D (“Discontinuous”, for discontinuous fibers)
- A first number identifying the nominal diameter (in μm) of the filament
- A second number indicating the linear mass of the fiber in TEX
- The direction and value of torsion (Figure 7-4), expressed in rpm (optional)

- The number of wires used to produce the twisted member (optional)
- A manufacturer label containing all the un-coded information necessary for the product characterization (optional).



Negative torsion (S).



Positive torsion (Z).

Figure 7-4 – Definition of the two possible directions of torsion.

Examples of labeling are listed as follows:

- EC10 40: continuous filament of E-glass, with a diameter of 10 μm and a linear mass of 40 TEX.
- EC9 34 Z 40: continuous filament of E-glass, with a diameter of 9 μm and a linear mass of 34 TEX, twisted at 40 rpm. The letter Z represents positive torsion according to ISO 1139:1973(E) (negative torsion is indicated with the letter S).
- EC9 34 Z 160 x 4 S 150: the letter “x” shows that the material is a wire containing a number of identical filaments. The code preceding the “x” identifies the characteristics of the filaments, while the following number (4) represents the number of filaments and the letter S represents a negative torsion, accomplished at 150 rpm.
- EC9 x 4 S 150: simplified labeling of the previous filament.

Yarns commonly used for structural composites are referred to as EC5 10 x 2 or SC5 4 x 2, depending on whether the material is E-glass or S-glass, respectively. For carbon fibers, yarns are usually classified by the symbol “k,” standing for “thousands” [e.g., a 1k yarn is made of 1000 filaments (66.6 Tex), a 3k yarn (200 Tex) has 3000 filaments, and so on]. Typical values are 0.5k, 1k, 3k, 6k, 12k, 18k, 24k, and 48k.

In addition to yarns or rovings, fibers are also commercially available as fabrics. In this case, fibers’ dispositions may provide quasi-isotropic properties of the fabric. In such materials, the main direction is named warp while the orthogonal direction is named weft.

7.2.1.1 Glass fibers

These fibers are commonly used in the naval and industrial fields to produce composites of medium-high performance. Their peculiar characteristic is their high strength. Glass is mainly made of silicon (SiO_2) with a tetrahedral structure (SiO_4). Some aluminum oxides and other metallic ions are then added in various proportions (Table 7-4) to either ease the working operations or modify the properties (e.g., S-glass fibers exhibit a higher tensile strength than E-glass).

Table 7-4 – Typical composition of fiberglass (% in weight).

	E-glass	S-glass
Silicon oxide	54.3	64.20
Aluminum oxide	15.2	24.80
Iron oxide	-	0.21
Calcium oxide	17.2	0.01
Magnesium oxide	4.7	10.27
Sodium oxide	0.6	0.27
Boron oxide	8.0	0.01
Barium oxide	-	0.20
Various	-	0.03

The production of fiberglass is essentially based on spinning a batch made of sand, alumina, and limestone. The constituents are dry mixed and melted (about 1260 °C) in a tank. The melted glass is carried directly on platinum bushings and, by gravity, passes through ad hoc holes located on the bottom. The filaments are then grouped to form a strand typically made of 204 filaments. A single filament has an average diameter of 10 µm and is typically covered with a sizing. The yarns are then bundled, in most cases without twisting, in a roving. The typical value of the linear mass for roving to be used in civil engineering applications is larger than 2000 TEX.

Glass fibers are also available as thin sheets, called *mats*. A *mat* may be made of both long continuous or short fibers (*e.g.*, discontinuous fibers with a typical length between 25 and 50 mm), randomly arranged (Figure 7-5) and are joined together by a chemical bond. The width of such *mats* varies between 5 cm and 2 m, with their density being roughly 0.5 kg/m².

Glass fibers typically have a Young modulus of elasticity (70 GPa for E-glass) lower than carbon or aramid fibers and their abrasion resistance is relatively poor; therefore, caution is required during manipulation. In addition, they are prone to creep and have low fatigue strength. To enhance the bond between the fibers and matrix, as well as to protect the fibers against alkaline agents and moisture, fibers undergo sizing treatments acting as coupling agents. Such treatments are useful to enhance the durability and fatigue performance (static and dynamic) of the composite material. FRP composites based on fiberglass are usually denoted as GFRP.



Discontinuous fibers.

Discontinuous fibers *mat*.**Figure 7-5** – Fiberglass *mat*.

7.2.1.2 Carbon fibers

Carbon fibers are used for their high performance and are characterized by high Young modulus of elasticity as well as high strength. They have an intrinsically brittle failure behavior with relatively low energy absorption. Nevertheless, the failure strength is large compared to glass and aramid fi-

bers. Carbon fibers are less sensitive to creep rupture and fatigue and show a slight reduction in long-term tensile strength.

The crystalline structure of graphite is hexagonal, with carbon atoms arranged in a planar structure, kept together by transverse Van der Waals interaction forces, much weaker than those acting on carbon atoms in the plane (covalent bonds). For this reason, their Young modulus of elasticity and strength are extremely high in the directions of fiber and much lower in the transverse direction (anisotropic behavior). The structure of carbon fibers is not as completely crystalline as that of graphite. The term “graphite fibers” is however used in the common language to represent fibers whose carbon content is larger than 99 %. The term “carbon fibers” denotes fibers whose carbon content is between 80 and 95 %. The number of filaments contained in the *tow* may vary from 400 to 160000. The modern production technology of carbon fibers is essentially based on pyrolysis (*e.g.*, the thermal decomposition in the absence of oxygen of organic substances), named precursors, among which the most frequent are polyacrylonitrile fibers (PAN), and rayon fibers. PAN fibers are first “stabilized,” with thermal treatments at 200-240 °C for 24 hrs, so their molecular structure becomes oriented in the direction of the applied load. As a second step, carbonization treatments are performed at 1500 °C in inert atmosphere to remove chemical components other than carbon. The carbonized fibers may then undergo a graphitization treatment in inert atmosphere at 3000 °C, to develop a fully crystalline structure similar to that of graphite. FRP composites based on carbon are usually denoted as CFRP.

7.2.1.3 Aramid fibers

Aramid fibers are organic fibers, made of aromatic polyamides in an extremely oriented form. First introduced in 1971, they are characterized by high toughness. The Young modulus of elasticity and tensile strength are intermediate between glass and carbon fibers (Figure 7-6 and Figure 7-7). The compressive strength is typically around 1/8 of the tensile strength. Due to the anisotropy of the fiber structure, compression loads promote localized yielding of the fibers resulting in fiber instability and formation of kinks. Aramid fibers may degrade from extensive exposure to sunlight, losing up to 50 % of their tensile strength. In addition, they may be sensitive to moisture. The creep behavior is similar to that of glass fibers, even though their failure strength and fatigue behavior is higher than GFRP.

The production technology of aramid fibers is based on high-temperature and high-speed extrusion of the polymer in a solution followed by fast cooling (quenching) and drying. The fibers produced in this way may undergo a hot orientation treatment through winding on fast rotating coils (post-spinning) to improve their mechanical characteristics. Aramid fibers are commercially available as *yarns*, *roving*, or *fabrics*. FRP composites based on aramid fibers are usually denoted as AFRP.

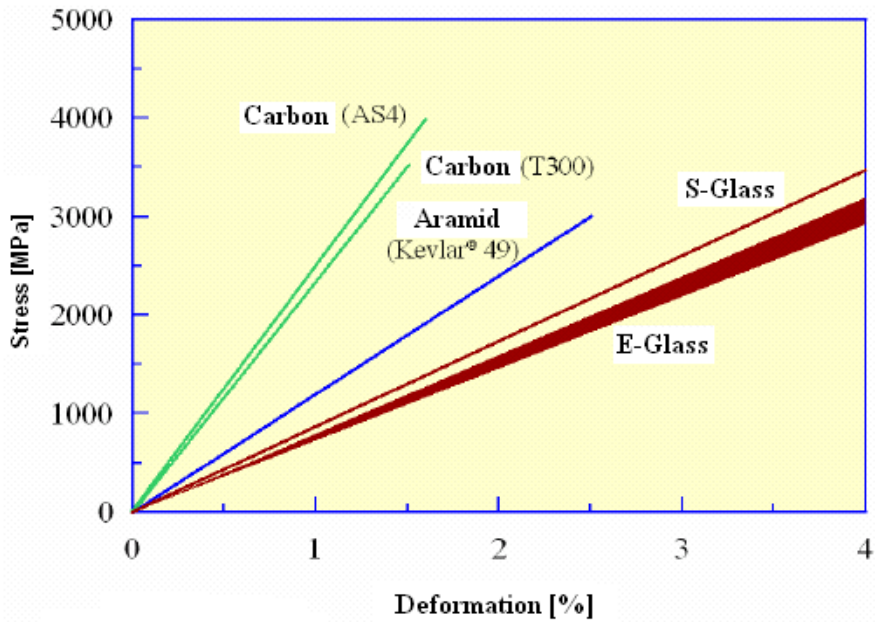


Figure 7-6 – Stress-strain diagram for different reinforcing fibers.

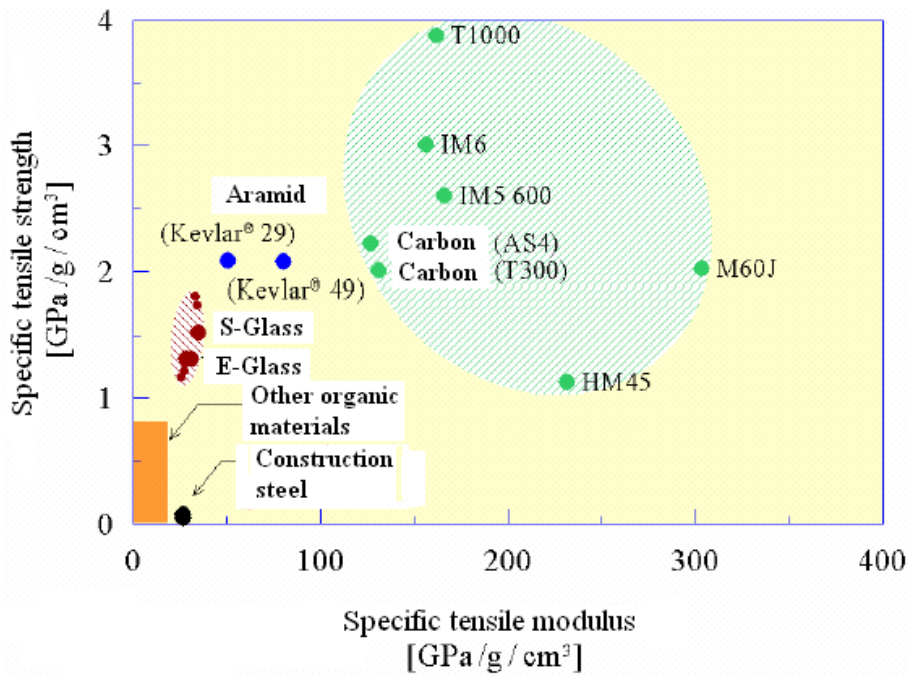


Figure 7-7 – Comparison between FRPs and steel.

7.2.1.4 Technical characteristics of yarn

Yarns are not commercially available as strengthening materials, but instead are used as raw material for the production of fabrics. Hereafter, the structure of a typical technical data sheet for yarn is proposed. The international reference standard is ISO 2113:1996(E).

ISO 1889:2009(E) can be used to determine the yarn count. A sample of given length should be taken from the fabric and should be weighted. The count value is given by the following ratio:

$$T_x = \frac{P \cdot 1000}{L}, \quad (7.1)$$

where T_x is the count of the yarn, expressed in Tex [g/km]; P is the weight of the sample, expressed in grams; and L is the length of the sample, expressed in meters.

The area A , in mm^2 , of the cross-section of a filament or bundle (*yarn, tow, or roving*), can be determined using the following equation:

$$A = \frac{T_x}{\rho \cdot 1000}, \quad (7.2)$$

where ρ is the yarn density, expressed in g/cm^3 . T_x is the count expressed in TEX. The evaluation of such parameters may be useful for production quality control.

7.2.2 Non-impregnated fabrics

A *fabric* that is not impregnated with resin is named “dry”. The simplest fabric is obtained starting from a roving and is named “woven roving”. Since the *roving* does not exhibit any twisting, the filament is transversely compressed where the weft and warp cross each other. The resulting *fabric* is suitable to achieve large products in size and thickness.

Fabrics obtained directly from the weaving of the yarns, being lighter and more compact, can be used for more specific applications that require an optimization of the structural weight. A composite laminate obtained from these fabrics has a lower volumetric fraction of fibers than a laminate made of a unidirectional fiber due to the crimp associated with weaving.

The most used types of fabric are plain, twill and satin. Plain fibers exhibit the stiffest and most stable structure. The primary disadvantages are the difficulty of resin impregnation as well as the crimp of the weft and warp. This latter characteristic implies a lower strengthening effectiveness on the plane of the laminate. The crimp for such fabrics is about 10 %. Twill fibers and satin fibers are more flexible but likely to be damaged during manipulation. The satin fabric is intrinsically stiffer in the lamination plane, since it has the least crimp of fibers in both directions.

Figure 7-8 shows the geometries of the most used fabrics in current applications. The representation complies with the following assumptions:

- Black or dashed box = weft yarn on top of warp yarn
- White box = weft yarn under warp yarn

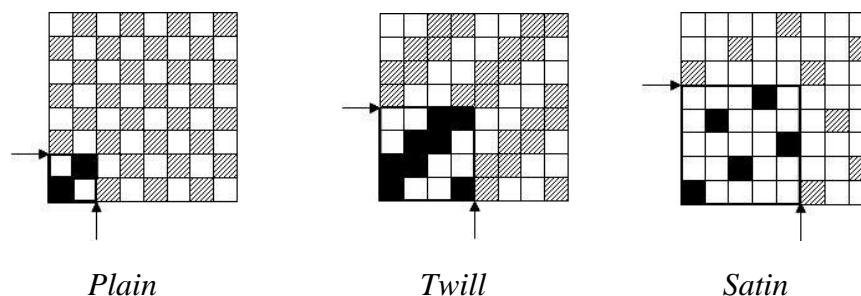


Figure 7-8 – Fabric examples.

There are also multi-axial fabrics, where the fibers are oriented in more than two directions. They can be made of woven yarns or simply sewn yarns. Finally, three-dimensional fabrics are also available, where the presence of a second weft in a direction orthogonal to the plane provides the

product with higher strength and special properties (e.g. the capability to inflate when they are impregnated with resin).

7.2.2.1 Technical characteristics of non-impregnated fabrics

Fabrics for structural strengthening are commonly distributed as a dry product to be impregnated with special resins at the job site. They can be unidirectional, where the fibers are all oriented in the direction of the length and kept together by a light non-structural weft, bi-directional, made of a orthogonal weft-warp weaving, usually balanced (same ratio of fibers in the two directions) and multi-axial, where fibers are oriented in different directions. Dry fiber manufacturers are required to provide material data sheets. The structure of a material data sheet is reported hereafter for mono- and bi-directional fabrics. Data sheets of commercially available fabrics may also include other information or parts of those indicated. The suggested structure is exhaustive regarding the type and amount of information provided.

The general reference standard is ISO 8099:1980. For multi-axial fabrics, in addition to the general information concerning the type of yarn and other characteristics of the fabric, the orientation of each layer of fibers should also be reported. Examples concerning the determination of some characteristic parameters of the fabrics used for structural strengthening are illustrated.

In cases where only the yarn count and geometry are provided, the mass of the fibers per unit area in a given direction can be determined with the following equation:

$$p_x = \frac{T_x \cdot N_f}{10}, \quad (7.3)$$

where p_x is the mass of the fabric in the principal direction [g/m^2], T_x is the *yarn* count in the principal direction, expressed in Tex [g/km], and N_f is the number of *yarns* per unit width in the principal direction [n°/cm].

For example, given a unidirectional fabric characterized by 3.8 yarns/cm and by a yarn count of 800 Tex, the resulting mass per unit area is:

$$p_x = \frac{800 [\text{Tex}] \cdot 3.8 [\text{fili}/\text{cm}]}{10} = 304 \text{ g}/\text{m}^2.$$

If it is necessary to evaluate the number of yarns arranged in a given direction per unit length in the orthogonal direction, ISO 4602:1997(E) can be applied and the yarns arranged in the orthogonal direction on a given fabric strip (e.g., 10 cm wide) are counted. The resulting number is varied proportionally to the chosen unit length.

7.3 MATRICES

Thermoset resins are the most commonly used matrices for the production of FRP materials. They are usually available in a partially polymerized state with fluid or pasty consistency at room temperature. When mixed with a proper reagent, they polymerize to become a solid, vitreous material. The reaction can be accelerated by adjusting the temperature. Thermoset resin have several advantages, including low viscosity that allows for a relative easy fiber impregnation, good adhesive properties, room temperature polymerization characteristics, good resistance to chemical agents, absence of melting temperature, etc. Disadvantages are limited to a range of operating temperatures, with the upper bound limit given by the glass transition temperature, poor toughness with respect to fracture (“brittle” behavior), and sensitivity to moisture during field applications. The most common thermosetting resins in civil engineering are the epoxy resin. Polyester or vinylester resins are also used. Considering the material is mixed directly at the construction site and obtains its final struc-

tural characteristics through a chemical reaction, it should always be handled by specialized personnel.

Fiber-reinforced composite materials with thermoplastic polymeric matrices are also available but require installation techniques different from the thermosetting resin. Composite bars with a thermoplastic matrix that may be bent at any time by means of special thermal treatment are currently being investigated.

7.3.1 Epoxy resins

Epoxy resins are characterized by a good resistance to moisture, chemical agents, and have excellent adhesive properties. They are suitable for the production of composite material in the civil engineering field. The maximum operating temperature depends both on the formulation and reticulation temperature. For operating temperatures higher than 60 °C, the resin should be suitably selected by taking into account the variations of its mechanical properties. There are usually no significant restrictions for the minimum operating temperature. The main reagent is composed of organic fluids with a low molecular weight, containing epoxy groups, rings composed by an oxygen atom and two carbon atoms:

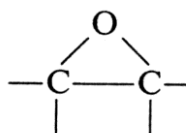


Figure 7-9 – Epoxy group.

Such materials may be produced by the reaction of epichlorohydrin with amino compounds or an acid compound of bisphenol A.

The epoxy pre-polymer is usually a viscous fluid, with a viscosity depending on the polymerization degree. A reticulating agent (typically an aliphatic amine) is to be added to this mixture in the exact quantity to obtain the correct structure and properties of the cross-linked resin. The reaction is exothermic and does not produce secondary products. It can be executed at both room and high temperatures, according to the technological requirements and the target final properties. The chemical structure of the resin may change based on the chemical composition of the epoxy pre-polymer. The most commonly used epoxy resin in composite materials for civil applications is the diglycidylether of bisphenol A (DGEBA).

7.3.2 Polyester resins

Polyester resins have a lower viscosity compared to epoxy resins, are very versatile, and highly reactive. Their mechanical strength and adhesive properties are typically lower than those of epoxy resins.

Unsaturated polyesters are linear polymers with a high molecular weight, containing double C=C bonds capable of producing a chemical reaction. The polymerization degree, and hence the molecule length may be changed. At room temperature the resin is always a solid substance. To be used, polyester resin has to be dissolved in a solvent, typically a reactive monomer, which reduces the resin viscosity and therefore assists with the fiber impregnation process. The monomer (typically styrene) shall also contain double C=C bonds, allowing the cross-linking of bridges between the polyester molecules to be created. The reaction is exothermic and no secondary products are generated. It is typically performed at room temperature, according to technological requirements and target final properties. The chemical structure of polyester resins may be adapted either by changing the acid and the glycol used in the polymer synthesis or by employing a different reactive monomer.

The family of polyester resins for composite materials is typically composed of isophthalic, orthophthalic, and bisphenolic resins. For both high temperatures and chemically aggressive environment applications, vinylester resins are often used. They represent a balance between the performance of traditional polyester resins and that of epoxy resins.

7.3.3 Other types of resins

The intrinsic limitations of thermosetting resins, particularly their poor toughness, relatively low operating temperatures, and tendency to absorb moisture from the environment, have recently led to the development of composites with a thermo-plastic matrix. Such resins have the flow capability after heating at a high enough temperature, specifically, higher than T_g (glass transition temperature) for amorphous materials and higher than T_m (melting temperature) for semi-crystalline materials. The shape of each component may be modified by heating the material at a suitable temperature (hot forming). Their use in the civil engineering field is rather limited, however, applications of potentially remarkable relevance are currently being developed (*e.g.*, reinforcing bars for concrete). In general, thermoplastic resins are tougher than thermosetting resin, and in some instances have higher operating temperatures. In addition, they have a better resistance to environmental factors. The main limitation for their use is their high viscosity, which makes fiber impregnation difficult, and requires complex and costly working equipment.

Moreover, the use of inorganic matrices (cement-based, metallic, ceramic, etc.) for production of fiber-reinforced composites for construction is rapidly growing. Although they are not discussed in this document, their use is deemed possible when accompanied by suitable technical documentation and experimental validation to prove their effectiveness.

7.4 ADHESIVES

The implementation of FRP-based structural strengthening (*e.g.*, pultruded laminate) requires the use of adhesives. Choosing of the most suitable adhesive as well as the type of surface treatment to be carried out prior to FRP application shall be made on the basis of available substrate and properties of the selected FRP system. Technical data sheets for FRP materials usually report the indications of the adhesive to be used as a function of the structure to be strengthened. Even the application of dry fabrics impregnated on-site may be considered as an assembling operation using adhesives. The type of surface treatment to be carried out prior to FRP application is important for the correct use of adhesives. For this reason, the rationale for a suitable substrate preparation that describes physical, chemical, and mechanical mechanisms of adhesion is presented. For a more comprehensive study, the reader is referenced to specific literature on the subject.

An adhesive is a material with a polymeric nature capable of creating a link between at least two surfaces and able to share loads. There are many types of natural and synthetic adhesives (elastomers, thermoplastics, and mono- or bi-component thermosetting resins); the most suitable adhesives for composite materials are based on epoxy resins. Epoxy adhesives usually are bi-component viscous mixture. Once hardened, through a cross-linking chemical reaction, they become suitable for structural applications.

There are several advantages in the use of adhesive bonding compared to mechanical anchorage. They include the possibility of connecting different materials, providing greater stiffness, uniform distribution of loads, and avoiding holes dangerous for stress concentrations.

8 APPENDIX B (MANUFACTURING TECHNIQUES)

8.1 INTRODUCTION

Manufacturing techniques of FRP systems for Civil Engineering application are introduced in this appendix.

8.1.1 Pultrusion

Pultrusion is a technology mainly used for production of fiber-reinforced laminates. Such products are widely used in civil engineering field. This technology is based on a continuous manufacturing process, consisting of three main phases:

- Forming.
- Impregnation.
- Hardening.

In the most common version designed for thermosetting resin, the components (resin and fibers) are separately fed into a machine that catches and pulls the fibers through the different production stages. A widespread version of the process includes impregnation with a resin bath, as shown in Figure 8-1.

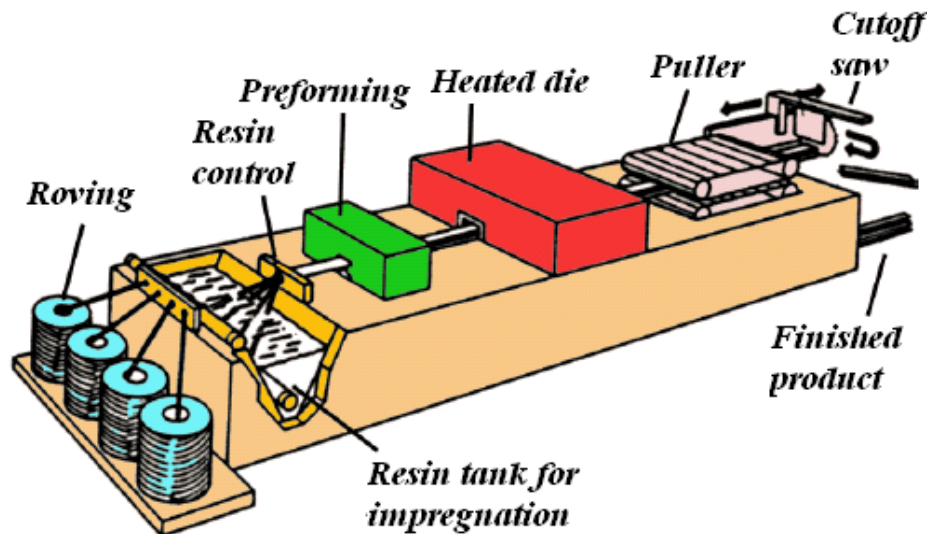


Figure 8-1 – Pultrusion process with resin bath impregnation.

The fibers are taken directly from the rovings and conveyed to a resin bath where impregnation occurs. Bundles of impregnated fibers enter the heating die where the material is formed and cross-linked under high pressure. During this phase, gaps between fibers are eliminated to ensure proper continuity in the transverse direction.

Heating is generally supplied by electrical resistances and the temperature is controlled by means of thermocouples. The duration of the heating stage is regulated by production speed. Upon exiting from the die, the matrix is cured and the composite is pulled at a constant speed. At the end of the process the material is cut to the appropriate length. Fabric layers may be added to ensure strength of FRP in directions other than the longitudinal. Weaving, winding, and twisting may be carried out directly on the production line with special equipment.

FRP pultruded material is light, corrosion-resistant, with a constant cross section and thicknesses up to few centimeters. Typically pultruded products include laminates, bars, structural shapes (C, double T, etc.), panels and plates. They are used as internal and external reinforcement for existing and new structures, structural components for transportation, supports for lighting and billposters, risers for oil industry, etc.

8.1.2 Lamination

Lamination is used exclusively to produce innovative and high performance composites. It is a discontinuous process that produces laminates of maximum thickness up to few centimeters by totally controlling fiber orientation and the complexity of the structure.

Compared to pultrusion, it allows complete freedom as to fiber orientation and curvature of the produced material. The main limitation regards the speed of production, which is roughly 0.5 kg/h for simple components.

The following fundamental phases can be identified in the lamination process:

- a) Material preparation.
- b) Lamination (cut of material, stacking of plies and compaction).
- c) Vacuum bag preparation.
- d) Material curing (at room temperature, oven, or autoclave).
- e) Inspection (visual, by ultrasound and X-rays).
- f) Finishing (cutting of edges with cutters or high pressure water jet).

Lamination may occur if dry fibers are impregnated during field installation, or pre-impregnated fibers running in either one or multiple directions.

The next phase in the lamination process requires preparation of a vacuum bag (phase c) as it is shown in Figure 8-2. The vacuum allows for a fast removal of solvents and entrapped air in the laminates prior to complete curing of the resin.

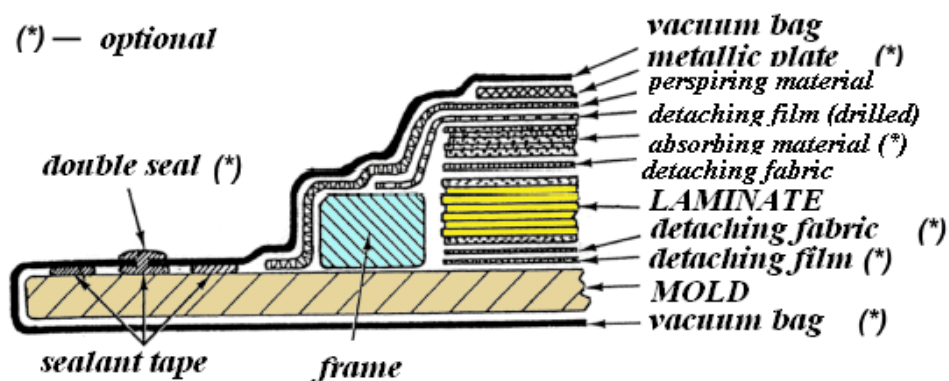


Figure 8-2 – Lamination system.

The primary advantage of this technology is the extreme versatility that allows for the production of complex components using inexpensive molds. Specific applications refer to the aeronautical and aerospace fields, car racing, sailing, and transportation. FRP strengthening of columns or RC beams by means of dry or pre-impregnated fibers represent one field of application where lamination can effectively be used in the construction field.

8.1.3 Wet lay-up

Wet lay-up is one of the most simple and traditional methods used for onsite FRP preparation, formed of two phases: a first one layering and a second one polymerization.

In detail, the first phase consists of manually arranging, on a specific support, a layer of fabric. This layer is immediately impregnated with a resin (Figure 8-3).

Impregnation is manually achieved through the use of rolls or brushes. Compaction of the material and elimination of bubbles within the layers are then achieved by rolling the surface.

The same procedure is repeated for any other layer of fabric up to the desired thickness.

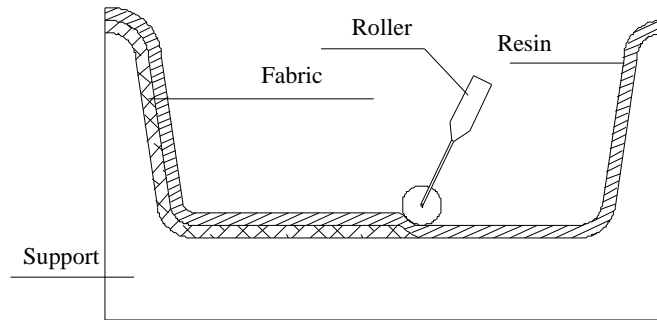


Figure 8-3 – Wet lay-up system.

Polymerization follows the layering and continues in an environmental temperature with relatively short time without warming the composite surface.

9 APPENDIX C (STRESS-STRAIN RELATIONSHIP OF FRP)

9.1 MECHANICAL BEHAVIOR OF COMPOSITES

Fiber-reinforced composites are heterogeneous (*e.g.*, made of different materials) and anisotropic (*e.g.*, exhibiting different properties when tested in different directions) materials. Because the application related to fiber-reinforced composites for civil engineering is far greater than the material micro-structure (see Table 7-2), the heterogeneity may be neglected, and the actual material may be considered to behave homogeneously. If the stress and strain at a generic location of the fiber-reinforced composite is represented by the components of the tensor of stress $\underline{\sigma}$ (Figure 9-1) and strain $\underline{\varepsilon}$, the mechanical behavior of a homogeneous, elastic, and anisotropic solid may be defined by 21 independent elastic constants as follows:

$$\underline{\sigma} = [C]\underline{\varepsilon} \Leftrightarrow \begin{bmatrix} \sigma_1 \\ \sigma_2 \\ \sigma_3 \\ \tau_{23} \\ \tau_{31} \\ \tau_{12} \end{bmatrix} = \begin{bmatrix} C_{11} & C_{12} & C_{13} & C_{14} & C_{15} & C_{16} \\ C_{12} & C_{22} & C_{23} & C_{24} & C_{25} & C_{26} \\ C_{13} & C_{23} & C_{33} & C_{34} & C_{35} & C_{36} \\ C_{14} & C_{24} & C_{34} & C_{44} & C_{45} & C_{46} \\ C_{15} & C_{25} & C_{35} & C_{45} & C_{55} & C_{56} \\ C_{16} & C_{26} & C_{36} & C_{46} & C_{56} & C_{66} \end{bmatrix} \begin{bmatrix} \varepsilon_1 \\ \varepsilon_2 \\ \varepsilon_3 \\ \gamma_{23} \\ \gamma_{31} \\ \gamma_{12} \end{bmatrix}, \quad (9.1)$$

where $[C]$ is the stiffness matrix.

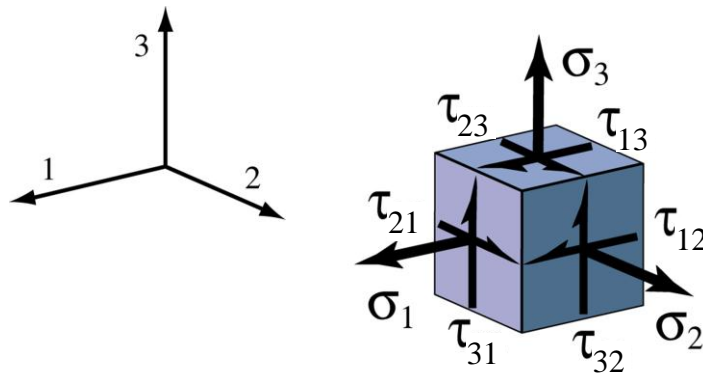


Figure 9-1 – Representation of stresses for an infinitesimal element.

The complete characterization of the stiffness matrix would require the evaluation of the 21 constants by means of combining tensile and shear tests. The number of tests to be performed can be significantly reduced if the material has some degree of symmetry, which is a circumstance that occurs in a majority of fiber-composite materials having engineering applications.

Many unidirectional composites may be considered transversely isotropic, as it is shown in Figure 9-2, where the 2-3 plane perpendicular to fibers is the isotropic plane. In this case, the independent elastic constants are reduced from 21 to 5 and the stiffness matrix becomes:

$$[C]=\begin{bmatrix} C_{11} & C_{12} & C_{12} & 0 & 0 & 0 \\ C_{12} & C_{22} & C_{23} & 0 & 0 & 0 \\ C_{12} & C_{23} & C_{22} & 0 & 0 & 0 \\ 0 & 0 & 0 & \frac{1}{2}(C_{22}-C_{23}) & 0 & 0 \\ 0 & 0 & 0 & 0 & C_{66} & 0 \\ 0 & 0 & 0 & 0 & 0 & C_{66} \end{bmatrix}. \quad (9.2)$$

It is often convenient to refer to the so-called engineering constants: E (Young modulus of elasticity), ν (Poisson ratio), and G (shear modulus) for which well-established procedures for their experimental evaluation exist. These constants have generally different values in different directions. The Young modulus of elasticity in the fiber direction, E_1 , is expected to be greater than that in the transverse direction, E_2 , which in turn can be different from that in the third direction, E_3 . The same consideration is applied to the modules G_{12} , G_{13} , G_{23} (directions 1, 2, and 3 are defined according to Figure 9-2).

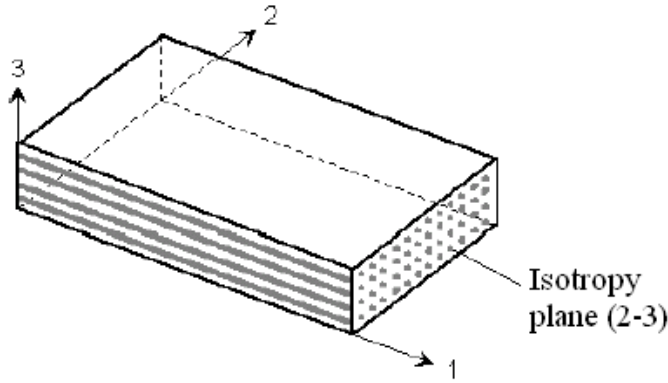


Figure 9-2 – Unidirectional composite with a transverse isotropy plane.

The deformability matrix, $[S]$, defined as the matrix inverse of the stiffness matrix $[C]$ (Eq. (9.2)), can be expressed as a function of the engineering constants as follows:

$$[S]=\begin{bmatrix} \frac{1}{E_1} & -\frac{\nu_{12}}{E_1} & -\frac{\nu_{12}}{E_1} & 0 & 0 & 0 \\ -\frac{\nu_{12}}{E_1} & \frac{1}{E_2} & -\frac{\nu_{23}}{E_2} & 0 & 0 & 0 \\ -\frac{\nu_{12}}{E_1} & -\frac{\nu_{23}}{E_2} & \frac{1}{E_2} & 0 & 0 & 0 \\ 0 & 0 & 0 & \frac{2 \cdot (1 + \nu_{23})}{E_2} & 0 & 0 \\ 0 & 0 & 0 & 0 & \frac{1}{G_{12}} & 0 \\ 0 & 0 & 0 & 0 & 0 & \frac{1}{G_{12}} \end{bmatrix}. \quad (9.3)$$

The independent engineering constants are as follows:

$$E_1, E_2, \nu_{12}, \nu_{23}, G_{12}.$$

9.2 PLANE STRESSES

For unidirectional thin laminate subjected to plane stresses, the deformability matrix becomes:

$$\begin{bmatrix} \varepsilon_1 \\ \varepsilon_2 \\ \gamma_{12} \end{bmatrix} = \begin{bmatrix} \frac{1}{E_1} & -\frac{\nu_{12}}{E_1} & 0 \\ -\frac{\nu_{12}}{E_1} & \frac{1}{E_2} & 0 \\ 0 & 0 & \frac{1}{G_{12}} \end{bmatrix} \begin{bmatrix} \sigma_1 \\ \sigma_2 \\ \tau_{12} \end{bmatrix}. \quad (9.4)$$

The mechanical behavior of unidirectional laminates can therefore be characterized by four independent elastic constants. For their determination, uniaxial tensile tests are typically performed with fibers inclined with an angle, θ , relative to the direction of the applied load. By setting $\theta = 0^\circ$, (e.g., fibers parallel to the load direction), E_1 and ν_{12} may be obtained, while with $\theta = 90^\circ$ (fibers perpendicular to the direction of load), E_2 may be determined. G_{12} can be determined and is dependent on the angle θ that is a function of the selected strengthening geometry.

Approximate values of the mentioned elastic constants can also be calculated using simple “micro-mechanical” models based on the properties of each components (fibers and matrix) and their volumetric fraction. For unidirectional laminate, longitudinal properties may be evaluated by using a relationship known as the “rule of mixtures.” It is derived from the application of a simple micro-mechanical model where fibers and matrix work in parallel. The model provides good results for the value E_1 of the Young modulus of the elasticity in the direction of fibers and the Poisson ratio ν_{12} .

$$\begin{aligned} E_1 &= V_{\text{fib}} \cdot E_{\text{fib}} + (1 - V_{\text{fib}}) \cdot E_{\text{mat}}, \\ \nu_{12} &= V_{\text{fib}} \cdot \nu_{\text{fib}} + (1 - V_{\text{fib}}) \cdot \nu_{\text{mat}}, \end{aligned} \quad (9.5)$$

where V_{fib} is the fiber volumetric fraction (ratio between the volume of fibers and the overall volume of composite), E_{fib} and E_{mat} are the Young modulus of elasticity of fibers and matrix, respectively, and ν_{fib} and ν_{mat} are the corresponding Poisson ratios.

Instead of the volumetric fraction, the weight fraction of fibers and matrix, P_{fib} and P_{mat} , respectively, are typically known. If ρ_{fib} and ρ_{mat} represent the density of the fibers and matrix, respectively, the following relationships apply:

$$\begin{aligned} V_{\text{fib}} &= \frac{P_{\text{fib}} / \rho_{\text{fib}}}{P_{\text{fib}} / \rho_{\text{fib}} + P_{\text{mat}} / \rho_{\text{mat}}}, \\ P_{\text{fib}} + P_{\text{mat}} &= 1. \end{aligned} \quad (9.6)$$

As an example, the computation of the volumetric fraction of fibers in a glass-fiber reinforced composite having a fraction of weight equal to 60%, is presented. The characteristics of each of the components are reported in Table 9-1.

Table 9-1

	Weight fraction	Density [g/cm ³]
Fiber	0.60	2.5
Matrix	0.40	1.2

By applying Eq. (9.6), a volumetric fraction of glass fibers equal to 42% is obtained. Considering the values of both fibers ($E_{\text{fib}} = 80 \text{ GPa}$, $\nu_{\text{fib}} = 0.3$) and matrix ($E_{\text{mat}} = 3 \text{ GPa}$, $\nu_{\text{mat}} = 0.34$) mechanical properties, the following values of the elastic constants can be obtained:

$$E_1 = 35.2 \text{ GPa},$$

$$\nu_{12} = 0.32.$$

For more details on micro-mechanical modes, the reader should refer to specialized literature.

9.2.1 Effect of loading acting on directions other than that of material symmetry

Once the elastic constants of the material are known, the behavior of fiber-reinforced material is completely determined for loading in any direction independent of the axes of symmetry of the material. For example, Figure 9-3 relates to a laminate with continuous unidirectional fibers, where the equivalent elastic constants E_x , E_y , G_{xy} and ν_{xy} , with respect to the reference axes x and y of the load system may be determined as a function of the angle θ and the elastic constants of the material $E_1, E_2, G_{12}, \nu_{12}$.

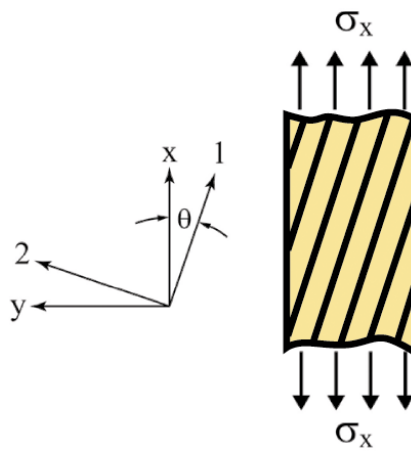


Figure 9-3 – Definition of the reference systems x, y and $1, 2$.

In Figure 9-4 and Figure 9-5, the values of both Young modulus of elasticity, E_x , and shear modulus, G_{xy} , are plotted as a function of the angle, θ , between the fibers and applied load, for different values of the modulus E_1 .

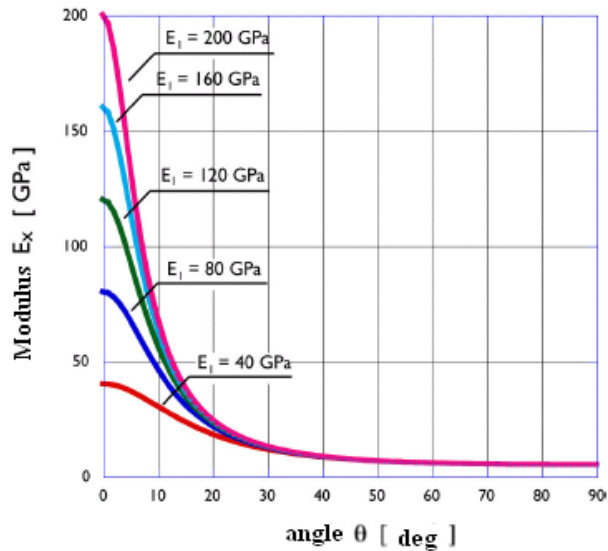


Figure 9-4 – Young modulus of elasticity E_x as a function of θ for fiber-reinforced composites for several values of the Young modulus of elasticity E_1 ($E_2 = 5$ GPa; $G_{12} = 3$ GPa; $\nu_{12} = 0.35$).

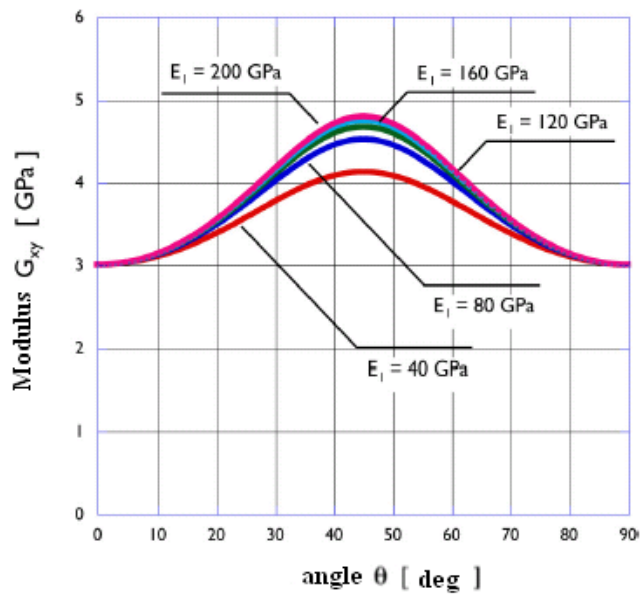


Figure 9-5 – Shear modulus G_{xy} as a function of θ for fiber-reinforced composites for several values of the Young modulus of elasticity E_1 ($E_2 = 5$ GPa; $G_{12} = 3$ GPa; $\nu_{12} = 0.35$).

Significant variations of the modulus E_x and G_{xy} with the angle θ are apparent. In case of fabrics, fibers are distributed along two or more directions (multi-axial fabrics). If one were to neglect the crimping due to weaving of fibers and assuming the fabric is comprised of two separate unidirectional layer of fibers running at 0° and 90° direction, the modulus of elasticity, E_x , can be evaluated with simplified methods neglecting the slip between layers. For this particular case of fabric having the same percentage of fibers in the two considered directions (balanced fabric), Figure 9-6 shows the relationship between E_x and θ .

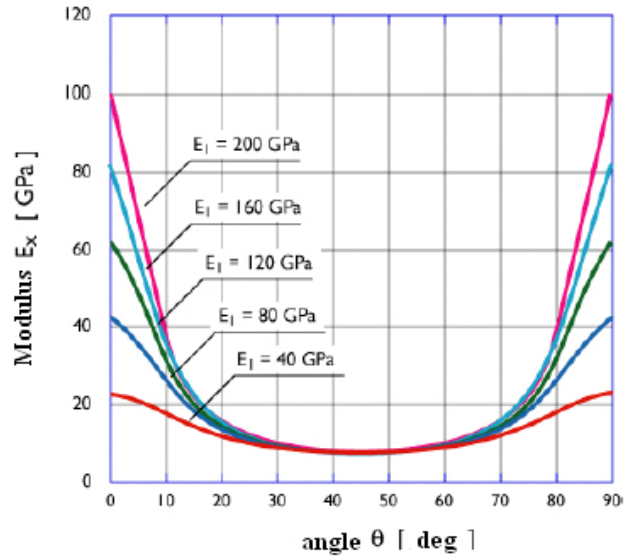


Figure 9-6 – Modulus of elasticity, E_x , as a function of θ for balanced fabric depending upon the modulus of elasticity, E_1
 ($E_2 = E_1$; $G_{12} = 3$ GPa; $\nu_{12} = 0.35$)

9.3 FAILURE CRITERIA

The micro-mechanic collapse mechanism of fiber-reinforced materials is a complex phenomenon that depends on a multitude of parameters that include type of loading, fiber, and resin type. For this reason, failure criteria for composites usually refer to the macro-mechanical level assuming that the composite itself can be considered a homogeneous material exhibiting a linear elastic behavior up to collapse. For laminates subjected to planar stresses, one of the simplest failure criteria is that of the maximum stress. If $\sigma_{1u,t}$ ($\sigma_{1u,c}$) and $\sigma_{2u,t}$ ($\sigma_{2u,c}$), represent the tensile (compressive) failure stress in the symmetry directions, and τ_{12u} is the corresponding shear stress at failure, this criterion can be represented as follows:

$$\begin{aligned} \sigma_1 & \begin{cases} \leq \sigma_{1u,t} \text{ per } \sigma_1 > 0, \\ \geq \sigma_{1u,c} \text{ per } \sigma_1 < 0, \end{cases} \\ \sigma_2 & \begin{cases} \leq \sigma_{2u,t} \text{ per } \sigma_2 > 0, \\ \geq \sigma_{2u,c} \text{ per } \sigma_2 < 0, \end{cases} \\ |\tau_{12}| & \leq \tau_{12u}. \end{aligned} \quad (9.7)$$

The criterion does not depend on the sign of the shear stress nor does it consider the interaction between different failure modes. Different failure modes can occur independent from one another. The maximum stress that the laminate can withstand is given by the lowest among the following values (Figure 9-3):

$$\begin{aligned} \sigma_{xu} & < \frac{\sigma_{1u}}{\cos^2 \theta}, \\ \sigma_{xu} & < \frac{\sigma_{2u}}{\sin^2 \theta}, \\ \sigma_{xu} & < \frac{\tau_{12u}}{\sin \theta \cdot \cos \theta}. \end{aligned} \quad (9.8)$$

Figure 9-7 shows the variation of σ_{xu} as a function of θ .

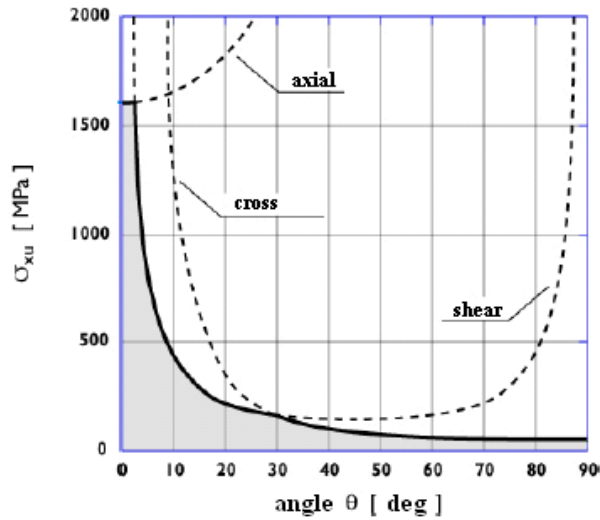


Figure 9-7 – Criterion of maximum stress: tensile failure stress as a function of θ for unidirectional laminates ($\sigma_{1u} = 1600$ MPa; $\sigma_{2u} = 40$ MPa; $\tau_{12u} = 70$ MPa).

The criterion of the maximum stress is usually in well agreement with experimental data only for a tensile test with θ smaller than 15° and larger than 45° . Otherwise, the measured values for compression are higher. Another widely used criterion to estimate the failure of a laminate is due to Tsai-Hill, which may be expressed as follows:

$$\left(\frac{\sigma_1}{\sigma_{1u}}\right)^2 + \left(\frac{\sigma_2}{\sigma_{2u}}\right)^2 - \frac{\sigma_1 \cdot \sigma_2}{\sigma_{1u}^2} + \left(\frac{\tau_{12}}{\tau_{12u}}\right)^2 \leq 1. \quad (9.9)$$

The stress at failure as function of θ can be written as follows (Figure 9-3):

$$\sigma_{xu} = \left[\frac{\cos^4 \theta}{\sigma_{1u}^2} + \left(\frac{1}{\tau_{12u}^2} - \frac{1}{\sigma_{1u}^2} \right) \cos^2 \theta \cdot \sin^2 \theta + \frac{\sin^4 \theta}{\sigma_{2u}^2} \right]^{-1/2} \quad (9.10)$$

and it is plotted in Figure 9-8.

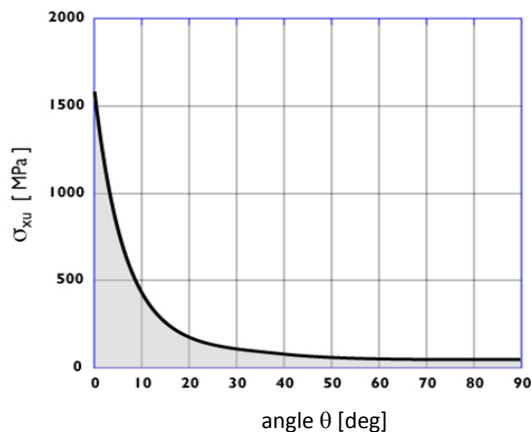


Figure 9-8 – Tsai-Hill criterion: tensile failure stress as a function of θ for unidirectional laminates ($\sigma_{1u} = 1600$ MPa; $\sigma_{2u} = 40$ MPa; $\tau_{12u} = 70$ MPa).

As previously shown, the variability of strength and elastic properties of the fiber-reinforced materials depends on the direction of the fibers compared to the direction of applied load.

10 APPENDIX D (DEBONDING)

10.1 FAILURE DUE TO DEBONDING

The primary failure modes of FRP-strengthened structural members due to debonding are summarized as follows:

- Mode 1 (plate end debonding)** (Figure 10-1). The end portions of the FRP system are subjected to high interfacial shear stresses for a length of approximately 100-200 mm. When strengthening is done with FRP laminates, tensile stress perpendicular to the interface between FRP and support (normal stress) may arise due to the significant stiffness of FRP laminate (Figure 10-2(a)). Normal stresses may reduce the value of interfacial shear stress as shown in Figure 10-2(b). Failure mode by end debonding is characterized by brittle behavior.

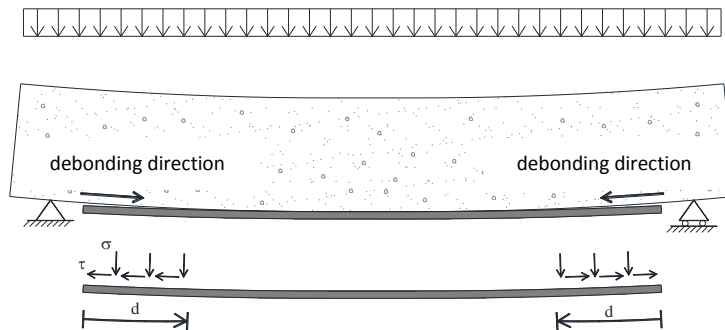


Figure 10-1 – Plate end debonding.

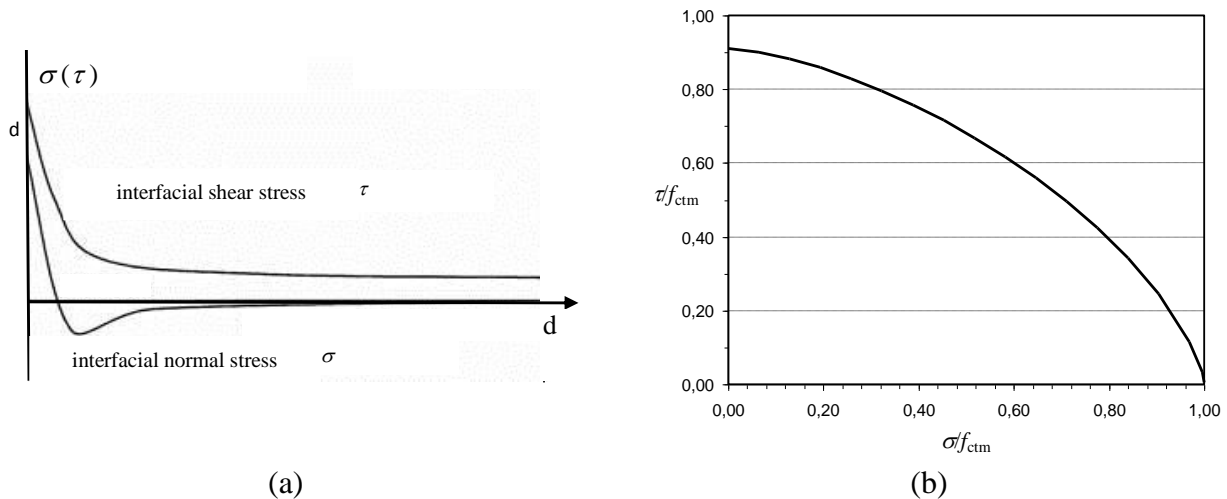


Figure 10-2 – (a) Interfacial shear and normal stress along the length of a bonded FRP laminate (linear-elastic analysis); (b) Strength domain represented by interfacial shear and normal stresses.

- Mode 2 (Debonding by flexural cracks in the beam)** (Figure 10-3). Flexural cracking generates discontinuity within the support that enhances interfacial shear stress causing FRP debonding. Cracking may be oriented perpendicular to the beam axis when flexural loads are predominant; inclined when there is a combination of flexure and shear.

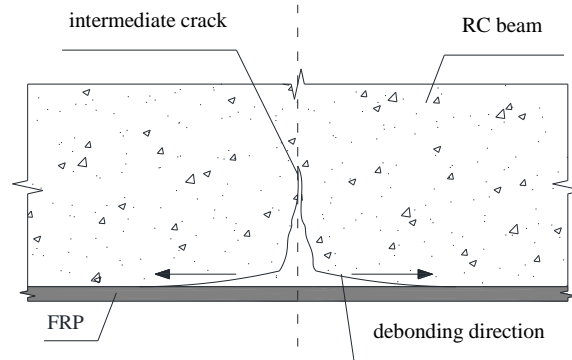


Figure 10-3 – Debonding starting from vertical cracks in concrete.

- Mode 3 (Debonding by diagonal shear cracks) (Figure 10-4). For members where shear stresses are predominant to flexural stresses, a relative displacement between the edges of the crack is displayed. Such displacement increases normal stress perpendicular to the FRP laminate responsible for FRP debonding. Such a debonding mechanism is active regardless of the presence of stirrups. Collapse due to debonding from diagonal shear cracks is peculiar in four-point-bending laboratory tests, and is not common for field application where the applied load is distributed over the beam's length. For heavily strengthened beams with low transverse reinforcement, debonding in the form of peeling typically occur at the end plate section.

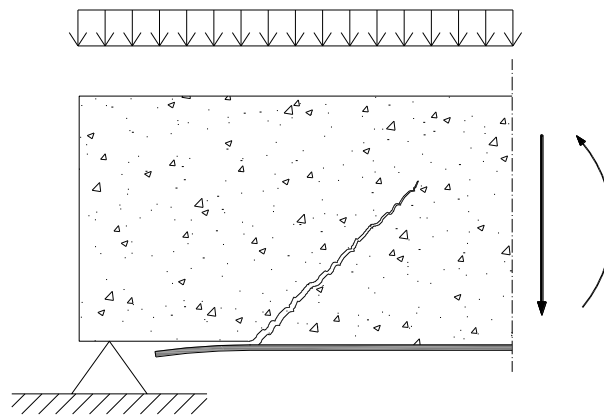


Figure 10-4 – Debonding by diagonal shear crack.

- Mode 4 (Debonding by irregularities and roughness of the concrete surface). Localized debonding due to surface irregularities of the concrete substrate may propagate and cause full debonding of the FRP system. This failure mode can be avoided if the concrete surface is treated in such a way to avoid excessive roughness.

10.2 BOND BETWEEN FRP AND CONCRETE

In the following section, additional recommendations related to bond between FRP and concrete support are given. Reference is made to Figure 10-5.

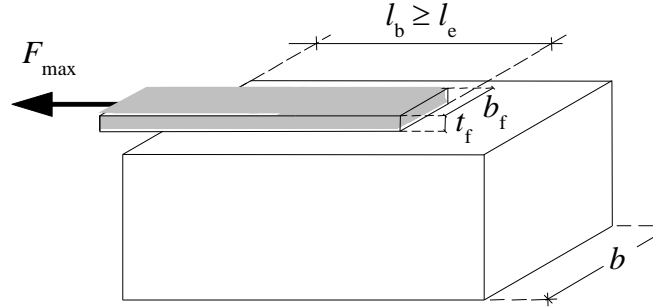


Figure 10-5 – Maximum force allowed to FRP reinforcement.

10.2.1 Specific fracture energy

The maximum force, F_{\max} , allowed in the FRP reinforcement, considered of infinite length, can be computer as:

$$F_{\max} = b_f \int_0^{\infty} \tau_b(x) dx, \quad (10.1)$$

where b_f is the width of FRP and τ_b is the shear stress at the adhesive-concrete interface. When the stiffness of the concrete elements is greater than the FRP, Equation (10.2) can be considered:

$$F_{\max} = b_f \cdot \sqrt{2 \cdot E_f \cdot t_f \cdot \Gamma_F}, \quad (10.2)$$

where t_f , b_f , E_f , Γ_F represent FRP thickness, width, Young modulus of elasticity in the direction of the applied force, and the specific fracture energy, respectively. In this document Equation (10.3) is used to compute the specific fracture energy:

$$\Gamma_F = k_b \cdot k_G \cdot \sqrt{f_{cm} \cdot f_{ctm}}, \quad (10.3)$$

where the symbols are defined in Chapter 4.

In particular:

- k_b is a geometrical corrective factor equal to:

$$k_b = \sqrt{\frac{2 - b_f/b}{1 + b_f/b}} \geq 1 \quad \text{per } b_f/b \geq 0.25, \quad (10.4)$$

where b is the width of the strengthened element (for $b_f/b < 0.25$, k_b is taken as function of $b_f/b = 0.25$).

- k_G is an experimental corrective factor expressed in terms of length.

The coefficient k_G was calibrated based on a large population of experimental results available in scientific national and international literature. Part of the experimental database gathers FRP-concrete bond tests performed by Task 8.2 of ReLUIS-DPC 2005-2008 Project. Calibration of mean and characteristic values were performed in accordance with the EN1990 – Annex D (Design assisted by testing) methodology, assuming uncertainties in the mechanical characteristic of the materials.

The calibration procedure was performed separately for pre-cured FRP (Section 2.3.2) and for wet lay-up FRP (Section 2.3.3). The following were obtained:

- for pre-cured FRP, mean value of 0.063 mm and 5% fractile of 0.023 mm.
- for wet lay-up FRP, mean value of 0.077 mm and 5% fractile of 0.037 mm

By using the mean values, 0.063 and 0.077, Equation (10.3) is used to compute the mean value of specific fracture energy, Γ_{Fm} .

Whereas, using the 5% fractiles, 0.023 mm and 0.037 mm, the characteristic value of energy is computed. The performed analysis considers the uncertainties related to the concrete strength. Therefore, in this Guideline, Γ_{Fk} was not reduced with the partial factor $\gamma_C = 1.5$.

The design debonding strength of FRP, f_{fdd} , can be obtained using Equation (10.2):

$$f_{fdd} = \frac{1}{\gamma_{f,d}} \sqrt{\frac{2 \cdot E_f \cdot \Gamma_{Fd}}{t_f}}, \quad (10.5)$$

where, $\Gamma_{Fd} = \Gamma_{Fk}/FC$ and $\gamma_{f,d}$ is the partial factor as per Section 3.4.1.

Figure 10-6 shows the experimental values of bond tests extracted from the database used for the k_G calibration. Values are divided for pre-cured and wet lay-up FRP.

The experimental data is compared to the design, mean and fractile values of debonding strength obtained from Equation (10.5).

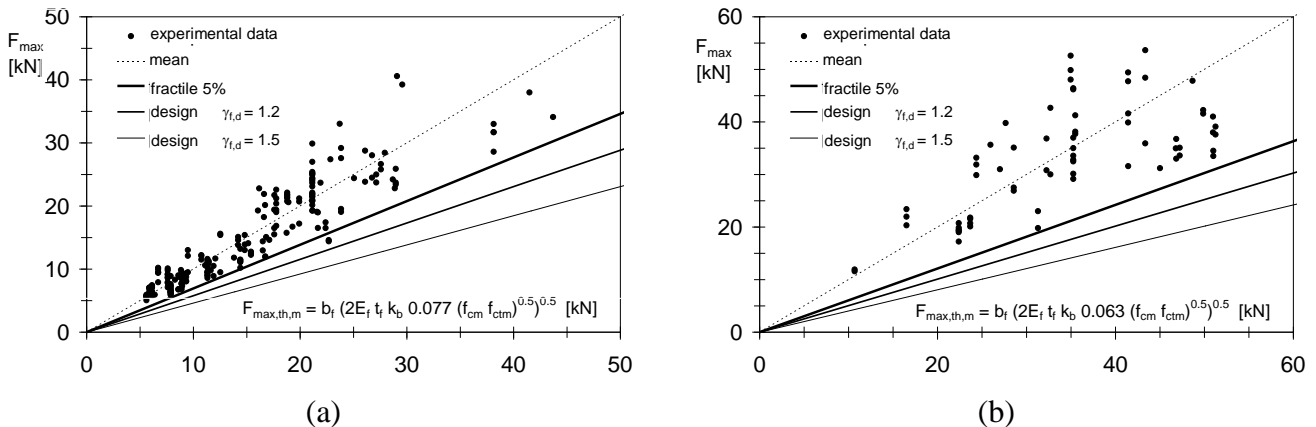


Figure 10-6 – Experimental calibration: (a) wet lay-up FRP, (b) pre-cured FRP.

10.2.2 Bond-slip law

The bond between FRP and concrete is typically expressed with a relationship between interfacial shear stress and the corresponding slip (“ $\tau_b - s$ ” relationship). Both FRP and concrete mechanical characteristics as well as geometry of the FRP system and concrete support shall be considered in the analysis.

The $\tau_b - s$ relationship is typically non linear with a descending nature. For design purposes, it may be treated as a bi-linear relationship as shown in Figure 10-7. The first ascending branch is defined by considering the deformability of adhesive layer and concrete support for an appropriate depth. Unless a more detailed analysis is performed, the average mechanical parameters defining the $\tau_b - s$ relationship, can be evaluated as follows.

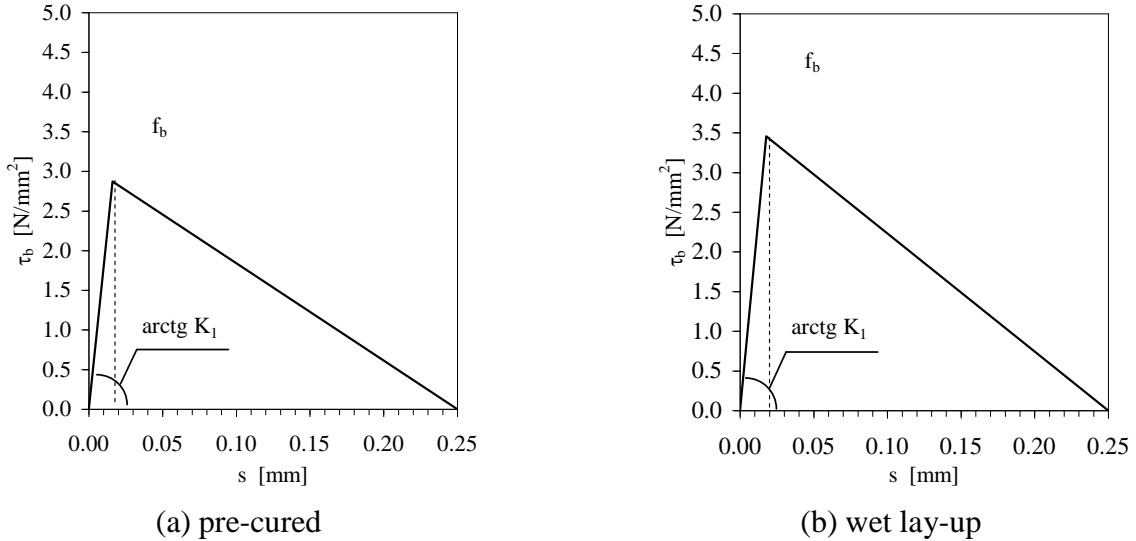


Figure 10-7 – Example of bilinear “ $\tau_b - s$ ” laws ($f_{cm} = 20$ MPa, $k_b=1$).

The slip interface corresponding to full debonding is assumed:

$$s_u = 0.25 \text{ mm} . \quad (10.6)$$

The mean values of shear stress to be used in the $\tau_b - s$ relationship can be computed by using the mean value of the specific fracture energy, Γ_{Fm} , as follows:

$$f_b = \frac{2 \cdot \Gamma_{Fm}}{s_u} . \quad (10.7)$$

K_1 is equal to:

$$K_1 = \frac{c_1}{t_a/G_a + t_c/G_c} , \quad (10.8)$$

where, G_a and G_c represent shear modules of adhesive and concrete, respectively, t_a is the nominal thickness of the adhesive; and t_c is the effective depth of concrete (suggested values for t_c and c_1 are $20 \div 30$ mm and $0.5 \div 0.7$, respectively). For SLS K_1 is given by Equation (10.8) with $c_1 = 1$.

10.2.3 Optimal bond length

In this guideline, the design optimal bond length is obtained by using a stiff-softening constitutive law ($K_1 \rightarrow \infty$) where the contribution of the stiff branch can be neglected compared to the branch demonstrating softening (assumption valid at ULS):

$$l_{ed} = \frac{1}{\gamma_{Rd} \cdot f_{bd}} \sqrt{\frac{\pi^2 \cdot E_f \cdot t_f \cdot \Gamma_{Fd}}{2}} , \quad (10.9)$$

where:

- $f_{bd} = \frac{2 \cdot \Gamma_{Fd}}{s_u}$ is the design bond strength between FRP reinforcement and concrete.
- $s_u = 0.25$ mm.
- $\gamma_{Rd} = 1.25$ is a corrective factor.

10.2.4 Debonding due to flexural cracks

In case of debonding due to flexural cracking (mode 2) ε_{fdd} , can be computed as follows:

$$\varepsilon_{fdd} = \frac{f_{fdd,2}}{E_f} = \frac{k_q}{\gamma_{f,d}} \cdot \sqrt{\frac{2 \cdot \frac{k_b \cdot k_{G,2}}{FC} \cdot \sqrt{f_{cm} \cdot f_{ctm}}}{E_f \cdot t_f}} \geq \varepsilon_{sy} - \varepsilon_0, \quad (10.10)$$

The relationship is similar to that proposed for maximum stress or strain in FRP reinforcement when mode 1 controls FRP debonding.

Calibration of the mean and characteristic values of $k_{G,2}$ in Equation (10.10) is performed by using a large population of experimental results available in the scientific national and international literature for FRP strengthened beams and slabs exhibiting failure due to flexural debonding (mode 2). Calibration of mean and characteristic values were performed in accordance with the EN1990 – Annex D (Design assisted by testing) methodology, assuming uncertainties in the mechanical characteristic of the materials. The statistical procedure provide mean and 5% fractile values of $k_{G,2}$ equal to 0.32 and 0.10 mm, respectively and independently of support type.

The introduction of k_q is justified based on the experimental and analytical results, furthermore is used to characterized distributed and concentrated loads (1.25 and 1.0, respectively). However, the assumption of $k_q = 1.25$ represent a precautionary value considering the small amount of data available on tests with distributed load.

10.3 BOND BETWEEN FRP AND MASONRY

In the following, additional recommendations related to bond between FRP and concrete support are given. Reference is made to Figure 10-8.

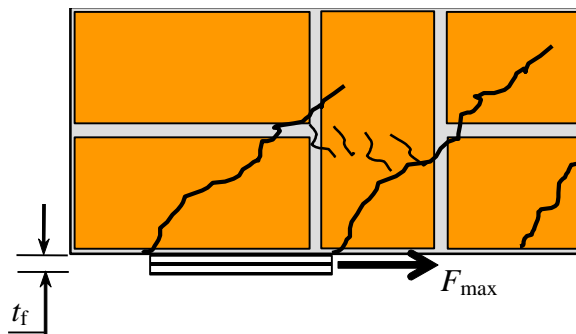


Figure 10-8 – Failure mode.

10.3.1 Specific fracture energy

The maximum force, F_{max} , allowed in the FRP reinforcement considered of infinite length is given by Equation (10.1), which becomes Equation (10.2) when the stiffness of masonry elements is

greater than that of the FRP. The specific fracture energy becomes:

$$\Gamma_F = k_b \cdot k_G \cdot \sqrt{f_{cm} \cdot f_{ctm}}, \quad (10.11)$$

where the symbols refer to Chapter 5. In particular:

- k_b is a geometrical corrective factor equal to:

$$k_b = \sqrt{\frac{3 - b_f/b}{1 + b_f/b}}, \quad (10.12)$$

where b is the width of the strengthened element, to be calculated as reported in Section 5.3.2.

- k_G is an experimental corrective factor expressed in terms of length.

The coefficient k_G was calibrated based on a large population of experimental results available in scientific national and international literature. The experimental database gathers FRP-concrete bond tests performed by Task 8.2 of ReLUIS-DPC 2005-2008 Project. Calibration of mean and characteristic values are performed in accordance with the EN1990 – Annex D (Design assisted by testing) methodology, assuming uncertainties in the mechanical characteristic of the materials.

The calibration procedure was performed separately for wet lay-up FRP (Section 2.2.3) on masonry made of perforated and natural bricks, with the following characteristics:

- for perforated brick 7.0-42.0 MPa;
- for tuff bricks 2.7-5.0 MPa;
- for calcarenite or Lecce stones 2.0-24.0 MPa.

The calibration results are:

- for perforated brick, mean value of 0.093 mm and a 5% fractile of 0.031 mm.
- for tuff bricks, mean value of 0.157 mm and a 5% fractile of 0.048 mm.
- for calcarenite or Lecce stones, mean value of 0.022 mm and a 5% fractile of 0.012 mm.

By using the mean and characteristic values of k_G in Equation (10.11), the mean and characteristic values of specific fracture energy, Γ_{Fm} and Γ_{Fk} , can be obtained.

The design debonding strength of FRP, f_{idd} , can be obtained by using Equation (10.2):

$$f_{idd} = \frac{1}{\gamma_{f,d}} \sqrt{\frac{2 \cdot E_f \cdot \Gamma_{Fd}}{t_f}}, \quad (10.13)$$

where, $\Gamma_{Fd} = \Gamma_{Fk}/FC$ and $\gamma_{f,d}$ the partial factor as per Section 3.4.1.

Consequentially, the design debonding strength value can be computed as follows:

$$F_{max,d} = \frac{b_f}{\gamma_{f,d}} \sqrt{2 \cdot E_f \cdot t_f \cdot \Gamma_{Fd}}. \quad (10.14)$$

Figure 10-9 shows the experimental values of bond tests extracted from the database used for the k_G calibration. Values are divided based on masonry types.

The experimental data are compared to the design, mean and fractile values of debonding strength, obtained from Equation (10.14).

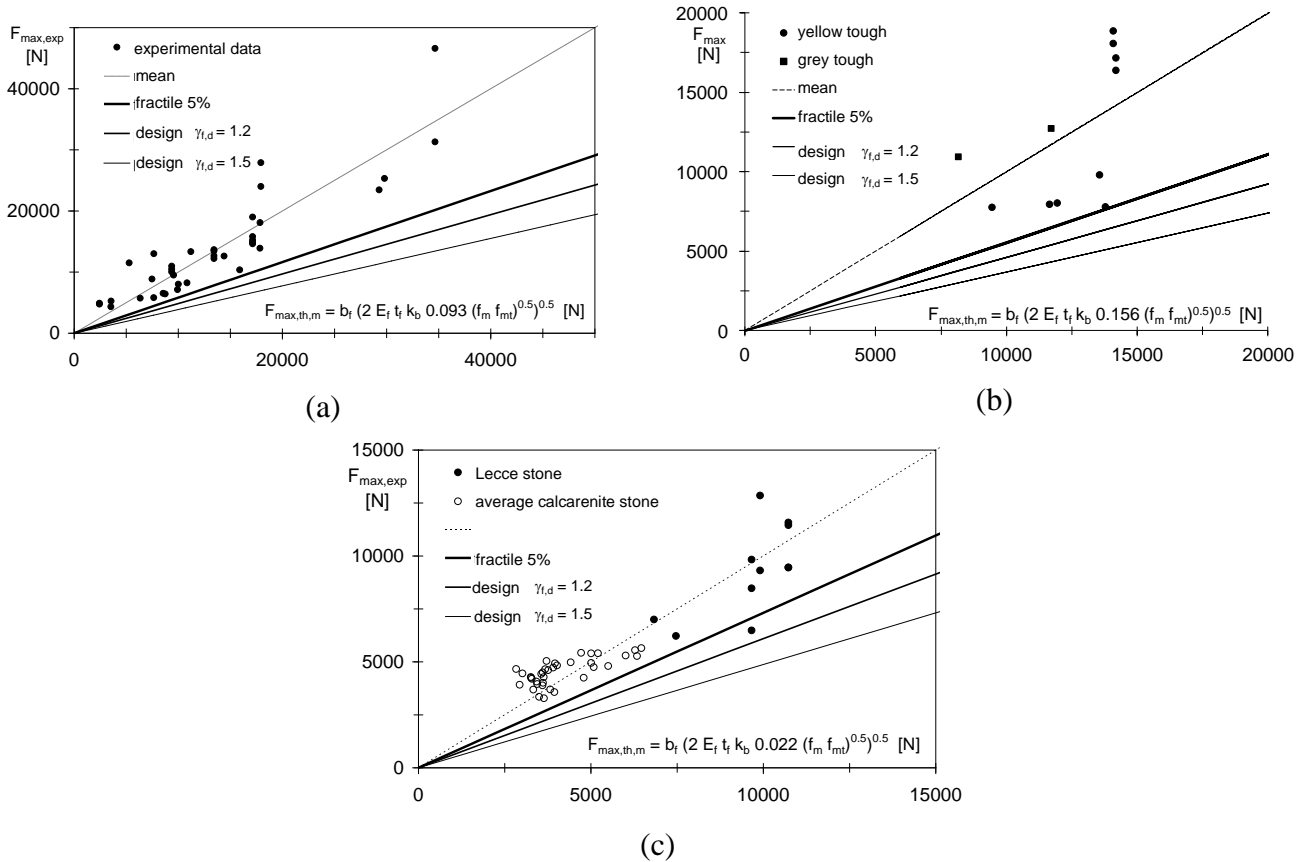


Figure 10-9 – Experimental calibration: (a) performed bricks, (b) tuff bricks, (c) calcarenite and Lecce stones.

When considering the limited numbers of experimental tests available in literature on FRP-strengthened masonry, the k_G values used for pre-cured FRP can be obtained by reducing 35% of the values of wet lay-up FRP systems.

10.3.2 Bond-slip law

Bond between FRP and concrete is typically expressed with a relationship between interfacial shear stress and the corresponding slip (“ $\tau_b - s$ ” relationship).

The $\tau_b - s$ relationship is typically non linear with a descending branch. For design purposes, this may be treated as a bi-linear relationship as shown in Figure 10-10.

The first ascending branch is defined by considering the deformability of the adhesive layer and masonry support for an appropriate depth. Unless a more detailed analysis is performed, the average mechanical parameters defining the $\tau_b - s$ relationship can be evaluated as follows.

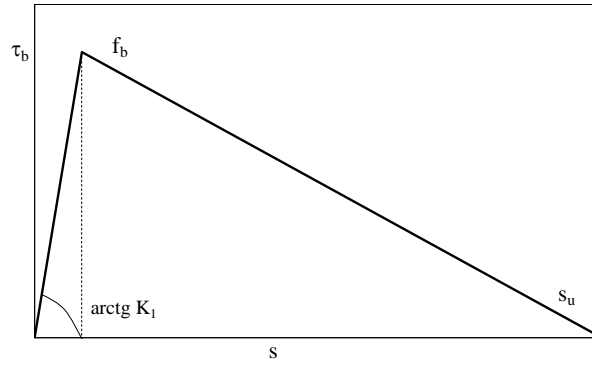


Figure 10-10 - Example of bilinear “ $\tau_b - s$ ” laws.

The interface slip corresponding to full debonding is assumed:

$$\begin{aligned} s_u &= 0.3 \text{ mm per murature di calcareniti e di pietra leccese;} \\ s_u &= 0.4 \text{ mm per murature di laterizio e di tufo.} \end{aligned} \quad (10.15)$$

The mean values of shear stress to be used in the $\tau_b - s$ relationship can be computed by using the mean value of the specific fracture energy, Γ_{Fm} , as follows::

$$f_b = \frac{2 \cdot \Gamma_{Fm}}{s_u}. \quad (10.16)$$

K_1 is equal to:

$$K_1 = \frac{c_1}{t_a/G_a + t_m/G_m}, \quad (10.17)$$

where, G_a and G_m represent shear modules of the adhesive and masonry, respectively. t_a is the nominal thickness of the adhesive and t_m is the effective depth of masonry (suggested values for t_c and c_1 are $20 \div 30$ mm and $0.5 \div 0.7$, respectively). For SLS, K_1 is given by Equation (10.17) with $c_1 = 1$.

10.3.3 Optimal bond length

In this guide, the design optimal bond length is obtained by using a stiff-softening constitutive law ($K_1 \rightarrow \infty$) where the contribution of the stiff branch can be neglected, compared to the softening branch (assumption valid at ULS):

$$l_{ed} = \frac{1}{\gamma_{Rd} \cdot f_{bd}} \sqrt{\frac{\pi^2 \cdot E_f \cdot t_f \cdot \Gamma_{Fd}}{2}} \geq 150 \text{ mm} \quad (10.18)$$

where:

- $f_{bd} = \frac{2 \cdot \Gamma_{Fd}}{s_u}$ is the design bond strength between FRP reinforcement and masonry, with $\Gamma_{Fd} = \Gamma_{Fk}/FC$;
- $s_u = 0.3$ mm for calcarenite or Lecce stones masonry and $s_u = 0.40$ mm for perforated and tuff bricks masonry;

- γ_{Rd} is a corrective factor equal to 1.5 for perforated and tuff bricks masonry and 1.25 for calcarenite or Lecce stones masonry.

10.3.4 Debonding due to flexural cracking

In case of debonding due to flexural cracking (mode 2) ε_{fdd} , can be computed as follows:

$$\varepsilon_{fdd} = \frac{f_{fdd,2}}{E_f} = \frac{\alpha \cdot f_{fdd}}{E_f} \quad (1.0 \leq \alpha \leq 1.5). \quad (10.19)$$

Considering the small amount of data available, α is extrapolated from the concrete experiences.

11 APPENDIX E (STRENGTHENING FOR COMBINED BENDING AND AXIAL LOAD OF REINFORCED CONCRETE MEMBERS)

11.1 FLEXURAL CAPACITY OF FRP STRENGTHENED MEMBERS SUBJECTED TO COMBINED BENDING AND AXIAL LOAD

FRP strengthened members subjected to combined bending and axial loading shall be designed as follows:

$$M_{Sd} \leq M_{Rd}(N_{Sd}), \quad (11.1)$$

where M_{Sd} is the design applied moment and M_{Rd} represents the flexural capacity of the strengthened member considering the design axial force N_{Sd} .

A possible design procedure is hereafter described. The mechanical ratio μ_s and μ_f related to tension steel reinforcement and FRP system, respectively, can be calculated as follows:

$$\mu_s = \frac{A_{s1} \cdot f_{yd}}{f_{ccd} \cdot b \cdot d}, \quad (11.2)$$

$$\mu_f = \frac{b_f \cdot t_f \cdot f_{fd}}{f_{ccd} \cdot b \cdot d}. \quad (11.3)$$

where A_{s1} and f_{yd} represent area and design yield strength of existing steel reinforcement, respectively. f_{ccd} is equal to the design strength of confined concrete, b and d are the width and effective depth of the FRP strengthened member, respectively, b_f e t_f are the FRP width and thickness, respectively; and f_{fd} is the FRP ultimate design strength calculated according to Section 4.2.2.4, item (2)P. Material design strengths for non-seismic applications shall be in accordance with Section 3.3.3, item (7). For seismic applications, such values shall be obtained from in-situ experimental tests. Unless a more detailed analysis regarding structural details and material properties is available, mechanical properties of existing materials shall be divided by an appropriate coefficient greater than 1.

The following non-dimensional equations reflecting applied loads are introduced:

$$n_{Sd} = \frac{N_{Sd}}{f_{ccd} \cdot b \cdot d}, \quad (11.4)$$

$$m_{Sd} = \frac{M_{Sd}}{f_{ccd} \cdot b \cdot d^2}. \quad (11.5)$$

When FRP width and mechanical properties are known, a trial and error procedure can be performed to evaluate the thickness of FRP reinforcement as follows.

Step 1

η is computed as follows:

$$\eta = n_{sd} + \mu_s \cdot (1-u) + \mu_f \cdot \quad (11.6)$$

Step 2

The following parameters η_i ($i = 0, 1, 2, 3$), are defined

$$\eta_0 = -\mu_s \cdot u, \quad \eta_1 = \frac{2}{3} \cdot \frac{r}{r+1}, \quad \eta_2 = 0.8 \cdot \frac{1.75 \cdot r}{1.75 \cdot r + 1}, \quad \eta_3 = 0.51 + \mu_f \cdot (1-r), \quad (11.7)$$

where:

- u is the ratio of steel existing compression, A_{s2} , and tension, A_{s1} area.
- $r = 2/1000 \varepsilon_{fd}$.

Step 3

From Table 11-1, the failure mode (Figure 4-5, 4.2.2.3) and corresponding value of the parameter $m_{(mr)}(\eta)$ can be determined as a function of η when compared with the limits presented in Step 2.

Table 11-1

Failure mode	η	$m_{(mr)}(\eta)$
1a	$\eta_0 \leq \eta \leq \eta_1$	$m_{(1a)}(\eta) = \frac{1}{2} \cdot \left\{ \eta_0 + \frac{\eta_1 \cdot (1-\eta_1) - \eta_0 \cdot (\eta - \eta_0)}{\eta_1 - \eta_0} \right\}$
1b	$\eta_1 \leq \eta \leq \eta_2$	$m_{(1b)}(\eta) = \frac{1}{2} \cdot \left\{ \eta_1 \cdot \eta_2 + [1 - (\eta_1 + \eta_2)] \cdot \eta \right\}$
2	$\eta_2 \leq \eta \leq \eta_3$	$m_{(2)}(\eta) = \frac{1}{2} \cdot \left\{ \eta_2 \cdot (1-\eta_2) + \frac{(0.75 - \eta_3) - \eta_2 \cdot (1-\eta_2)}{\eta_3 - \eta_2} \cdot (\eta - \eta_2) \right\}$

Step 4

The non-dimensional flexural capacity, $m_{Rd}(n_{sd})$, of the strengthened member is evaluated as follows:

$$m_{Rd}(n_{sd}) = m_{(mr)}(\eta) + \frac{1}{2} \cdot [\mu_s \cdot (1+u) + \mu_f] \cdot \quad (11.8)$$

Step 5

The following relationship shall be met:

$$m_{Rd}(n_{sd}) \geq m_{sd} \cdot \quad (11.9)$$

If this is not the case, the thickness, t_f , of the strengthening system is increased as well as its mechanical ratio, μ_f , and the iterative procedure is repeated from Step 1.

12 APPENDIX F (CONFINED CONCRETE)

12.1 CONSTITUTIVE LAW OF CONFINED CONCRETE

Modeling the mechanical behavior of FRP-confined concrete members calls for the preliminary definition of a suitable constitutive law $\sigma(\varepsilon)$ related to the mechanical behavior of members subjected to uni-axial compression (σ and ε are considered positive in compression).

In this context, as an alternative method to the parabolic-rectangular model proposed in 4.5.3, a non-linear relationship can be adopted similar to that shown in Figure 12-1, where a parabolic branch is followed by a linear ascending branch. At the intersection point between the two branches, the first derivative of the function $\sigma(\varepsilon)$ shall be assumed as continuous.

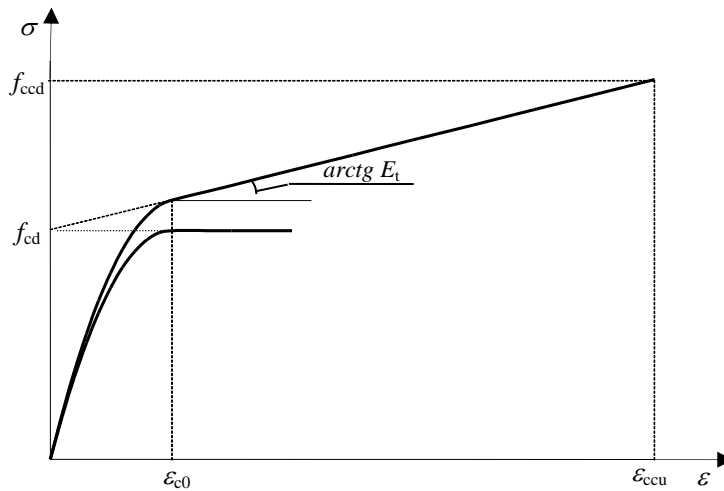


Figure 12-1 – Stress-strain model of FRP-confined concrete.

The mathematical expression of such relationship can be written as follows:

- (parabolic branch)
$$\frac{f_c}{f_{cd}} = a \cdot \bar{\varepsilon} - \bar{\varepsilon}^2 \quad \text{per } 0 \leq \bar{\varepsilon} \leq 1, \quad (12.1)$$

- (linear branch)
$$\frac{f_c}{f_{cd}} = 1 + b \cdot \bar{\varepsilon} \quad \text{per } 1 \leq \bar{\varepsilon} \leq \frac{\varepsilon_{ccu}}{\varepsilon_{c0}}. \quad (12.2)$$

where:

- $\bar{\varepsilon}$ is a non-dimensional coefficient defined as follows:

$$\bar{\varepsilon} = \frac{\varepsilon_c}{\varepsilon_{c0}}; \quad (12.3)$$

- f_{cd} and ε_{c0} are the design strength of unconfined concrete and the concrete strain at peak (typically assumed equal to 0.2%), respectively.
- ε_{ccu} is the design ultimate strain of confined concrete corresponding to the design strength f_{ccd} (Chapter 4).

- the coefficients a and b are taken as follows:

$$a = 1 + \gamma, \quad b = \gamma - 1, \quad (12.4)$$

where (see Figure 12-1):

$$\gamma = \frac{f_{cd} + E_t \cdot \varepsilon_{c0}}{f_{cd}}, \quad (12.5)$$

$$E_t = \frac{f_{ccd} - f_{cd}}{\varepsilon_{ccu}}. \quad (12.6)$$

13 APPENDIX G (EXAMPLES OF FRP STRENGTHENING DESIGN ON RC STRUCTURES)

In this Appendix, numerical examples of non-seismic FRP strengthening of RC members are provided. It is assumed that FRP strengthening is necessary due to the increase of applied loads. Design is only performed at ultimate limit state. Serviceability limit state design is not performed because of similarities to traditional theory of RC members.

13.1 GEOMETRICAL, MECHANICAL AND LOADING DATA

The building considered for design is shown in Figure 13 – 1 structural elements are defined as follows:

- Primary rectangular beams with cross-section of 30 cm x 50 cm (concrete cover $d_1=d_2=3$ cm).
- Secondary rectangular beams with cross-section of 30 cm x 40 cm (concrete cover $d_1=d_2=3$ cm).
- Rectangular columns with cross-section of 20 cm x 30 cm (concrete cover $d_1=d_2=3$ cm).

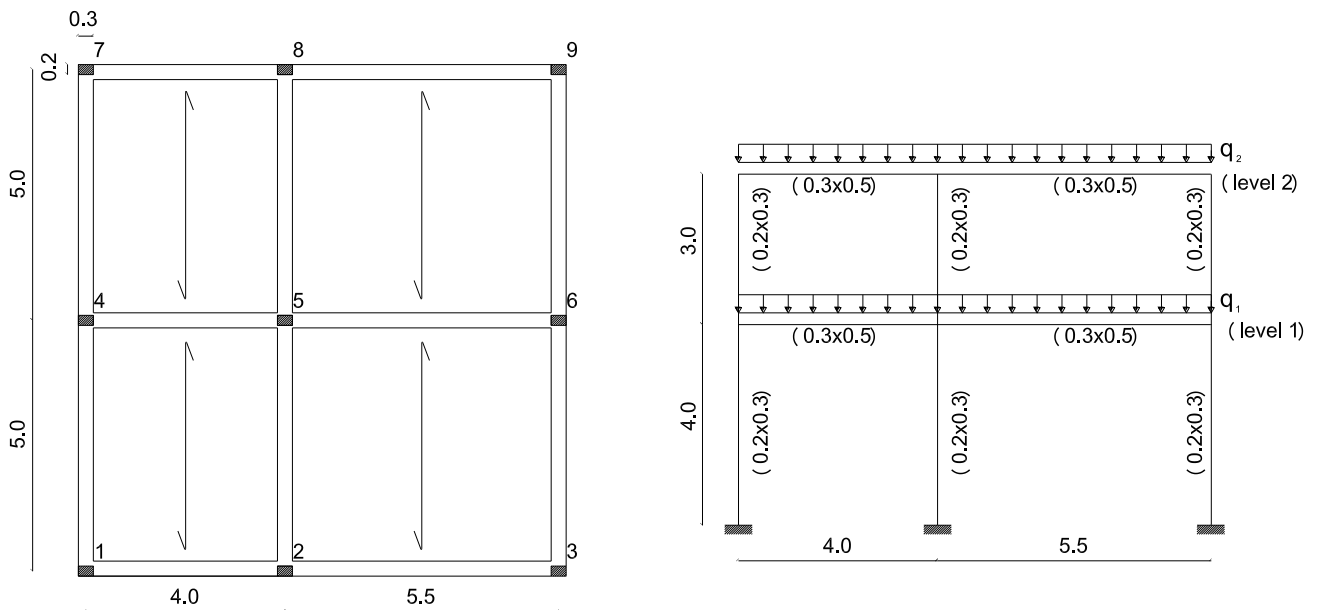


Figure 13-1 – Building geometry (dimensions in m).

Material mechanical properties are as follows:

- Concrete: $R_{ck} = 20 \text{ N/mm}^2$.
- Steel: FeB38k ($f_{yk}=31.5 \text{ N/mm}^2$).

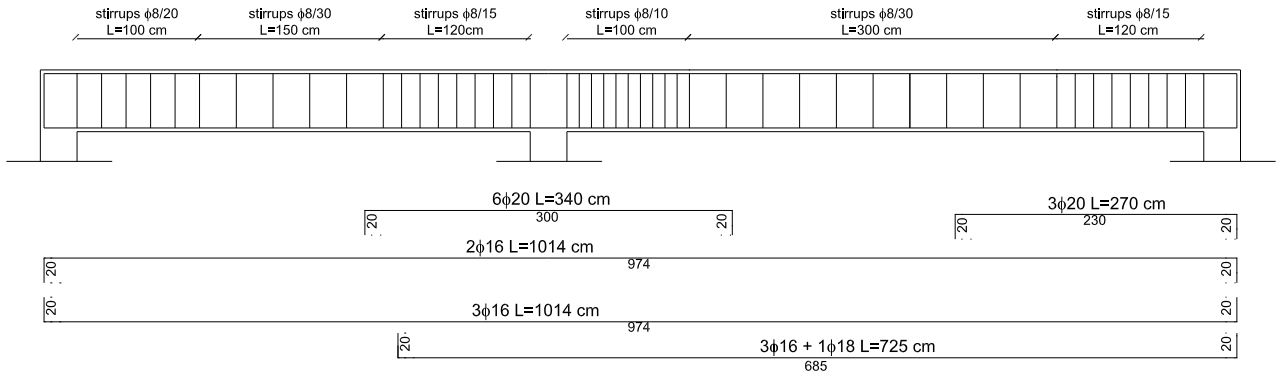
Loading conditions are defined as follows:

- Live load at level 1: $a_1 = 2.00 \text{ kN/m}^2$;
- Live load at level 2: $a_2 = 0.50 \text{ kN/m}^2$;
- Snow (zone III, height $a_s < 200 \text{ m}$): $b = 0.75 \text{ kN/m}^2$;
- Dead load due to flooring (for each level): $g = 6.00 \text{ kN/m}^2$.

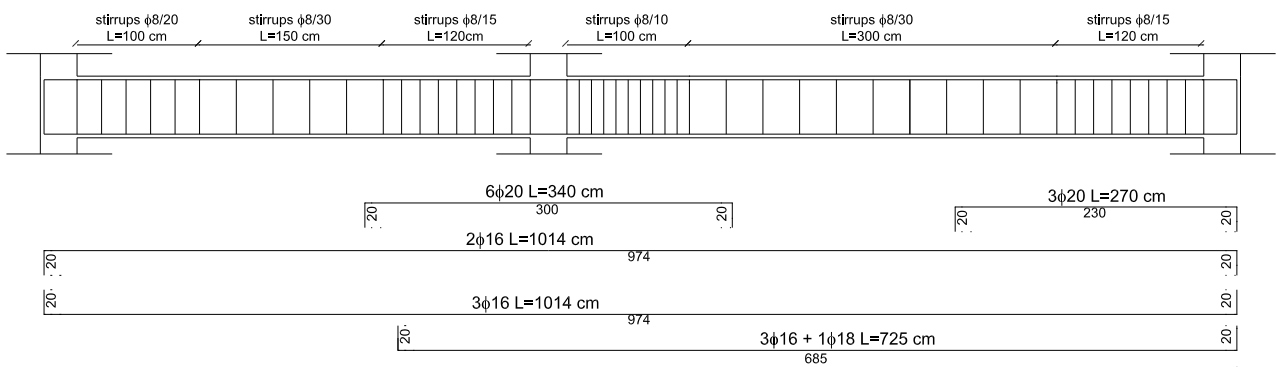
Factored loads acting at ULS can be evaluated as follows:

- level 1: $q_1 = 62.25$ kN/m;
- level 2: $q_2 = 55.00$ kN/m.

METALLIC REINFORCEMENT
LEVEL 2



METALLIC REINFORCEMENT
LEVEL 1



METALLIC REINFORCEMENT
COLUMNS AT LEVEL 1 AND 2

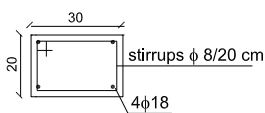


Figure 13-2 shows existing steel bar arrangement for beams and columns.

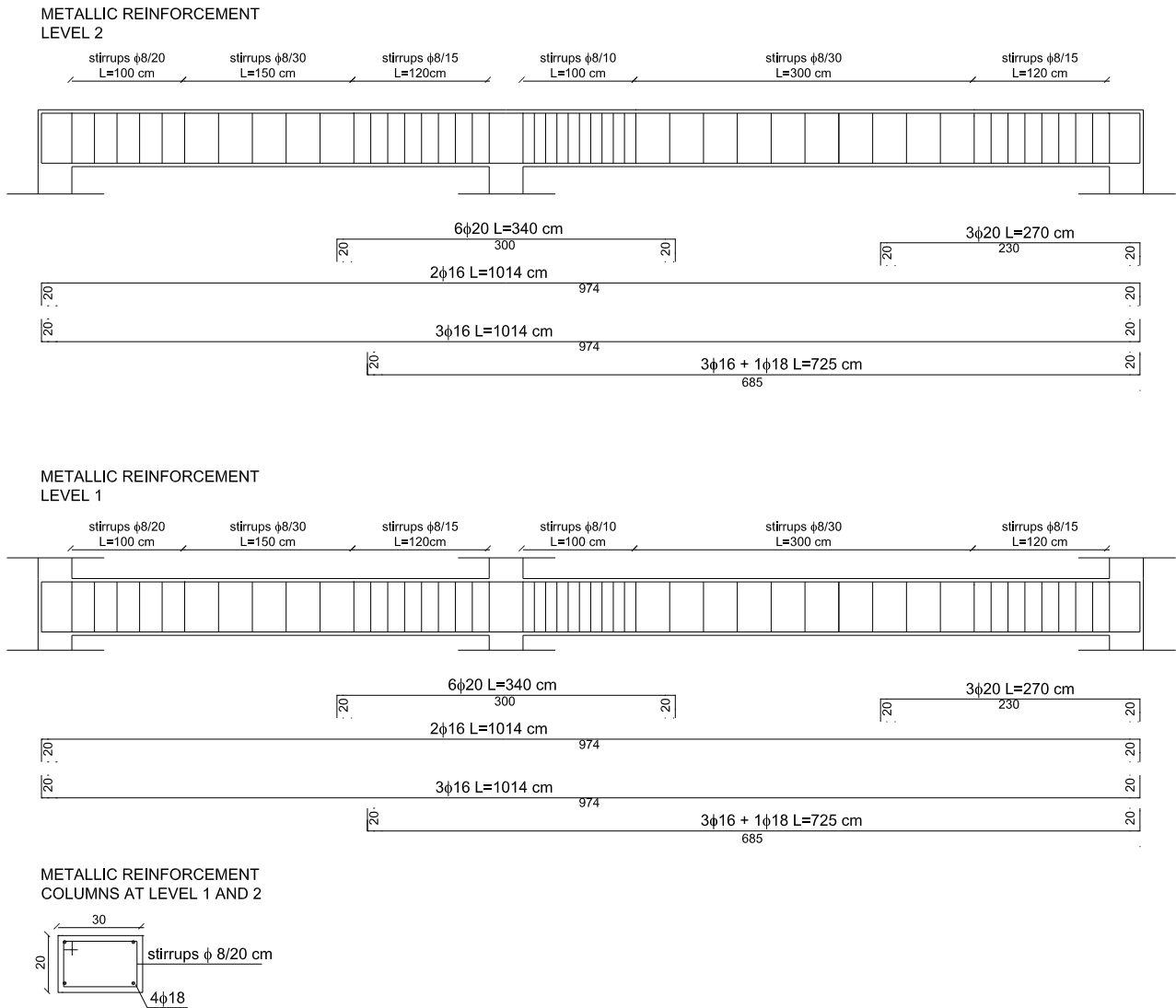


Figure 13-2 – Steel bars location for beams and columns.

13.2 INCREASE OF APPLIED LOADS

New loads are defined as follows:

- Level 1: $a_1 = 6.00 \text{ kN/m}^2$.
- Level 2: $a_2 = 4.00 \text{ kN/m}^2$.

New factored loads acting at ULS can be evaluated as follows:

- Level 1: $q_1 = 92.25 \text{ kN/m}$.
- Level 2: $q_2 = 81.20 \text{ kN/m}$.

13.3 DESIGN OF FLEXURAL REINFORCEMENT

Design material properties are determined as follows:

- Concrete ($f_{cm} = 20.00 \text{ N/mm}^2$, $\gamma_c = 1$, $FC = 1.35$, $f_{cd} = 14.81 \text{ N/mm}^2$, $f_{ck} = 12.00 \text{ N/mm}^2$, $f_{ctm} = 1.57 \text{ N/mm}^2$);
- Steel ($f_{ym} = 380.00 \text{ N/mm}^2$, $\gamma_s = 1$, $FC = 1.35$, $f_{yd} = 281.48 \text{ N/mm}^2$).

The following relationship shall be met:

$$M_{Sd} \leq M_{Rd} \quad (13.1)$$

As indicated in Table 13-1, Equation (10.7) is not met at mid-span of both levels for 5.5 m long beams.

Table 13-1

Level	Span [m]	Section	M_{Sd} [kN m]	A_{s1} [cm ²]	A_{s2} [cm ²]	M_{Rd} [kN m]	$M_{Sd} \leq M_{Rd}$
1	4.0	left support	-49	4.02	6.03	-51.7	SI
	4.0	mid-span	69	6.03	4.02	76.6	SI
	4.0	right support	-195	22.90	14.60	-284.3	SI
	5.5	left support	-242	22.90	14.00	-283.9	SI
	5.5	mid-span	182	14.60	4.02	179.5	NO
	5.5	right support	-99	13.40	14.60	-167.9	SI
2	4.0	left support	-35	4.02	6.03	-51.7	SI
	4.0	mid-span	65	6.03	4.02	76.6	SI
	4.0	right support	-175	22.90	14.60	-284.3	SI
	5.5	left support	-207	22.90	14.00	-283.9	SI
	5.5	mid-span	173	14.60	4.02	179.5	SI
	5.5	right support	-67	13.40	14.60	-167.9	SI

FRP flexural strengthening is performed by installing carbon fiber reinforcement using the wet-lay-up method with the following geometrical and mechanical characteristics (System 1, Section 2.2.3.2: $\alpha_{fE} = \alpha_{ff} = 0.9$):

- CFRP thickness: $t_{f,1} = 0.167$ mm.
- CFRP width: $b_f = 240.0$ mm.
- CFRP Young modulus of elasticity in fibers direction (beam axis): $E_f = 270000$ N/mm².
- CFRP characteristic strength: $f_{fk} = 2700$ N/mm².

For a Type A application, the partial factors γ_f and $\gamma_{f,d}$ are 1.10 and 1.20, respectively (Section 3.4.1).

The environmental conversion factor, η_a , is equal to 0.85 (Table 3-2, Section 3.5.1).

A trial and error procedure is initiated for the determination of the number of CFRP plies, n_f , required to satisfy Equation (10.7). Therefore, assuming $n_f = 1$, the maximum CFRP design strain, ε_{fd} , can be calculated as follows (Equation (4.14)):

$$\varepsilon_{fd} = \min \left\{ \eta_a \cdot \frac{\varepsilon_{fk}}{\gamma_f}, \varepsilon_{fdd} \right\} = \varepsilon_{fdd} = 0.0045, \quad (13.2)$$

where:

$$\varepsilon_{fk} = \frac{f_{fk}}{E_f} = 0.01, \quad (13.3)$$

$$\varepsilon_{fdd} = \frac{f_{fdd,2}}{E_f} \geq \varepsilon_{sy} - \varepsilon_0 = 0.0045 \geq 0.0014 - 0.0007 = 0.0007. \quad (13.4)$$

CFRP design strength, $f_{fdd,2}$, when failure mode 2 (debonding) controls and when k_G , $k_{G,2}$ and k_q are equal to 0.037 mm, 0.10 mm and 1.25, respectively, can be calculated as follows

$$k_b = \sqrt{\frac{2 - b_f/b}{1 + b_f/b}} \geq 1, \quad (13.5)$$

$$\Gamma_{Fd} = \frac{k_b \cdot k_G}{FC} \cdot \sqrt{f_{cm} \cdot f_{ctm}} = 0.154 \text{ N/mm}, \quad (13.6)$$

$$f_{fdd,2} = \frac{k_q}{\gamma_{f,d}} \cdot \sqrt{\frac{E_f}{t_f} \cdot \frac{2 \cdot k_b \cdot k_{G,2}}{FC} \cdot \sqrt{f_{cm} \cdot f_{ctm}}} = 1207.3 \text{ N/mm}^2. \quad (13.7)$$

CFRP flexural failure mechanism may be of two types, depending on whether CFRP maximum tensile strain, ε_{fd} , or concrete maximum compressive strain, ε_{cu} , is reached (Figure 13-3).

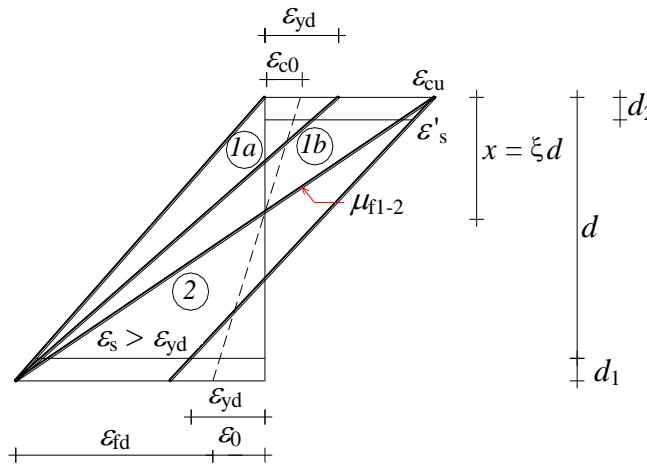


Figure 13-3 – Failure regions of RC members strengthened with FRP.

To identify the failure mode for this particular case, the CFRP mechanical ratio, μ_f , is computed:

$$\mu_f = \frac{b_f \cdot (n_f \cdot t_{f,1}) \cdot f_{fdd,2}}{f_{cd} \cdot b \cdot d}, \quad (13.8)$$

and compared with the balanced mechanical ratio, μ_{f1-2} , defined as follows:

$$\mu_{f1-2} = \frac{0.8 \cdot \varepsilon_{cu} \cdot \frac{h}{d}}{\varepsilon_{cu} + \varepsilon_{fd} + \varepsilon_0} - \mu_s \cdot (1 - u). \quad (13.9)$$

where:

- μ_s may be defined as follows:

$$\mu_s = \frac{A_{s1} \cdot f_{yd}}{f_{cd} \cdot b \cdot d}; \quad (13.10)$$

- u represents the ratio between steel compression, A_{s2} , and tension, A_{s1} , area;
- ε_0 is the initial strain of the tension side of concrete, evaluated as:

$$\varepsilon_0 = \frac{M_{gk}}{0.9 \cdot d \cdot E_s \cdot A_{s2}}; \quad (13.11)$$

- M_{gk} is the moment due to dead loads at SLS.

If $\mu_f \leq \mu_{f1-2}$, failure occurs in region 1; if $\mu_f > \mu_{f1-2}$, failure occurs in region 2 (Figure 13-3). Once the failure mode is known, the position, x , of the neutral axis can be identified from Equation (4.15). The flexural capacity, M_{Rd} , can be calculated from Equation (4.16), assuming that the partial factor, γ_{Rd} , is set equal to 1.00 (Table 3-1, Section 3.4.2). The calculated flexural capacity, M_{Rd} , for a single layer of CFRP reinforcement (Table 13-2) is greater than the applied moment, M_{Sd} .

Table 13-2

Level	Span [m]	Section	M_{Sd} [kN m]	n_f	ε_{fd}	$\mu_{f,1}$	$\mu_{f,1-2}$	Region	x [m]	M_{Rd} [kN m]	l_e [m]
1	5.5	mid-span	182	1	0.0045	0.027	0.18	1	0.11	214	0.12

If Equation (13.1) is not satisfied, the number, n_f , of CFRP plies shall be progressively increased, in the interaction of the design procedure. CFRP strengthening shall be installed along the beam axis until Equation (13.1) is not met. Proper anchorage length shall be provided to CFRP reinforcement according to Section 4.2.2.5. Table 13-2 also summarizes the value of the optimal bond length, l_{ed} , calculated according to Equation (4.1):

$$l_{ed} = \frac{1}{\gamma_{Rd} \cdot f_{bd}} \sqrt{\frac{\pi^2 \cdot E_f \cdot n_f \cdot t_{f,1} \cdot \Gamma_{Fd}}{2}} = 120 \text{ mm}, \quad (13.12)$$

where:

- $\gamma_{Rd} = 1.25$;
- $f_{bd} = \frac{2 \cdot \Gamma_{Fd}}{s_u} = 1.23 \text{ MPa}$, with $s_u = 0.25 \text{ mm}$.

The debonding capacity is verified with $M_{Sd} = 179.5 \text{ kNm}$ and $\sigma_f = 411 \text{ MPa}$, and f_{fd} equal to:

$$f_{fdd} = \frac{1}{\gamma_{f,d}} \cdot \sqrt{\frac{2 \cdot E_f \cdot F_{Fd}}{t_f}} = 587.0 \text{ MPa.} \quad (13.13)$$

13.4 DESIGN OF SHEAR REINFORCEMENT

The following relationship shall be met:

$$V_{Sd} \leq V_{Rd}. \quad (13.14)$$

where V_{Sd} is the design applied shear force, and V_{Rd} represent the shear capacity to be calculated as follows:

$$V_{Rd} = \min \{ V_{Rd,s}, V_{Rd,c} \}, \quad (13.15)$$

where $V_{Rd,s}$ and $V_{Rd,c}$ are the steel and concrete contributions to shear capacity, respectively. In this example only inclined stirrups are considered. According to the current building code, the above-mentioned quantities may be expressed as follows:

$$V_{Rd,c} = 0.9 \cdot d \cdot b \cdot \alpha_c \cdot 0.5 \cdot f_{cd} \cdot (\text{ctg}\alpha + \text{ctg}\theta) / (1 + \text{ctg}^2\theta), \quad (13.16)$$

$$V_{Rd,s} = 0.9 \cdot d \cdot \frac{A_{sw}}{s} \cdot f_{ywd} \cdot (\text{ctg}\alpha + \text{ctg}\theta) \cdot \sin \alpha. \quad (13.17)$$

where:

- A_{sw} and s are area and spacing of steel stirrups, respectively.
- f_{cd} and f_{ywd} are design concrete strength equal to 9.88 MPa and design steel stirrups strength equal to 244.77 MPa, respectively, with material safety factors equal to $\gamma_c=1.5$ and $\gamma_s=1.15$.

Table 13-3 summarizes the as-built shear capacity. As it can be seen, all members require shear strengthening.

Table 13-3

Level	Span [m]	Section	V_{Sd} [kN]	A_{sw} [cm ²]	s [cm]	$V_{Rd,s}$ [kN]	$V_{Rd,c}$ [kN]	V_{Rd} [kN]	Satisfied
1	4.0	left support	148	1.00	20	51.8	313.3	51.8	NO
	4.0	right support	221	1.00	15	69.0	313.3	69.0	NO
	5.5	left support	280	1.00	10	103.5	313.3	103.5	NO
	5.5	right support	228	1.00	15	69.0	313.3	69.0	NO
2	4.0	left support	127	1.00	20	51.8	313.3	51.8	NO
	4.0	right support	198	1.00	15	69.0	313.3	69.0	NO
	5.5	left support	248	1.00	10	103.5	313.3	103.5	NO
	5.5	right support	197	1.00	15	69.0	313.3	69.0	NO

FRP shear strengthening is performed by installing U-wrap carbon fiber reinforcement with the following geometrical and mechanical characteristics:

- CFRP thickness (equivalent): $t_{f,1} = 0.167$ mm;
- CFRP width: $b_f = 150.0$ mm;
- CFRP Young modulus of elasticity: $E_f = 270000$ N/mm²;

- CFRP characteristic strength: $f_{fk} = 2700 \text{ N/mm}^2$.

The partial factors γ_f and $\gamma_{f,d}$ are 1.10 and 1.20, respectively (Section 3.4.1). Fiber orientations with respect to the beam axis is considered for both first and second level equal $\beta = 45^\circ$.

The design shear capacity of the strengthened member may be evaluated from Equation (4.18):

$$V_{Rd} = \min \{ V_{Rd,s} + V_{Rd,f}, V_{Rd,c} \}. \quad (13.18)$$

where:

- $V_{Rd,s}$ is the steel contribution to the shear capacity ($\alpha = 90^\circ$).
- $V_{Rd,c}$ is the concrete contribution to the shear capacity ($\alpha = \beta = 45^\circ$).
- $V_{Rd,f}$ is the CFRP U-wrap contribution to the shear capacity computed in accordance to Equation (4.19):

$$V_{Rd,f} = \frac{1}{\gamma_{Rd}} \cdot 0.9 \cdot d \cdot f_{fed} \cdot 2 \cdot t_f \cdot (\cot \theta + \cot \beta) \cdot \frac{b_f}{p_f}, \quad (13.19)$$

where γ_{Rd} equal to 1.2 (Table 3-1, Section 3.4.2) and θ equal to 45° .

For CFRP U-wrap reinforcement, the effective design strength, f_{fed} , can be evaluated from Equation (13.19) as follows:

$$f_{fed} = f_{idd} \cdot \left[1 - \frac{1}{3} \cdot \frac{l_{ed} \cdot \sin \beta}{\min \{ 0.9 \cdot d, h_w \}} \right]. \quad (13.20)$$

where:

- h_w is the beam depth.
- l_{ed} is the effective bond length from Equation (13.12).
- f_{idd} is the bond strength for mode 1 from Equation (13.13).

Assuming the CFRP strip width, b_f , equal to 150 mm, both center-to-center spacing, p_f , and number of CFRP plies, n_f , can be determined with a trial and error procedure until Equation (13.14) is satisfied.

Table 13-4 and Table 13-5 as well as Table 13-6 and Table 13-7 summarize the shear design of a CFRP U-wrapped strengthened member for both level 1 and 2, respectively.

Table 13-4

Span [m]	Section	n_f	p_f [mm]	k_b	Γ_{Fk} [N/mm ²]	f_{fd} [N/mm ²]	l_{ed} [mm]	f_{fd} [N/mm ²]	$V_{Rd,f}$ [kN]
4.0	left support	1	150	1.0	0.154	587	120	548	129
4.0	right support	2	150	1.0	0.154	415	170	376	177
5.5	left support	3	150	1.0	0.154	339	208	300	212
5.5	right support	2	150	1.0	0.154	415	170	376	177

Table 13-5

Span [m]	Section	$V_{Rd,c}$ [kN]	$V_{Rd,s}$ [kN]	$V_{Rd,f}$ [kN]	V_{Sd} [kN]	V_{Rd} [kN]
4.0	left support	627	52	129	148	181
4.0	right support	627	69	177	221	246
5.5	left support	627	104	212	280	316
5.5	right support	627	69	177	228	246

Table 13-6

Span [m]	Section	n_f	p_f [mm]	Γ_{Fk} [N/mm ²]	f_{fd} [N/mm ²]	l_{ed} [mm]	f_{fd} [N/mm ²]	$V_{Rd,f}$ [kN]
4.0	left support	1	200	0.154	587	120	548	97
4.0	right support	2	200	0.154	415	170	376	133
5.5	left support	2	150	0.154	415	170	376	177
5.5	right support	2	150	0.154	415	170	376	177

Table 13-7

Span [m]	Section	$V_{Rd,c}$ [kN]	$V_{Rd,s}$ [kN]	$V_{Rd,f}$ [kN]	V_{Sd} [kN]	V_{Rd} [kN]
4.0	left support	627	52	97	127	149
4.0	right support	627	69	133	198	202
5.5	left support	627	104	177	248	281
5.5	right support	627	69	177	197	246

13.5 DESIGN OF COLUMNS REINFORCEMENT

Starting from the values of factored moment and axial force, reinforcement design is required for columns subjected to slightly eccentric axial force, if the following equation is not verified:

$$N_{Sd} \leq N_{Rd}. \quad (13.21)$$

When the columns are subjected to combined bending and axial force, the strengthening intervention is required if the point (N_{Sd} ; M_{Sd}) lies outside the P-M domain based on the specified material mechanical properties (

Table 13-8).

Table 13-8

Level	Column	Section	N_{Sd} [kN]	M_{Sd} [kN m]	Eccentricity [cm]	Semi diameter of the central core of inertia [cm]
1	left side	bottom	-290	-10	3.4	6.5
	left side	top	-282	16	-5.7	6.5
	central	bottom	-962	-9	0.9	6.5
	central	top	-954	15	-1.6	6.5
	right side	bottom	-441	16	-3.6	6.5
	right side	top	-432	-34	7.9	6.5
2	left side	bottom	-134	-34	25.4	6.5
	left side	top	-128	35	-27.3	6.5
	central	bottom	-453	-32	7.1	6.5
	central	top	-447	33	-7.4	6.5
	right side	bottom	-204	66	-32.4	6.5
	right side	top	-198	-67	-33.8	6.5

As summarized in Table 13-9 and Table 13-10, there are two cases for each level where columns require strengthening.

Table 13-9

Level	Column	Section	N_{Sd} [kN]	N_{Rd} [kN]	$N_{Rd} > N_{Sd}$
1	left side	bottom	-290	-953	SI
	left side	top	-282	-953	SI
	central	bottom	-962	-953	NO
	central	top	-954	-953	NO
	right side	bottom	-441	-953	SI

Table 13-10

Level	Column	Section	N_{Sd} [kN]	M_{Sd} [kN m]	Strengthening required
1	right side	top	-432	-34	SI
	left side	bottom	-134	-34	SI
	left side	top	-128	35	SI
2	central	bottom	-453	-32	SI
	central	top	-447	33	SI
	right side	bottom	-204	66	NO
	right side	top	-198	-67	NO

13.5.1 Confinement of columns subjected to slightly eccentric axial force

Because the central column of level 1 is subjected to a slightly eccentric axial force, FRP confinement is performed to ensure that the following equation is met:

$$N_{Sd} \leq N_{Rec,d} \quad (13.22)$$

A continuous CFRP wrapping of the column is used assuming the following parameters:

- CFRP thickness (equivalent): $t_{f,1} = 0.167$ mm.

- CFRP Young modulus of elasticity: $E_f = 270000 \text{ N/mm}^2$.
- CFRP characteristic strength: $f_{fk} = 2700 \text{ N/mm}^2$.

The partial factors γ_f and $\gamma_{f,d}$ are set equal to 1.10 and 1.20 (Section 3.4.1). The environmental conversion factor, η_a , is set equal to 0.85 (Table 3-2, Section 3.5.1).

A trial and error procedure is initiated for the determination of the number of CFRP plies, n_f , needed to satisfy Equation (13.22) Therefore, assuming $n_f=1$, the design axial capacity, $N_{Rcc,d}$ can be written as follows (Equation (4.30)):

$$N_{Rcc,d} = \frac{1}{\gamma_{Rd}} \cdot A_c \cdot f_{ccd} + A_s \cdot f_{yd} \quad (13.23)$$

where:

- γ_{Rd} is the partial factor for the resistance model, equal to 1.10 (Section 3.4.2).
- A_c is the concrete cross section area.
- f_{ccd} is the design strength of confined concrete.
- A_s is the area of steel existing reinforcement.
- f_{yd} is the design strength of steel existing reinforcement, calculated according to the current building code.

The design strength, f_{ccd} , for confined concrete may be evaluated according to Equation (4.31):

$$\frac{f_{ccd}}{f_{cd}} = 1 + 2.6 \cdot \left(\frac{f_{l,eff}}{f_{cd}} \right)^{2/3}, \quad (13.24)$$

where f_{cd} is the design strength of unconfined concrete according to the current building code, and $f_{l,eff}$ is the effective confinement pressure, dependent on member cross section and type of FRP application. The latter is given by Equation(4.32) as follows:

$$f_{l,eff} = k_{eff} \cdot f_l = k_{eff} \cdot \left(\frac{1}{2} \cdot \rho_f \cdot E_f \cdot \varepsilon_{fd,rid} \right) \quad (13.25)$$

where:

- $k_{eff} (\leq 1)$ is the coefficient of efficiency defined by Equation (4.34)

$$k_{eff} = k_H \cdot k_V \cdot k_\alpha; \quad (13.26)$$

- ρ_f is the CFRP geometric ratio. A rectangular cross section confined with continuous FRP reinforcement it may be defined as follows:

$$\rho_f = \frac{2 \cdot t_f \cdot (b+h)}{b \cdot h}, \quad (13.27)$$

- b and h are dimensions of the column cross-section.

- E_f represents CFRP Young modulus of elasticity in the direction of fiber.
- $\varepsilon_{fd,rid}$ is the CFRP reduced design strain, taken from Equation (4.37):

$$\varepsilon_{fd,rid} = \min\{\eta_a \cdot \varepsilon_{fk} / \gamma_f; 0.004\} = 0.004. \quad (13.28)$$

The coefficient of vertical efficiency, k_v , as well as the k_α coefficient can be set equal to 1 when continuous wrapping with fibers running perpendicular to the member axis. The coefficient of horizontal efficiency, k_H , for rectangular cross sections can be written as follows (Equation (4.40)):

$$k_H = 1 - \frac{b'^2 + h'^2}{3 \cdot A_g}, \quad (13.29)$$

where b' and h' are the dimension shown in Figure 4-13 of Section 4.5.2.1.2 and A_g is the member cross-sectional area.

The calculated axial capacity, $N_{Rcc,d}$, of the CFRP confined column is summarized in (Table 13-11).

Table 13-11

Section	n_f	k_H	k_{eff}	ρ_f	$f_{l,eff}$ [N/mm ²]	f_{ccd} [N/mm ²]	$N_{Rcc,d}$ [kN]
bottom	1	0.41	0.41	0.0033	0.74	20.03	1106
top	1	0.41	0.41	0.0033	0.74	20.03	1106

13.5.2 Confinement and flexural strengthening of columns subjected to combined bending and axial force

In this paragraph, design of CFRP strengthening for level 2 of the right side column subjected to combined bending and axial force is performed (Table 13-10). Flexural CFRP reinforcement is carried out, given the following geometrical and mechanical parameters:

- CFRP thickness (equivalent): $t_{f,1} = 0.167$ mm;
- CFRP width: $b_{f,1} = 160$ mm;
- CFRP Young modulus of elasticity: $E_f = 270000$ N/mm²;
- CFRP characteristic strength: $f_{fk} = 2700$ N/mm².

In the regions of the column near the beams, the same CFRP material is applied as column wrapping.

The partial factors γ_f is set equal to 1.10.

The environmental conversion factor, η_a , is set equal to 0.85 (Table 3-2, Section 3.5.1).

Due to confinement, the concrete design compressive strength can be written as follows (Section 13.5):

$$f_{ccd} = f_{cd} \cdot \left[1 + 2.6 \cdot \left(\frac{f_{l,eff}}{f_{cd}} \right)^{2/3} \right] = 15.10 \text{ N/mm}^2. \quad (13.30)$$

A trial and error procedure is initiated according to Appendix E by calculating the non-dimensional coefficients.

Design is satisfied when the number, n_f , of CFRP plies is equal to 2 (Table 13-12 e Table 13-13).

Table 13-12

Section	n_{Sd}	m_{Sd}	μ_s	u	n_f	μ_f
bottom	0.251	0.301	0.18	1	2	0.13
top	0.244	0.306	0.18	1	2	0.13

Table 13-13

Section	η_0	η_1	η_2	η_3	η	Failure mode	$m_{(2)}(\eta)$	$m_{Rd}(n_{Sd})$	$m_{Rd} > m_{Sd}$
bottom	-0.177	0.137	0.249	0.606	0.380	2	0.0857	0.3267	SI
top	-0.177	0.137	0.249	0.606	0.373	2	0.0861	0.3272	SI

14 APPENDIX H (EXAMPLES OF FRP STRENGTHENING DESIGN ON MASONRY STRUCTURES)

This appendix reports on the design of FRP strengthening system of masonry panel located in the perimeter wall of a three stores building.

The example discusses in the following items:

- geometrical, mechanical and loading data
- capacity of preexistent masonry panels for combined axial and flexural loads
- design of FRP for combined axial and flexural loads
- shear capacity of preexistent masonry panels
- design of FRP for shear.

14.1 GEOMETRICAL, MECHANICAL AND LOADING DATA

The masonry taken under examination is comprised of four panels of 2.0 m or 3.0 m width as in Figure 14-1. The thickness of the panels decreases with the height and is equal to 500 mm, 375 mm and 250 mm for first, second and third floor, respectively. The height is the same for each panel and equal to 9.0 m (3.0 m per floor).

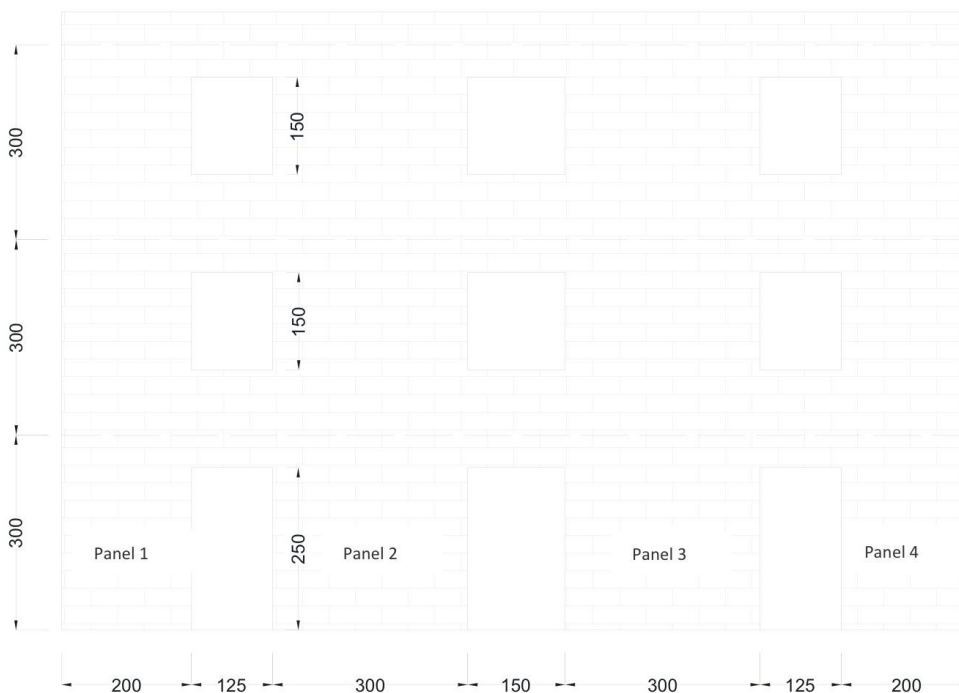


Figure 14-1 – Geometry (dimensions are reported in cm).

Table 14-1 shows data related to the mechanical property of the bricks and values of safety factors. The assumed constitutive law of the masonry is indicated in Section 5.2.3 (8) with $\bar{\varepsilon}_m = 2\text{‰}$ and $\varepsilon_{mu} = 3.5\text{‰}$.

Table 14-1 – Masonry data.

Young modulus of elasticity	E [N/mm ²]	4000
Shear modulus	G [N/mm ²]	1000
Specific weight	γ [kN/m ³]	18.0
Factor of confidence	FC	1.0
Partial factor	γ_M	2
Compressive strength of masonry in the horizontal direction		
Characteristic strength	f_{mk} [N/mm ²]	8.0
Design strength	f_{md} [N/mm ²]	4.0
Shear capacity		
Characteristic strength without any axial load	f_{vk0} [N/mm ²]	0.8
Masonry block strength		
Mean value of compressive strength	f_{bm} [N/mm ²]	38
Mean value of tensile strength	f_{btm} [N/mm ²]	3.8

Wet-layup CFRP with monodirectional fibers is used. Geometrical and mechanical characteristics are reported in Table 14-2. Partial factors and design values of the FRP are shown in Table 14-3.

Table 14-2–FRP geometry and mechanical properties.

Thickness	t_f [mm]	0.165
Width	b_f [mm]	100
Young modulus of elasticity in the fiber direction	E_f [GPa]	230
Ultimate strain	ε_{fk}	0.0175
Spacing	p_f [mm]	500

Table 14-3–Partial factors and design values of the FRP.

Partial factor for debonding	$\gamma_{f,d}$ (Section 3.4.1)	1.2
Partial factor for ULS	γ_f (Section 3.4.1)	1.1
Conversion factor for environment	η_a (Section 3.5.1)	0.95
Ultimate tensile strain	$\eta_a \cdot \varepsilon_{fk} / \gamma_f$ (Section 5.2.3)	0.0151
Width of the bond strength distribution area	b_d [mm] (Section 5.3.2)	250
Geometrical corrective factor	k_b (Section 5.3.2)	1.363
Interface slip at full debonding	s_u [mm] (Section 5.3.2)	0.4
Corrective factor	k_G [mm] (Section 5.3.2)	0.031
Specific fracture energy	Γ_{Fd} [N/mm] (Section 5.3.2)	0.5077
Optimal bond length	l_{ed} [mm] (Section 5.3.2)	150
Design debonding strength of FRP (mode 1)	f_{fdd} [N/mm ²] (Section 5.3.2)	991
Design debonding strength of FRP (mode 2)	$f_{fdd,2} = 2.0 \cdot f_{fdd}$ [N/mm ²] (5.3.3)	1982
Design bond strength between FRP and masonry	f_{bd} [N/mm ²] (Section 5.3.2)	2.5
Maximum strain of FRP before debonding	ε_{idd} (5.3.3)	0.0086
Design strain of FRP	ε_{fd} (Section 5.2.3)	0.0086
Partial factor for combined bending and axial load	γ_{Rd} (Section 3.4.2)	1.00
Partial factor for shear	γ_{Rd} (Section 3.4.2)	1.20

Horizontal and vertical loads of the masonry walls are represented in Figure 14-2. Axial, shear and bending moment diagrams are computed assuming a linear elastic behavior of the structural elements (see Figure 14-3; Table 14-4, Table 14-5, Table 14-6 and Table 14-7).

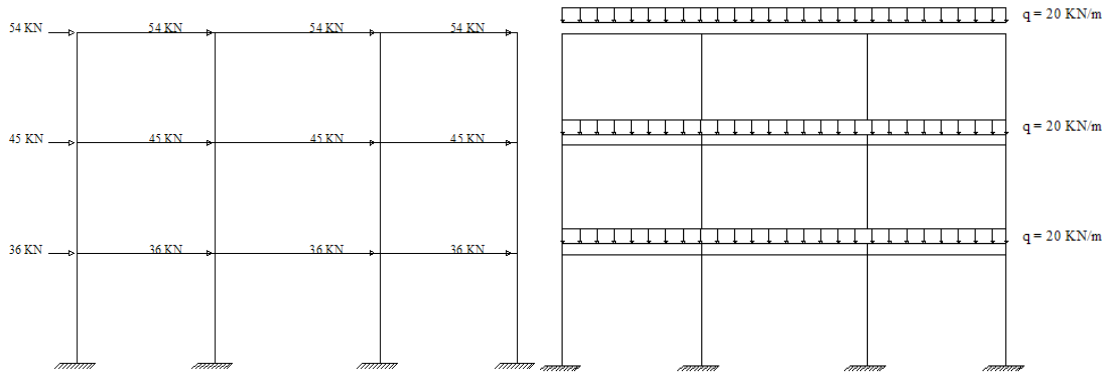


Figure 14-2 – Frame model and loads.

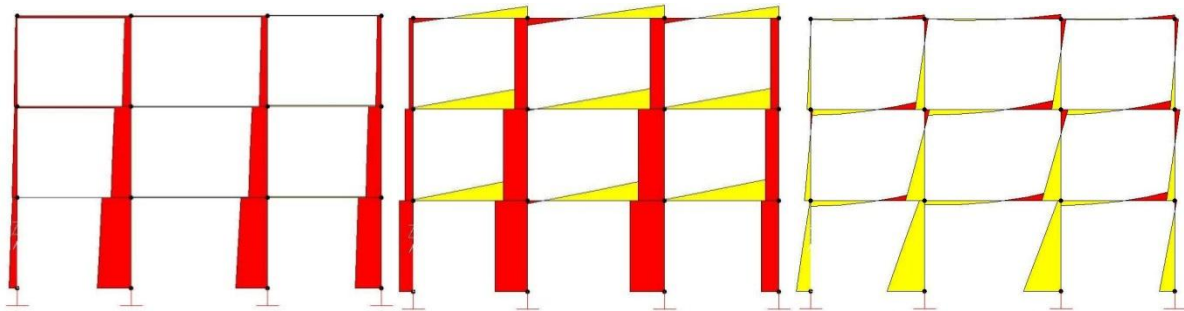


Figure 14-3 – Axial, shear and moment diagrams.

Table 14-4 – Moment capacity: panel 1.

Level	Length	Thickness	Factored axial load	Factored moment	Factored shear
[m]	L [m]	t [m]	N_{Sd} [kN]	M_{Sd} [kNm]	V_{Sd} [kN]
0	2	0.5	133.38	240.98	76.58
1	2	0.5	115.73	164.4	76.58
2	2	0.5	98.07	87.82	76.58
3	2	0.5	80.41	11.23	76.58
3	2	0.375	84.04	103.39	46.48
4	2	0.375	70.8	56.92	46.48
5	2	0.375	57.56	10.44	46.48
6	2	0.375	44.31	36.04	46.48
6	2	0.25	52.72	55.5	21.85
7	2	0.25	43.89	33.65	21.85
8	2	0.25	35.06	11.81	21.85
9	2	0.25	26.23	10.04	21.85

Table 14-5 – Moment capacity: panel 4.

Level	Length	Thickness	Factored axial load	Factored moment	Factored shear
[m]	L [m]	t [m]	N_{Sd} [kN]	M_{Sd} [kNm]	V_{Sd} [kN]
0	2	0.5	434.71	250.51	95.43
1	2	0.5	417.05	155.08	95.43
2	2	0.5	399.39	59.65	95.43
3	2	0.5	381.74	35.78	95.43
3	2	0.375	252.33	131.73	72.51
4	2	0.375	239.09	59.21	72.51
5	2	0.375	225.84	13.3	72.51
6	2	0.375	212.6	85.81	72.51
6	2	0.25	90.5	72.98	45.1
7	2	0.25	81.67	27.89	45.1
8	2	0.25	72.84	17.21	45.1
9	2	0.25	64.01	62.3	45.1

Table 14-6 – Moment capacity: panel 2.

Level	Length	Thickness	Factored axial load	Factored moment	Factored shear
[m]	L [m]	t [m]	N_{Sd} [kN]	M_{Sd} [kNm]	V_{Sd} [kN]
0	3	0.5	557.52	619.07	178.52
1	3	0.5	531.03	440.55	178.52
2	3	0.5	504.55	262.04	178.52
3	3	0.5	478.06	83.52	178.52
3	3	0.375	331.42	311.06	131.92
4	3	0.375	311.55	179.14	131.92
5	3	0.375	291.69	47.22	131.92
6	3	0.375	271.82	84.7	131.92
6	3	0.25	143.71	152.28	70.56
7	3	0.25	130.47	81.72	70.56
8	3	0.25	117.22	11.16	70.56
9	3	0.25	103.98	59.4	70.56

Table 14-7 – Moment capacity: panel 3.

Level	Length	Thickness	Factored axial load	Factored moment	Factored shear
[m]	L [m]	t [m]	N_{Sd} [kN]	M_{Sd} [kNm]	V_{Sd} [kN]
0	3	0.5	521.43	618.68	189.47
1	3	0.5	494.94	429.21	189.47
2	3	0.5	468.46	239.74	189.47
3	3	0.5	441.97	50.27	189.47
3	3	0.375	315.46	316.02	145.09
4	3	0.375	295.59	170.93	145.09
5	3	0.375	275.73	25.83	145.09
6	3	0.375	255.86	119.26	145.09
6	3	0.25	138.48	152.36	78.5
7	3	0.25	125.24	73.86	78.5
8	3	0.25	111.99	4.64	78.5
9	3	0.25	98.75	83.13	78.5

14.2 COMBINED AXIAL AND BENDING MOMENT CAPACITY

The combined axial and bending moment capacity of the unstrengthen masonry panels is computed assuming a constitutive law as per Section 14.1. The moment capacity, M_{Rd} (N_{Sd}) is computed for the design axial load N_{Sd} in accordance to the prescriptions on concrete structures reported in Sec-

tion 4.2.2.4. The translational and rotational equilibriums are used assuming the linearity of the strain distribution.

Results of the analysis are shown in Table 14-8, Table 14-9, Table 14-10 and Table 14-11. Figure 14-4 displays a comparison between the factored moment and flexural capacity. The equation $M_{Rd}(N_{Sd}) \geq M_{Sd}$ is not satisfied in some sections of the panels 1 and 4.

For these panels, FRP is chosen as strengthening system and applied over the all height of the panel with a distance of 10 cm from the panel edge.

Table 14-8–Design for combined bending and axial load: panel 1.

Section height [m]	$M_{Rd}(N_{Sd})$ [kN m]	$M_{Rd}(N_{Sd}) \geq M_{Sd}$
0	128.93	not satisfied
1	112.38	not satisfied
2	95.67	satisfied
3	78.79	satisfied
3	81.69	not satisfied
4	69.13	satisfied
5	56.46	satisfied
6	43.66	satisfied
6	51.33	not satisfied
7	42.93	satisfied
8	34.45	satisfied
9	25.89	satisfied

Table 14-9 – Design for combined bending and axial load: panel 4.

Section height [m]	$M_{Rd}(N_{Sd})$ [kN m]	$M_{Rd}(N_{Sd}) \geq M_{Sd}$
0	387.47	satisfied
1	373.57	satisfied
2	359.51	satisfied
3	345.31	satisfied
3	231.11	satisfied
4	220.04	satisfied
5	208.84	satisfied
6	197.53	satisfied
6	86.40	satisfied
7	78.34	satisfied
8	70.19	satisfied
9	61.96	not satisfied

Table 14-10 – Design for combined bending and axial load: panel 3

Section height [m]	$M_{Rd}(N_{Sd})$ [kN m]	$M_{Rd}(N_{Sd}) \geq M_{Sd}$
0	758.57	satisfied
1	726.05	satisfied
2	693.18	satisfied
3	659.95	satisfied
3	460.52	satisfied
4	434.97	satisfied
5	409.17	satisfied
6	383.10	satisfied
6	205.24	satisfied
7	187.19	satisfied
8	168.96	satisfied
9	150.56	satisfied

Table 14-11 – Design for combined bending and axial load: panel 4.

Section height [m]	$M_{Rd}(N_{Sd})$ [kN m]	$M_{Rd}(N_{Sd}) \geq M_{Sd}$
0	714.17	satisfied
1	681.17	satisfied
2	647.83	satisfied
3	614.12	satisfied
3	440.02	satisfied
4	414.26	satisfied
5	388.25	satisfied
6	361.97	satisfied
6	198.13	satisfied
7	180.02	satisfied
8	161.71	satisfied
9	143.25	satisfied

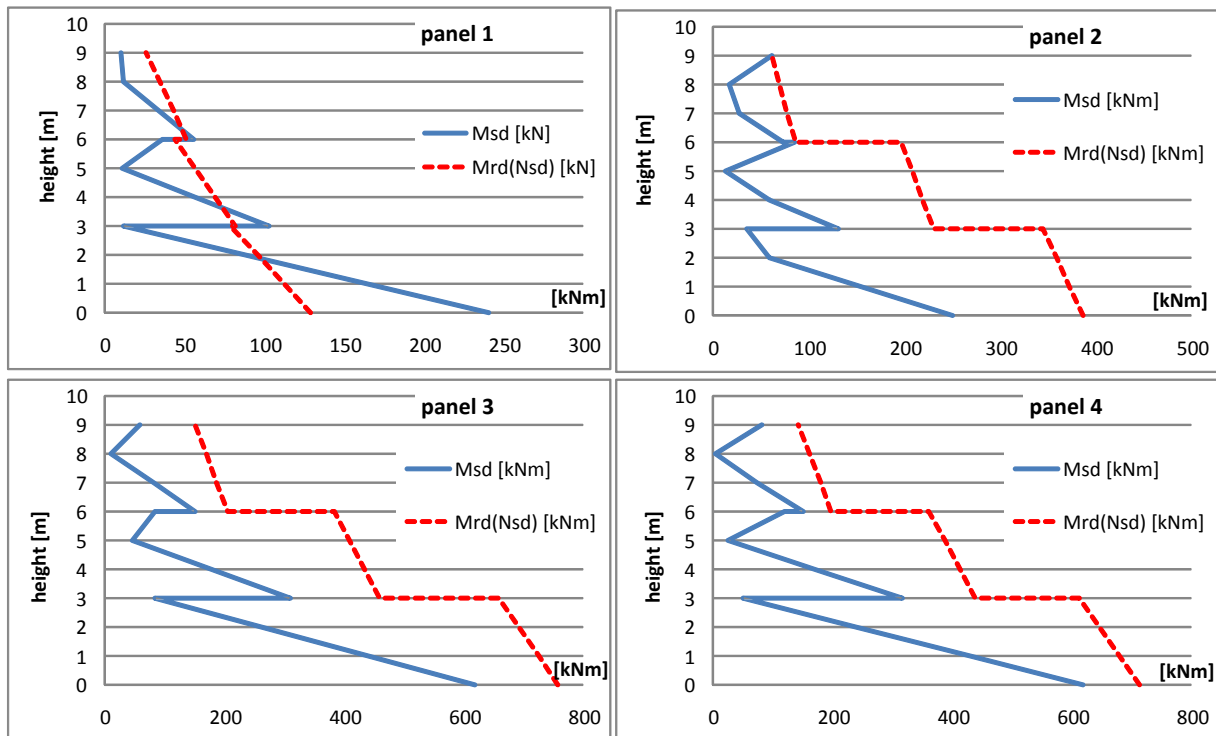


Figure 14-4– Flexural capacity and factored moment.

14.3 DESIGN OF FRP FOR COMBINED AXIAL AND BENDING MOMENT

The FRP properties are reported in Section 14.1 and installed continuously from the level 0.0 m to level 9.0 m on both internal and external side of the panels.

Mechanical anchoring devices are used at the lower levels.

The ULS stress distribution is simplified with *stress-block* distribution and depth equal to $0.8 \cdot x$ (where x is the distance from extreme compression fiber to the neutral axes).

The results of the FRP strengthened panels 1 and 2 are reported in Table 14-12 and Table 14-13, respectively.

Table 14-12 – Combined axial and bending capacity of the FRP strengthened panel 1.

Level [m]	FRP failure	ε_{fd}	$M_{Rd}(N_{Sd})$ [kN m]	$M_{Rd}(N_{Sd}) \geq M_{Sd}$
0	FRP failure	0.0151	335.8	verified
1	intermediate debonding	0.0086	231.6	verified
2	intermediate debonding	0.0086	215.4	verified
3	intermediate debonding	0.0086	199.1	verified
3	intermediate debonding	0.0086	200.6	verified
4	intermediate debonding	0.0086	188.6	verified
5	intermediate debonding	0.0086	176.6	verified
6	intermediate debonding	0.0086	164.3	verified
6	intermediate debonding	0.0086	169.8	verified
7	intermediate debonding	0.0086	162.0	verified
8	intermediate debonding	0.0086	154.0	verified
9	end debonding	0.0043	86.5	verified

Table 14-13 – Combined axial and bending capacity of the FRP strengthened panel 2.

Level [m]	FRP failure	ε_{fd}	$M_{Rd}(N_{Sd})$ [kN m]	$M_{Rd}(N_{Sd}) \geq M_{Sd}$
0	FRP failure	0.0151	577.0	verified
1	intermediate debonding	0.0086	482.9	verified
2	intermediate debonding	0.0086	469.4	verified
3	intermediate debonding	0.0086	455.8	verified
3	intermediate debonding	0.0086	342.7	verified
4	intermediate debonding	0.0086	332.2	verified
5	intermediate debonding	0.0086	321.6	verified
6	intermediate debonding	0.0086	310.9	verified
6	intermediate debonding	0.0086	202.4	verified
7	intermediate debonding	0.0086	194.9	verified
8	intermediate debonding	0.0086	187.3	verified
9	end debonding	0.0043	121.3	verified

14.4 SHEAR CAPACITY

Shear capacity of the unstrengthen panels 3 and 4 is reported in Table 14-14 and Table 14-15, respectively. Figure 14-5 displays a comparison between the factored shear and shear capacity. In these panels the equation $V_{Rd} \geq V_{Sd}$ is always satisfied. Therefore, the panels do not require any installation of shear strengthening systems.

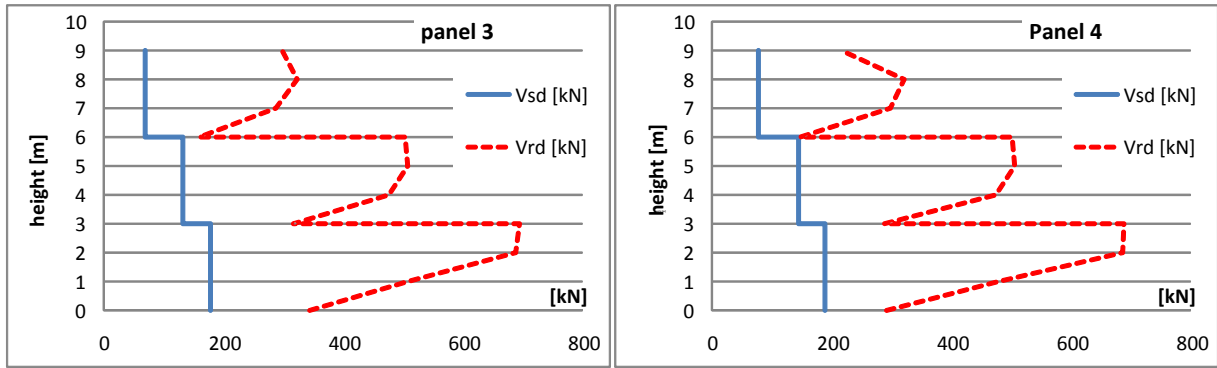


Figure 14-5 – Shear capacity and factored shear diagrams of panels 3 and 4.

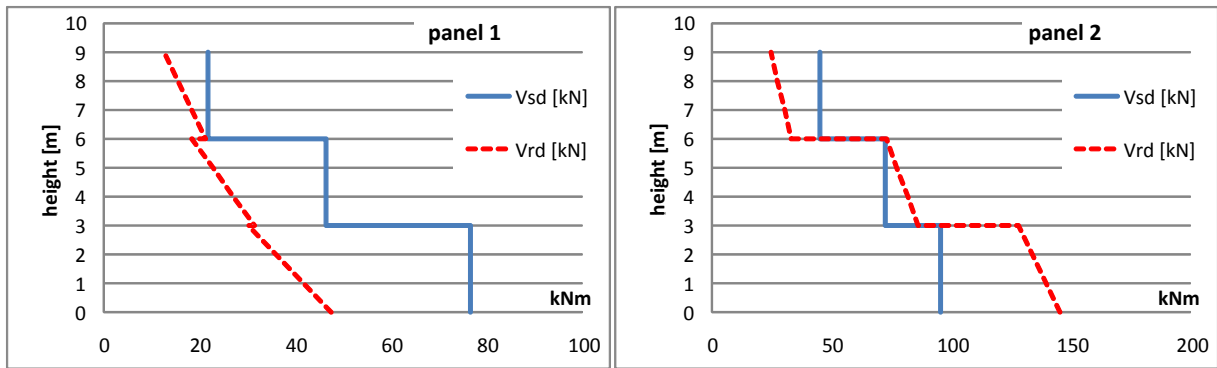


Figure 14-6 – Shear capacity and factored shear diagrams of panels 1 and 2.

Table 14-14 – Shear capacity of panel 3.

Level	Factored shear	Eccentricity	Optimal length	Characteristic shear strength	Shear capacity	$V_{Rd} \geq V_{Sd}$
[m]	V_{Sd} [kN]	e [m]	l_c [m]	f_{vk} [kN/m ²]	V_{Rd} [kN]	
0	178.52	1.11	1.17	1181.60	345.26	satisfied
1	178.52	0.83	2.01	1011.2	508.4	satisfied
2	178.52	0.52	2.94	937.2	689.3	satisfied
3	178.52	0.17	3.00	927.5	695.6	satisfied
3	131.92	0.94	1.68	1009.9	318.9	satisfied
4	131.92	0.57	2.78	919.8	478.6	satisfied
5	131.92	0.16	3.00	903.7	508.3	satisfied
6	131.92	0.31	3.00	896.6	504.4	satisfied
6	70.56	1.06	1.32	974.0	160.9	satisfied
7	70.56	0.63	2.62	879.6	288.2	satisfied
8	70.56	0.10	3.00	862.5	323.4	satisfied
9	70.56	0.57	2.79	859.7	299.4	satisfied

Table 14-15 – Shear capacity of panel 4.

Level	Factored shear	Eccentricity	Optimal length	Characteristic shear strength	Shear capacity	$V_{Rd} \geq V_{Sd}$
[m]	V_{Sd} [kN]	e [m]	l_c [m]	f_{vk} [kN/m ²]	V_{Rd} [kN]	
0	189.47	1.19	0.94	1243.54	292.38	satisfied
1	189.47	0.87	1.90	1008.6	478.7	satisfied
2	189.47	0.51	2.96	926.4	686.6	satisfied
3	189.47	0.11	3.00	917.9	688.4	satisfied
3	145.09	1.00	1.49	1025.1	287.3	satisfied
4	145.09	0.58	2.77	914.0	473.9	satisfied
5	145.09	0.09	3.00	898.0	505.1	satisfied
6	145.09	0.47	3.00	891.0	501.2	satisfied
6	78.5	1.10	1.20	984.7	147.6	satisfied
7	78.5	0.59	2.73	873.4	298.1	satisfied
8	78.5	0.04	3.00	859.7	322.4	satisfied
9	78.5	0.84	1.97	880.0	217.2	satisfied

Table 14-16 and Table 14-17 show the result of the shear analysis of panels 1 and 4, respectively.

Table 14-16 – Shear capacity of panel 1.

Level	Factored shear	Neutral axis	Characteristic shear strength	Shear capacity	$V_{Rd} \geq V_{Sd}$
[m]	V_{Sd} [kN]	x [m]	f_{vk} [kN/m ²]	V_{Rd} [kN]	
0	76.58	0.15	1488.4	57.7	non satisfied
1	76.58	0.11	1618.4	45.8	non satisfied
2	76.58	0.10	1568.5	40.0	non satisfied
3	76.58	0.09	1506.5	34.3	non satisfied
3	46.48	0.12	1520.4	35.5	non satisfied
4	46.48	0.11	1466.0	31.2	non satisfied
5	46.48	0.10	1399.8	26.9	non satisfied
6	46.48	0.09	1317.6	22.6	non satisfied
6	21.85	0.15	1371.9	25.3	satisfied
7	21.85	0.14	1314.6	22.4	satisfied
8	21.85	0.13	1247.3	19.6	non satisfied
9	21.85	0.07	1370.3	12.6	non satisfied

Table 14-17 – Shear capacity of panel 4.

Level	Factored shear	Neutral axis	Characteristic shear strength	Shear capacity	$V_{Rd} \geq V_{Sd}$
[m]	V_{Sd} [kN]	x [m]	f_{vk} [kN/m ²]	V_{Rd} [kN]	$V_{Rd} \geq V_{Sd}$
0	95.43	0.34	1812.9	155.6	satisfied
1	95.43	0.30	1906.8	143.7	satisfied
2	95.43	0.29	1900.2	138.0	satisfied
3	95.43	0.28	1893.1	132.2	satisfied
3	72.51	0.26	1816.9	90.2	satisfied
4	72.51	0.25	1805.5	85.9	satisfied
5	72.51	0.24	1793.0	81.6	satisfied
6	72.51	0.23	1779.3	77.3	satisfied
6	45.1	0.19	1543.6	37.6	non satisfied
7	45.1	0.18	1511.4	34.7	non satisfied
8	45.1	0.17	1475.1	31.8	non satisfied
9	45.1	0.12	1647.8	24.9	non satisfied

14.5 DESIGN OF FRP FOR SHEAR

FRP (Section 14.1) are used throughout the total height of the panels assuming a distance between strips, p_f , equal to 50 cm. The analysis is performed according to Section 5.4.1.2.2. Results are shown in Table 14-18 and Table 14-19 for panel 1 and 2, respectively, in which the chosen p_f satisfies the shear requirements.

Table 14-18– Shear capacity of panel 1.

Level [m]	Factored shear V_{Sd} [kN]	Masonry contribution $V_{Rd,m}$ [kN]	FRP contribution $V_{Rd,f}$ [kN]	$V_{Rd,max}$ [kN]	Shear capacity V_{Rd} [kN]	$V_{Rd} \geq V_{Sd}$	Failure
0	76.58	57.7	124.02	1140	181.7	satisfied	FRP failure
1	76.58	45.8	124.02	1140	169.8	satisfied	FRP failure
2	76.58	40.0	124.02	1140	164.1	satisfied	FRP failure
3	76.58	34.3	124.02	1140	158.3	satisfied	FRP failure
3	46.48	35.5	124.02	855	159.5	satisfied	FRP failure
4	46.48	31.2	124.02	855	155.2	satisfied	FRP failure
5	46.48	26.9	124.02	855	150.9	satisfied	FRP failure
6	46.48	22.6	124.02	855	146.6	satisfied	FRP failure
6	21.85	25.3	124.02	570	149.3	satisfied	FRP failure
7	21.85	22.4	124.02	570	146.4	satisfied	FRP failure
8	21.85	19.6	124.02	570	143.6	satisfied	FRP failure
9	21.85	12.6	124.02	570	136.6	satisfied	FRP failure

Table 14-19 – Shear capacity of panel 2.

Level [m]	Factored shear V_{Sd} [kN]	Masonry contribution $V_{Rd,m}$ [kN]	FRP contribution $V_{Rd,f}$ [kN]	$V_{Rd,max}$ [kN]	Shear capacity V_{Rd} [kN]	$V_{Rd} \geq V_{Sd}$	Failure
0	95.43	155.61	124.02	1140.0	279.6	satisfied	FRP failure
1	95.43	143.70	124.02	1140.0	267.7	satisfied	FRP failure
2	95.43	137.96	124.02	1140.0	262.0	satisfied	FRP failure
3	95.43	132.22	124.02	1140.0	256.2	satisfied	FRP failure
3	72.51	90.17	124.02	855.0	214.2	satisfied	FRP failure
4	72.51	85.86	124.02	855.0	209.9	satisfied	FRP failure
5	72.51	81.56	124.02	855.0	205.6	satisfied	FRP failure
6	72.51	77.25	124.02	855.0	201.3	satisfied	FRP failure
6	45.1	37.57	124.02	570.0	161.6	satisfied	FRP failure
7	45.1	34.70	124.02	570.0	158.7	satisfied	FRP failure
8	45.1	31.83	124.02	570.0	155.9	satisfied	FRP failure
9	45.1	24.88	124.02	570.0	148.9	satisfied	FRP failure

Figure 14-7 shows the FRP installation details of panels 1 and 4 for both shear and combined axial and bending moment.

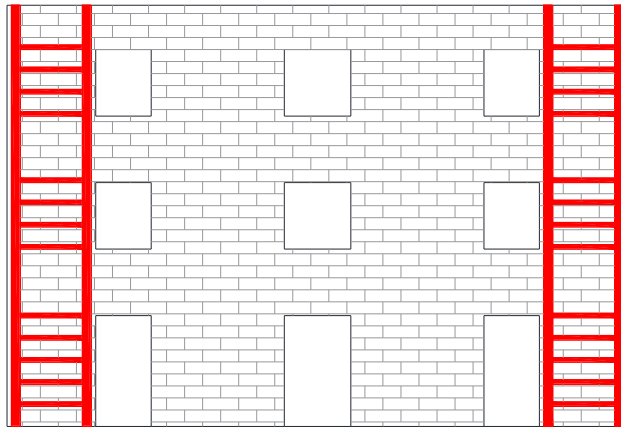


Figure 14-7 – Layout of the FRP installation.

14.6 DESIGN FOR SIMPLE OVERTURNING

Following the assumption reported in Section 5.4.1.1, Figure 14-8 shows the system of forces to consider while design the masonry panels for simple overturning. The FRP with characteristic as per Section 14.1 are used by embracing the entire perimeter of the building in each floor (Figure 14-9). The FRP reinforcement at the third floor is comprised of two layers with a thickness equal to 0.33 mm. The FRP width is equal to 350 mm at the third and second floors, and 200 mm at the first floor.

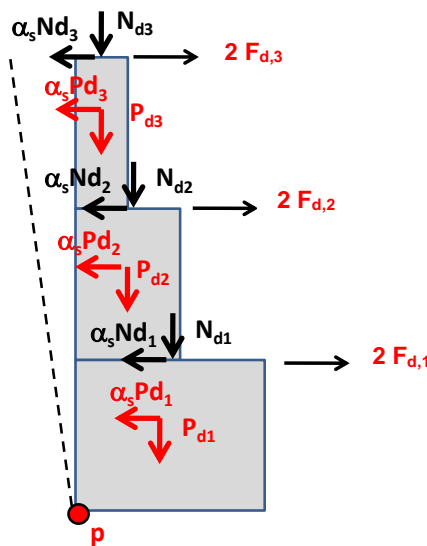


Figure 14-8 –Scheme of simple overturning.

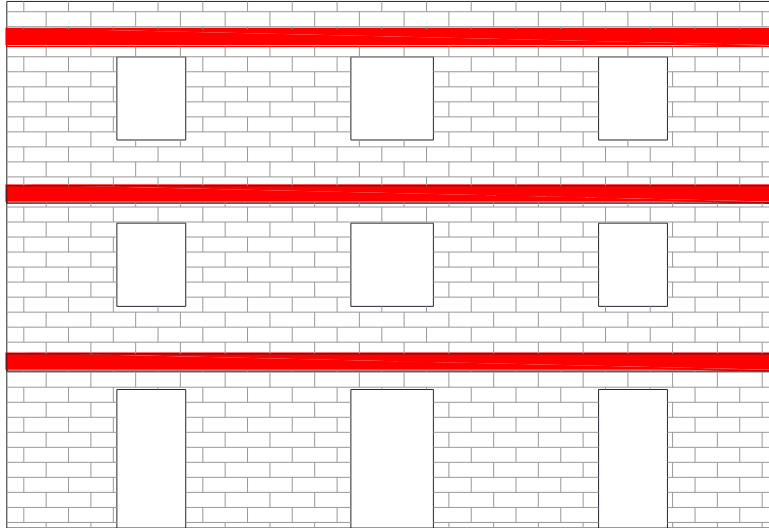


Figure 14-9 – FRP installation for simple overturning.

Assuming that the symbols reported in Figure 14-8 are equal as follows:

- $P_{d1}=288$ kN, $P_{d2}=243$ kN, $P_{d3}=162$ kN.
- $N_{d1}=155$ kN, $N_{d2}=155$ kN, $N_{d3}=155$ kN.
- $\alpha_s= 1.5$.

The following can be computed:

- $2 \cdot F_{d,1}=188$ kN,
- $2 \cdot F_{d,2}=377$ kN,
- $2 \cdot F_{d,3}=566$ kN,

where $F_{d,k}$ represent the force carried by the FRP system at the level k (with $k=1, 2, 3$), and:

$$F_{d,1} \leq (230000 \cdot 200 \cdot 0.165 \cdot 10^{-3} \cdot 0.0151) \text{ kN} = 115 \text{ kN.}$$

$$F_{d,2} \leq (230000 \cdot 350 \cdot 0.165 \cdot 10^{-3} \cdot 0.0151) \text{ kN} = 201 \text{ kN.}$$

$$F_{d,3} \leq (230000 \cdot 350 \cdot 0.330 \cdot 10^{-3} \cdot 0.0151) \text{ kN} = 401 \text{ kN.}$$

The last three equations satisfy the requirement for simple overturning.

This Technical Document has been prepared by a Task Group whose members are:

AIELLO Prof. Maria Antonietta	- University of Lecce
ASCIONE Prof. Luigi	- University of Salerno
BARATTA Prof. Alessandro	- University of Napoli “Federico II”
BASTIANINI Ing. Filippo	- University of Bologna
BATTISTA dott. Umberto	- SACEN S.r.l. Restauri – Napoli, Italy
BENEDETTI Prof. Andrea	- University of Bologna
BERARDI Ing. Valentino Paolo	- University of Salerno
BILOTTA Ing. Antonio	- University of Napoli “Federico II”
BORRI Prof. Antonio	- University of Perugia
BRICCOLI BATI Prof. Silvia	- University of Firenze
CASADEI Ing. Paolo	- Kerakoll S.p.a. - Sassuolo (MO), Italy
CERONI Ing. Francesca	- University of Sannio - Benevento
CERSOSIMO Ing. Giuseppe	- Interbau S.r.l.- Milano
COSENZA Prof. Edoardo	- University of Napoli “Federico II”
CREDALI Prof. Lino	- Ardea S.r.l. - Casalecchio (BO), Italy
DE LORENZIS Prof. Laura	- University of Lecce
FAELLA Prof. Ciro	- University of Salerno
FAVA Ing. Giulia	- Politecnico of Milano
FEO Prof. Luciano	- University of Salerno
FERRACUTI Ing. Barbara	- University of Bologna
FORABOSCHI Prof. Paolo	- IUAV – Venezia, Italy
FRASSINE Prof. Roberto	- Politecnico of Milano
GIACOMIN Ing. Giorgio	- G&P Intech S.r.l. - Altavilla Vicentina (VI), Italy
IMBIMBO Prof. Maura	- University of Cassino
LA TEGOLA Prof. Antonio	- University of Lecce
LAGOMARSINO Prof. Sergio	- University of Genova
LUCIANO Prof. Raimondo	- University of Cassino
MACERI Prof. Franco	- University of Roma “Tor Vergata”
MAGENES Prof. Guido	- University of Pavia
MANFREDI Prof. Gaetano	- University of Napoli “Federico II”
MANTEGAZZA Dott. Giovanni	- Ruredil S.p.a. – Milano, Italy
MARRA Ing. Gianfranco	- University of Salerno
MARTINELLI Ing. Enzo	- University of Salerno
MODENA Prof. Claudio	- University of Padova
MONTALBANO Ing. Antonino	- Sika Italia S.p.a. – Milano, Italy
MONTI Prof. Giorgio	- University of Roma “La Sapienza”
MORANDINI Ing. Giulio	- Mapei S.p.a. – Milano, Italy
NANNI Prof. Antonio	- University of Napoli “Federico II”
NIGRO Prof. Emidio	- University of Napoli “Federico II”
OLIVITO Prof. Renato Sante	- University of Calabria - Cosenza
PARRETTI Ing. Renato	- Fibrwrap Italia S.r.l. - Sesto Fiorentino (FI), Italy
PASCALE Prof. Giovanni	- University of Bologna
PECCE Prof. Maria Rosaria	- University of Sannio - Benevento
PISANI Prof. Marco Andrea	- Politecnico of Milano
POGGI Prof. Carlo	- Politecnico of Milano
PROTA Prof. Andrea	- University of Napoli “Federico II”
REALFONZO Prof. Roberto	- University of Salerno
ROSATI Prof. Luciano	- University of Napoli “Federico II”
SACCO Prof. Elio	- University of Cassino

SAVOIA Prof. Marco - University of Bologna
SPACONE Prof. Enrico - University of Chieti
ZAMPA Ing. Andrea - Fibre Net S.r.l. – Udine, Italy

Coordinators:

- for the chapter on “Materials”: FRASSINE Prof. Roberto, POGGI Prof. Carlo;
- for the chapter on “Basic notions on the strengthening design and special issues”: MONTI Prof. Giorgio, NANNI Prof. Antonio;
- for the chapter on “Reinforced concrete and prestressed concrete structures”: ASCIONE Prof. Luigi, MANFREDI Prof. Gaetano, MONTI Prof. Giorgio;
- for the chapter on “Masonry structures”: BENEDETTI Prof. Andrea, SACCO Prof. Elio;
- for the chapter on “Monitoring and quality control”: OLIVITO Prof. Renato Sante, PASCALE Prof. Giovanni, PROTA Prof. Andrea.

General Coordinator:

ASCIONE Prof. Luigi.

Technical Office:

FEO Prof. Luciano, ROSATI Prof. Luciano.

This Technical Document has been approved by the “Advisory Committee on Technical Recommendation for Construction” as a draft version on 08/03/2012 and submitted for public hearing. The members of the “Advisory Committee on Technical Recommendation for Construction” present were:

ANGOTTI Prof. Franco	- University of Firenze
ASCIONE Prof. Luigi	- University of Salerno
BARATTA Prof. Alessandro	- University of Napoli “Federico II”
COSENZA Prof. Edoardo	- University of Napoli “Federico II”
JAPPELLI prof. Ruggiero	- University of Roma “Tor Vergata”
MACERI Prof. Franco	- University of Roma “Tor Vergata”
MANCINI Prof. Giuseppe	- Politecnico of Torino
MAZZOLANI Prof. Federico Massimo	- University of Napoli “Federico II”
PINTO Prof. Paolo Emilio	- University of Roma “La Sapienza”
SAVOIA Prof. Marco	- University of Bologna
SOLARI Prof. Giovanni	- University of Genova
URBANO Prof. Carlo	- Politecnico of Milano
VINCI Arch. Roberto	- Italian National Council of Researches
ZANON Prof. Paolo	- University di Trento

This Technical Document has been approved in its final version on 10/10/2013 and includes the modifications derived from the public hearing. The members of the “Advisory Committee on Technical Recommendation for Construction” present were:

ANGOTTI Prof. Franco	- University of Firenze
AURICCHIO Prof. Ferdinando	- University of Pavia
ASCIONE Prof. Luigi	- University of Salerno
BARATTA Prof. Alessandro	- University of Napoli “Federico II”
COSENZA Prof. Edoardo	- University of Napoli “Federico II”
MACERI Prof. Franco	- University of Roma “Tor Vergata”
MANCINI Prof. Giuseppe	- Politecnico of Torino
MAZZOLANI Prof. Federico Massimo	- University of Napoli “Federico II”
PINTO Prof. Paolo Emilio	- University of Roma “La Sapienza”
POGGI Prof. Carlo	- Politecnico of Milano
ROYER CARFAGNI Prof. Gianni	- University of Parma
SAVOIA Prof. Marco	- University of Bologna
SCARPELLI prof. Giuseppe	- University of Marche
SOLARI Prof. Giovanni	- University of Genova
URBANO Prof. Carlo	- Politecnico of Milano
VINCI Arch. Roberto	- Italian National Council of Researches
ZANON Prof. Paolo	- University of Trento